UNIVERSITÀ
DEGLI STUDI
DI PADOVA

Sede Amministrativa: Università degli Studi di Padova

Dipartimento di Neuroscienze

CORSO DI DOTTORATO DI RICERCA IN SCIENZE PSICOLOGICHE
CICLO XXXII

TRACKING COGNITIVE CONTROL: HOW DO WE SOLVE INTERFERENCE?

Coordinatore: Prof. Giovanni Galfano
Supervisore: Prof. Antonino Vallesi
Co-Supervisore: Dott.ssa Luisa Sartori

Dottoranda: Alessandra Tafuro

Publications

Chapter 1 is derived from the following publication:

Tafuro, A., Ambrosini, E., Puccioni, O., & Vallesi, A. (2019). Brain oscillations in cognitive control: A cross-sectional study with a spatial stroop task. *Neuropsychologia*, 107190.

Abstract in English

Selecting relevant information in the presence of distracting one is a core component of cognitive control, referred as interference resolution. This process has been often investigated through the Stroop task, where responses are longer when two stimulus features are incongruent, compared to when they are congruent (Stroop effect). Despite a large body of literature about this process, the mechanisms of interference resolution are still matter of debate. The present PhD project aimed at shedding light on the temporal dynamics of interference resolution and the related neural underpinnings. In Study 1 we focused on investigating the brain oscillations involved in this process during a spatial Stroop task, aiming at understanding if these correlates and their temporal course change across the lifespan by recruiting younger and older adults. We found age-related differences in theta and beta bands. Theta may represent an early mechanism signalling the need to exert control, which seems to be impaired with aging. Beta may correspond to the process of relevant information selection and older adults showed an over-recruitment of these frequencies. Previous evidence suggested that these results may be attributed to age-related differences in the use of proactive and reactive control, in line with the DMC (Dual Mode of Control) model. Proactive control is defined as an anticipatory attentional bias, whereas reactive control as a late correction mechanism. To study more in depth the different contribution of these control modes, we developed Study 2. We used the same task, manipulating the percentage of congruency (PC) at different levels, list or item, to elicit proactive and reactive control respectively. We also recorded computer mouse trajectories because the high temporal resolution of this tool can shed light on the underlying temporal dynamics of these control modes. Analysis of mouse-derived measures showed that the Stroop effect was present as costs in responding to incongruent trials, reflected in a greater attraction toward the irrelevant information, less smooth trajectories, and longer time to respond due to the updating and adjustments of the trajectories. We found that the magnitude of the interference varied as a function of the PC manipulations, with smaller Stroop interference for low-PC manipulations. Our results suggested also that reactive control may work faster than previously thought, possibly triggering a rapid attentional bias toward the relevant information similar to the one predicted for proactive control. To investigate further the role of proactive control it was necessary to study the time preceding stimulus appearance. Hence, we developed Study 3 in which we used the same mouse-tracking task, manipulating the PC at the list level to mainly elicit proactive control, and we recorded EEG signal to have a window on the brain dynamics before stimulus presentation. We found clear PC-dependent modulations of the interference, both at the behavioural and the neural level, for which we found smaller Stroop effect for blocks with low PC. Behavioural results generally replicated those of Study 2. EEG results showed PC-related modulations of interference, which mirrored the same pattern observed in mouse-derived measures and mainly involved theta and beta bands. This project provides confirmations and new suggestions in the study of interference resolution. We confirmed the involvement of theta in this process, interpreted as an early mechanism of interference detection that signals the need to exert control. We also found a main involvement of beta that may represent the imposition of early attentional biases toward the relevant information. We interpreted these results in line with the Cascade of Control and the DMC models. This project represents a first attempt to evaluate more deeply the temporal course of proactive and reactive control, taking advantages of two techniques with high temporal resolution.

Abstract in Italiano

Selezionare informazioni rilevanti in presenza di altre distraenti è un aspetto chiave del controllo cognitivo, conosciuto come risoluzione dell'interferenza. Questo processo è spesso investigato con il paradigma di Stroop, in cui sono registrate risposte più lunghe per stimoli con caratteristiche incongruenti. Tuttavia, i meccanismi della risoluzione dell'interferenza non sono ancora stati chiariti. Il presente progetto, attraverso tre studi, mira a far luce sulle dinamiche temporali di questo processo e sui suoi correlati neurali. Nello Studio 1, sono state investigate le oscillazioni neurali coinvolte in questo processo durante la somministrazione di uno Stroop spaziale, e se questi correlati cambiassero durante l'invecchiamento, reclutando partecipanti giovani e anziani. È emerso principalmente un coinvolgimento delle onde theta e beta. Theta può corrispondere ad un segnale che comunica la necessità di aumentare il controllo, che pare essere ridotto nell'invecchiamento. Beta può riflettere un meccanismo di selezione dell'informazione rilevante, e gli anziani hanno mostrato un aumento di queste frequenze. Alcuni studi hanno suggerito che questi risultati possano riflettere cambiamenti dovuti all'età nell'uso del controllo proattivo o reattivo, in linea col modello DMC (Dual Mode of Control). Il controllo proattivo è un meccanismo che anticipa l'interferenza, mentre il reattivo è una correzione tardiva. Per studiare meglio queste differenze è stato sviluppato lo Studio 2. È stato usato lo stesso compito con una manipolazione della percentuale di congruenza (PC) a livello di lista o di item, per elicitare rispettivamente il controllo proattivo e reattivo. Sono state anche registrate le traiettorie del mouse per poter far luce sulle dinamiche temporali sottostanti questi due controlli. È emerso un costo nel rispondere a stimoli incongruenti, tradotto in una maggiore attrazione verso l'informazione irrilevante, traiettorie meno omogenee e tempi di risposta più lunghi dovuti agli aggiustamenti in corso. Effetti Stroop più piccoli sono emersi per la manipolazione a bassa PC. Inoltre, i risultati hanno suggerito che il controllo reattivo possa essere più veloce del previsto, probabilmente usando rapidi meccanismi attentivi simili a quelli del proattivo. Per studiare meglio il ruolo del proattivo, è stato necessario focalizzarsi sul tempo che precede l'apparizione dello stimolo. Nello Studio 3 è stato usato lo stesso paradigma, con una manipolazione di PC sulla lista per elicitare il controllo proattivo. È stato inoltre registrato il segnale EEG per avere una finestra sul tempo precedente alla comparsa dello stimolo. Sono state trovate delle modulazioni dovute all'uso della PC, sia dalle analisi cinematiche che neurali, con un effetto Stroop minore per blocchi a bassa PC. Le analisi della cinematica hanno replicato i risultati dello Studio 2. Dai risultati EEG è emerso un maggior coinvolgimento delle onde theta e beta, con una modulazione dell'interferenza simile a quella delle misure del mouse. Questo progetto, dunque, fornisce conferme e nuovi spunti nello studio della risoluzione dell'interferenza. È stato confermato il ruolo di theta, interpretato come un meccanismo precoce che segnala il bisogno di aumentare controllo in presenza di un'interferenza. È stata riscontrata anche un'attività beta che potrebbe rappresentare un meccanismo attentivo di selezione dell'informazione rilevante. I risultati sono stati interpretati in linea con i modelli Cascade of Control e DMC. Questo progetto costituisce un primo tentativo di studiare in profondità il decorso temporale del controllo proattivo e reattivo, traendo vantaggio da due tecniche ad alta risoluzione temporale.

Acknowledgments

I would like to thank my supervisor Prof. Antonino Vallesi for supporting and encouraging me during my PhD. A special thank goes also to Dr. Ettore Ambrosini for being a mentor who guided me patiently in these three years and who taught me everything I have been able to report in this dissertation.

I would like to thank my lab members (and friends) Ettore, Maria, Antonino, Mariagrazia, Vincenza, Laila, Ilaria, Chiara and Francesca for always being ready to help me and cheer me up.

Last, but not least, I would like to thank Luca, my parents and my friends for their tireless support and love.

Table of Contents

List of Figures

CHAPTER 1

CHAPTER 2

CHAPTER 3

CHAPTER 4

APPENDIX

List of Tables

CHAPTER 2

CHAPTER 3

CHAPTER 4

APPENDIX

Chapter 1
General introduction

1.1. How do we deal with cognitive interference?

As I am organizing my ideas thinking about how to fill the blank pages of this thesis, I already got two e-mail notifications popped up on the lower corner of my desktop. However, I know that, right now, I need to ignore these distractions and focus on my goal. If you are reading this thesis, it means that, more or less successfully, I exerted cognitive control. Cognitive control, sometimes also referred as executive control, is a broad term often used to indicate the ability to flexibly regulate our behaviour according to contexts and internal goals, maintaining the representations of action plans and updating them according to environmental changes. Indeed, this ability allows us to select relevant information even in the presence of irrelevant and distracting information. A large body of evidence indicates that it preferentially engages prefrontal regions of the brain that, working in connection with other frontal, parietal and subcortical circuits, mediate a set of top-down processes allowing us to deal with complex situations (Diamond, 2013; Miller & Cohen, 2001; Stuss, 2011; Stuss & Levine, 2002). However, even if there is a general agreement that cognitive control plays a crucial role in a variety of high-level processes, a precise and formal classification of these is still missing. The most common interpretation defined cognitive control as the ability to bias information processing in face of competing representations, novel or habitual behaviours (Norman & Shallice, 1986), often considered to be exerted in a top-down fashion (Miller & Cohen, 2001).

Drawing back to my current situation, where I am exerting cognitive control to remain focussed despite the popped-up notifications, the particular process involved is referred in this thesis as interference resolution, and it is engaged when we need to focus on relevant goals, while ignoring distracting information. In laboratory settings, one of the most used paradigms to investigate this ability is the Stroop task (Stroop, 1935). In the classic version of this task, the so-called colour-word Stroop task, participants have to name the colour of the ink in which a colour word is written. Critically, the stimuli are thus denoted by two features (or two stimulus dimensions): the ink colour, which is the task-relevant feature, and the meaning of the word denoting the colour, which is the task-irrelevant, interfering feature. It is well known that, because of the extensive practice we have in reading, this process has priority in the elaboration, thus eliciting a prepotent response, that in this task needs to be overcome to give the correct answer. Therefore, responses are faster when the two features of the stimuli are congruent (e.g., the word "red" written in red ink), compared to when they are incongruent (e.g., the word "red" written in blue ink). To respond to incongruent trials, it is indeed necessary to exert cognitive control, and specifically interference resolution, in order to solve the interference of the to-be-ignored information (i.e., the word meaning), in favour of the task-relevant information (i.e., the ink colour). The cost in responding to incongruent trials, compared to the facilitation in responding to the congruent ones, is referred as the Stroop effect.

Nonetheless, how the resolution of interference is carried out is still matter of debate. Concerning the mechanisms implicated in this process, previous evidence suggested that it is achieved through inhibitory processing (Friedman & Miyake, 2004; Miyake et al., 2000; Nigg, 2000). However, other authors seemed to be sceptical in embracing inhibitory accounts to explain the Stroop effect, since these findings can be interpreted also as an activation or boosting of relevant information (MacLeod, Dodd, Sheard, Wilson, & Bibi, 2003; Roelofs, 1997). However, Munakata and colleagues (2011) suggested that the active maintenance of the task-relevant representations would also indirectly produce a form of "competitive inhibition" via diffuse lateral inhibitory connectivity, which results in the inhibition of alternative representations and the amplification of the most active representation. Moreover, the facilitation effect often reported in Stroop tasks (i.e., the advantage in responding to congruent items compared to the neutral ones) can be hardly explained through inhibitory processing, because there is no irrelevant information needing to be inhibited, leaving open the possibility that other mechanisms influence the Stroop performance (Lindsay & Jacoby, 1994; MacLeod, 1991). Related to this issue, much work has been done to understand where the locus of the interference is in the Stroop task, that is, if at the stimulus-processing or response level. There is evidence for both accounts, indeed the interference may arise at the stimulus-processing stage, because the relevant and irrelevant features of the stimulus usually overlap (i.e., stimulus-stimulus competition), but the Stroop effect may also be explained, at least in part, as an interference at the response selection level, because the irrelevant feature can activate an associated response (i.e., stimulus-response competition; De Houwer, 2003; Zhang & Kornblum, 1998). Indeed, the classical Stroop task requires participants to respond vocally to the ink colour of the stimulus, so that it not only involves a stimulus-stimulus overlap, but also a response dimension overlap that occurs with both the relevant and the irrelevant stimulus dimensions (i.e., the ink colour and the meaning of the word denoting the colour, respectively; Kornblum & Stevens, 2002). Nonetheless, it seems that the Stroop interference mainly arises at the stimulus-processing stage, as a result of the competition between the relevant and irrelevant features of the stimulus. This was evidenced by the fact that clear interference effects have been observed in Stroop-like tasks even when they did not entail stimulus-response competitions, but only stimulus-stimulus competition, for instance in variants of the classic colour-word Stroop task requiring manual responses (Augustinova, Parris, & Ferrand, 2019; Augustinova, Silvert, Spatola, & Ferrand, 2018; Luo, 1999; Sturz, Green, Locker, & Boyer, 2013).

These same processes are also involved in other versions of the Stroop task that have been extensively used in the literature, for example the picture-word Stroop task or the spatial Stroop task. In the picture-word Stroop task a word is presented superimposed on a picture, and participants have to name the picture ignoring the word, leading to the similar stimulus-stimulus and stimulus-response competitions of the classical version of the Stroop task. Concerning the spatial Stroop task, participants are generally presented with arrows appearing in different positions of the screen and pointing to either the same or different directions, and they are asked to attend to the direction of the arrow, while ignoring the position. Similar to what previously described, this entails a stimulus-stimulus competition, because the dimensions of position and direction overlap, but also a stimulus-response competition, because the position dimension triggers a primary processing and elicits a prepotent response, as compared to the direction dimension. Nevertheless, it is important to notice that other paradigms, such as the Flanker task (Eriksen & Eriksen, 1974) or the Simon task (Simon & Small, 1969), have been used to study interference resolution process, even though they do not imply the same loci of interference and competitions as the Stroop task (e.g., stimulus-stimulus or stimulus-response).

1.2. The cascade of interference resolution

There is however general agreement in considering the Stroop effect as having multiple loci and it has been suggested that the mechanisms involved in interference resolution may occur in a cascade-like manner, so that the magnitude of the interference in later stages is modulated by the efficiency of the earlier stages (Banich, 2009). In particular, there is one model that is tailored on the resolution of Stroop interference: The Cascade of Control Model (Banich, 2009). This model suggests that multiple, sequential steps are implicated in solving the interference. Based on different neuroimaging findings, the model proposes a temporal cascade of processing steps involving selection processes that are implemented in different portions of the prefrontal cortex (PFC; see Banich et al., 2000; Milham et al., 2001; Milham & Banich, 2005; Milham, Banich, & Barad, 2003). Firstly, posterior regions of the dorso-lateral PFC (DLPFC) are recruited to set an attentional bias toward task-relevant processes, that is, a top-down bias toward regions implicated in the elaboration of the to-be-attended information. For instance, in the classic version of the Stroop, posterior DLPFC sends a bias toward the regions implied in the identification of the ink colour and that must be strong to overcome the natural bias toward automatized word reading. The second step concerns the involvement of the mid portion of the DLPFC to bias task-relevant representations actively maintained in working memory, and it is fundamental to determine which stimulus information is the relevant one. The posterior portion of the dorsal anterior cingulate cortex (dACC) is then recruited as a late stage (third step) to select the correct response, and it has been reported that its involvement is essential in contexts implying response competitions (Milham et al., 2001). The fourth and last step is carried by the anterior portion of the dorsal ACC and involves the evaluation of the response, in line also with the Conflict Monitoring theory suggesting that ACC triggers adjustments in cognitive control (Botvinick, Cohen, & Carter, 2004). Figure 1.1 provides a summary of the steps predicted by the Cascade of Control model.

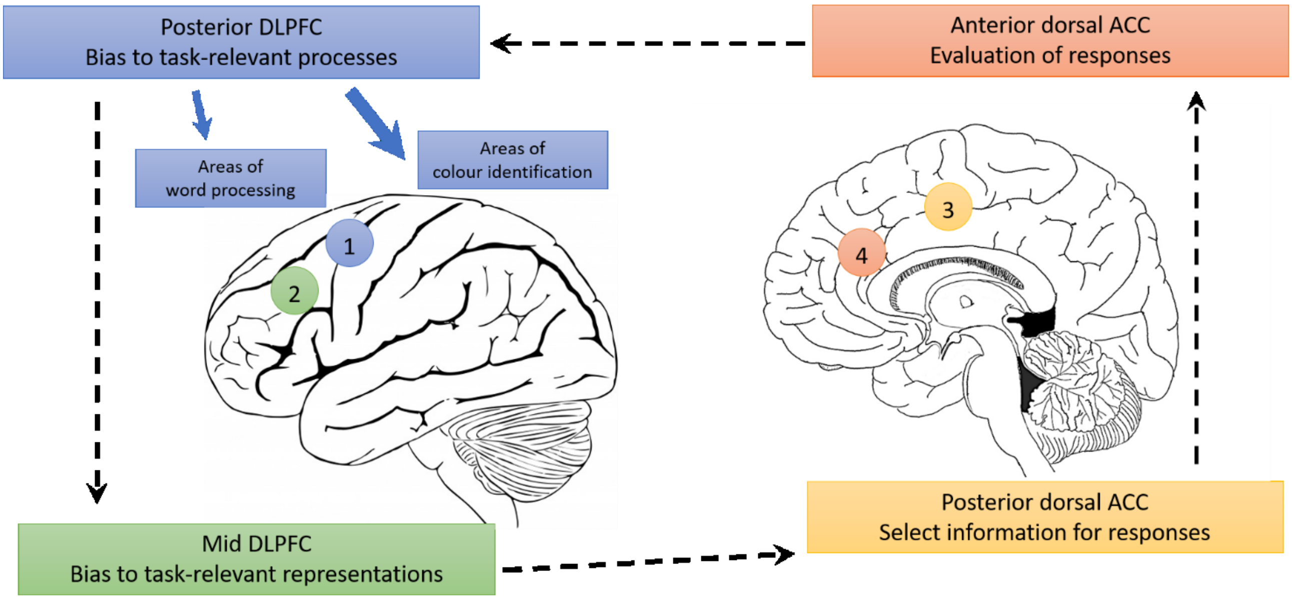

Figure 1.1. Cascade of Control model
The figure represents a schematic illustration of the Cascade of Control model. For the original figure of the model see Banich (2009). Posterior DLPFC is involved in the first step, imposing an attentional bias toward the task-relevant processes (e.g., colour identification); mid-DLPFC carries out the second step, imposing a bias toward the task-relevant representation actively maintained; posterior dACC is involved in the third step, selecting the information that should guide responses; the anterior dACC carries out the fourth and last step, evaluating the given response and feeding back to the DLPFC.

A critical aspect of the Cascade of Control model is that the need to invoke any of the selection (cognitive control) processes depends on how successfully cognitive control was applied at earlier steps. According to this model, thus, the activity of the ACC is influenced by the efficiency with which DLPFC exerts cognitive control (Milham, Banich, Claus, & Cohen, 2003). For example, a failure to effectively exert control by DLPFC requires increased involvement of dACC to resolve the interference. This is in line with evidence showing that, during the performance of a colour-word Stroop task, older adults showed an increase in ACC activity and less activity in DLPFC

(Milham et al., 2002) and, also in younger adults, activity in DLPFC is negatively correlated with that of ACC across participants (Floden, Vallesi, & Stuss, 2011). Furthermore, this model fits well with both evidence in favour of stimulus-stimulus and stimulus-response competitions reported in the literature (e.g., De Houwer, 2003) and is particularly suited to investigate the temporal dynamics and the different processes involved in interference resolution, providing significant insights in the understanding of how cognitive control works. Indeed, the debate is still open about the underlying cognitive and brain mechanisms during the processing of the different loci of interference in the Stroop task. It is currently still unclear whether and how the different cognitive processes involved in interference resolution might temporally interact and whether they share common or distinct neural mechanisms.

In this regard, another important issue to consider concerns the nature of cognitive control, that is, cognitive control may work with two distinct modes that entail different temporal dynamics (Braver, 2012).

1.3. The dual mechanisms of control framework

The Dual Mechanisms of Control (DMC) model suggests that cognitive control works through two distinct control modes with different underlying temporal dynamics (Braver, 2012; Braver, Gray, & Burgess, 2007; Braver, Paxton, Locke, & Barch, 2009). According to this model, the two distinct modes with which cognitive control can be employed are the proactive and the reactive control. Proactive control can be considered as an early anticipatory mechanism that is implemented in advance and that actively maintains in a sustained manner the task-relevant information, biasing attention and action processes in a goal-directed way and optimizing behaviour. In contrast, reactive control can be considered as a late correction mechanism engaged on-demand only after the occurrence of an event requiring control. This model of cognitive control is particularly relevant also for the process of interference resolution. For instance, in the case of the Stroop task, engaging proactive control can help in anticipating the interference imposing an early attentional bias toward the relevant information (i.e., ink colour), whereas reactive control would be engaged after the detection of interference (i.e., incongruent trial).

Different findings also indicate that the two modes of cognitive control rely on different brain areas (Braver et al., 2007). Indeed, proactive control has been mainly associated with activation of the lateral PFC, reflecting the maintenance of task goal (Braver et al., 2007), whereas reactive control has been reported to engage not only lateral PFC, but also ACC, which is critical for detecting the need to exert control (Botvinick, Braver, Barch, Carter, & Cohen, 2001). However, it should be noted that these areas are not the only executives of cognitive control, and that this process is achieved through an orchestration of complex interactions between these areas and other parietal and subcortical areas.

In the study of these two modes of cognitive control, the AX-Continuous Performance Test (AX-CPT) has been frequently used. In this task participants are presented with a cue (a letter), that after a delay is followed by a probe (another letter). Participants are asked to detect a specific sequence of letters, that is an X probe when it is preceded by an A cue, and they need to respond with different key presses for targets (AX sequence only) or non-targets (any sequence of letters other than AX). This task allows making different predictions depending on the use of proactive and reactive control. If participants rely on proactive control, they will prepare a target response only when they meet A letters as cue. In this way, they will be fast in responding to the target AX sequences, but they will be slow and more prone to errors in responding to AY sequences (where Y indicates any letter other than X). On the contrary, if participants rely on reactive control, they will not prepare responses in advance when they see an A cue, and they will be slower and more prone to mistakes in BX sequences (where B denotes any letter other than A), because the X letter activates a target response, but they will be faster in responding to AY sequences (Braver et al., 2007). Obviously optimal performance on this task entails a fine-tuned balance between these two cognitive control strategies. However, this task is not the only one through which it is possible to elicit proactive or reactive control.

1.4. DMC and interference resolution in the Stroop task

There is extensive evidence showing that also in the Stroop task it is possible to favour the use of one or the other modes of control by manipulating the proportion of congruency (PC, proportion of congruent trials; see Bugg & Crump, 2012, for a review). PC can be manipulated in different ways, for example at the list-wide level, at the item-specific level, or at the context-specific level. The first type of manipulation, a list-wide PC (LWPC), consists in presenting blocks with high PC (mostly congruent) and blocks with low PC (mostly incongruent). Different studies reported a smaller interference (i.e., smaller Stroop effect) for blocks with low PC as compared to those with high PC (Lindsay & Jacoby, 1994; Logan & Zbrodoff, 1979). The second approach concerns in manipulating the PC at an item-specific level (ISPC), so that a given item (e.g., a given word in a colour-word Stroop task) is presented with high PC (mostly congruent) or low PC (mostly incongruent). For this type of manipulation high- and low-PC items are presented in the same block, yielding a LWPC where congruent and incongruent trials are equally probable (LWPC of 50%). Similar to what demonstrated for LWPC manipulation, the Stroop effect is reduced for low-PC items as compared to high-PC ones (Bugg, Jacoby, & Chanani, 2011; Jacoby, Lindsay, & Hessels, 2003). The third kind of manipulation is similar to the ISPC one, but the PC is manipulated according to different contexts (i.e., context-specific level, CSPC), which constitutes another task-irrelevant feature that does not overlap with the response dimension. For example, one of the most used types of manipulation concerns the variation of the position where a specific item is presented (Crump, Gong, & Milliken, 2006), but similar results have been reported also manipulating the font of the words presented (Bugg, Jacoby, & Toth, 2008). As previously seen for the ISPC effect, the Stroop interference is reduced for the specific contexts that are manipulated with a low PC compared to the high PC, and the LWPC is kept always at the 50%.

Therefore, all these findings showed that, independently of the type of manipulations adopted, a smaller Stroop effect is obtained in low-PC condition as compared to high-PC condition. However, in line with the DMC model, many studies suggested that proactive and reactive cognitive control modes may be differentially engaged by LWPC or ISPC/CSPC manipulations (see Bugg & Crump, 2012, for a review). Indeed, given the anticipatory nature of proactive control, this mode can be involved mainly in the resolution of the interference in LWPC blocks. This happens because in this manipulation the likelihood of occurrence of conflicts in a given block allows the imposition of an early and preparatory attentional bias on the task-relevant dimension for all the trials in that block. In contrast, for ISPC and CSPC manipulations, it is not possible to prepare in advance a response, because congruent and incongruent trials are equally probable and it is not possible to know in advance if the forthcoming trial will include a low-PC or a high-PC item/context. Thus, reactive mode is the best candidate to resolve the interference in these conditions, as the likelihood of a conflict for a given item/context can still allow the employment of an attentional filter toward the relevant dimension (explaining the smaller Stroop effect for low-PC items/contexts compared to high-PC ones), but this can happen only after the presentation of the stimulus.

However, there is still some debate about how cognitive control is specifically implicated in interference resolution in all these manipulations. For instance, it has been suggested that the ISPC effects can be driven by a stimulus-response contingency-learning process, for which participants are faster in responding to items frequently associated to a given response, and that cognitive control may be not implied in this (Logan, 1998; Schmidt & Besner, 2008). Indeed, according to this account, participants do not rely on cognitive control to resolve the interference, because they implicitly learn contingencies between stimuli and responses, becoming able to predict which responses are associated with specific distracting stimuli. Bugg and Hutchison (2013) suggested that both mechanisms may work under specific circumstances, and in particular that a contingency-learning process may be the responsible for ISPC effects especially when a small set size (e.g., two items) is used, because there are high-contingency responses. With a small set size, indeed, it is possible to predict responses in the majority of trials relying on the correlations between stimuli and responses, thus shortcutting some higher-level processes (Schmidt & Besner, 2008). Instead, when using larger set size (e.g., four items) it is much harder to detect such extreme contingencies and to predict associated responses because, even though it is still possible to create some high-contingency associations for congruent items, the most challenging incongruent items do not entail any high contingency with specific responses.

Another debate to consider concerns studies challenging the view that the interference is resolved, in LWPC manipulations, through proactive control processes (i.e., by imposing an attentional bias before stimulus presentation) and suggesting that item-specific mechanisms may have a role in explaining both LWPC and ISPC effects (Blais & Bunge, 2010; Bugg et al., 2008). These concerns emerged because the LWPC manipulation confounds perfectly with the ISPC one, since blocks that are mostly congruent are constituted by mostly congruent items (i.e., a block with a LWPC of 25% is composed by items with an ISPC of 25% only). However, the inclusion of an additional set of unbiased items (i.e., items with an ISPC of 50%, for which congruent and incongruent trials are equally probable) in the low- and high-PC blocks allows to disentangle the specific contribution of proactive control (Bugg & Chanani, 2011). Indeed, it has been reported that interference is reduced for these unbiased items in the low-PC blocks compared to the same unbiased items in the high-PC blocks. This can only be explained by assuming that participants relied on the use of proactive control, imposing an early attentional bias to anticipate the interference that creates an advantage also for the unbiased items (Bugg, McDaniel, Scullin, & Braver, 2011). Therefore, ISPC effects cannot account entirely for the interference reduction reported in LWPC manipulations.

Finally, it is noteworthy that, despite LWPC and ISPC effects (associated with proactive and reactive control) have been extensively investigated, to the best of our knowledge only one study assessed independent estimates of these effects in the same participants (Gonthier, Braver, & Bugg, 2016).

1.5. The temporal dynamics of proactive and reactive control

As we already mentioned, LWPC and ISPC manipulations have been linked to the DMC model, proposing that, if PC is modulated globally in the blocks, participants can use the LWPC information to impose an early attentional bias toward the relevant dimension (i.e., in the case of the Stroop task, the ink colour) relying on proactive control, otherwise if PC is modulated locally (e.g., at the item level) participants must wait for the presentation of each stimulus and then they can use the ISPC information to exert reactive control. This evidence can be interpreted and integrated also in light of the Cascade of Control model (Banich, 2009; see section 1.2). Indeed, given the definition of proactive control as "a form of early selection […] prior to the occurrence of cognitively demanding events" (Braver, 2012), it may correspond and overlap to the earlier steps of the Cascade of Control model, and in particular to the first one that imposes a bias to the task-relevant processes. For instance, as reported above, in tasks where PC is manipulated at the block level, participants can engage proactive control in low-PC conditions because incongruent trials are more likely to occur, and they can impose an early bias to task-relevant information before the occurrence of the interference. This can be linked to the first step of the Cascade of Control model, where the bias to task-relevant processes allows increasing the weights on brain regions involved in the processing of task-relevant information (e.g., elaboration of the ink colour). This bias would be particularly strong when participants can anticipate the interference (even if they are unaware of the manipulation), as in the case of LWPC manipulation with low-PC blocks. Therefore, the cascade of steps engaged for the resolution of the interference may start earlier in time, indeed even before the stimulus presentation. As a consequence of this increased control at earlier steps, control processes at later stages will be invoked to a lesser degree (Banich, 2009).

By contrast, since reactive control has been defined as "a late correction mechanism that is mobilized only as needed in a just-in-time manner" (Braver, 2012), it can come into play only after the detection of the interference. Since participants cannot rely on the anticipation of the interference in ISPC manipulations, the cascade of steps involved in interference resolution has to start later in time as compared to proactive control, definitely after the stimulus presentation, and the bias of the first step may not be as strong as for proactive control. As a consequence of this inability to exert effective control at earlier steps, control processes at later steps would be recruited more. However, it has also been reported that Stroop interference is reduced for low-PC even in ISPC conditions (when PC is manipulated only at the item level but congruent and incongruent trials are globally equally probable), thus suggesting that a fast attentional setting is involved also here (Bugg, 2017; Bugg & Crump, 2012) and that reactive control may even operate at the earlier steps of the Cascade of Control model.

Hence, it appears clear that, broadly speaking, the two modes of cognitive control (i.e., proactive and reactive) entail intrinsic differences in the temporal dynamics with which they come into play. However, as seen in the evidence reviewed above, it seems important to understand further in depth the boundary between the two and the specific cascade of mechanisms that they engage in interference resolution. In this investigation, it is important to highlight which are the neural correlates and the specific temporal dynamics of these mechanisms, also in the light of the Cascade of Control model. Therefore, our main purpose was to study the temporal cascade of neural and cognitive mechanisms implicated in interference resolution. To do so, we took advantage of two techniques with high temporal resolution: the analysis of electroencephalographic (EEG) signal and the analysis of computer mouse trajectories.

EEG is a widely used tool in the study of cognitive processes, because it allows to have a window on the brain dynamics in a non-invasive way and it allows to make inferences on the processes engaged (Cohen, 2017). Other neuroimaging techniques have been used to shed light on cognitive processes (e.g., functional magnetic resonance imaging), but only EEG (or related techniques such as Magnetoencephalography) can capture their fast temporal course. Of particular interest for our purposes is the study of neural oscillations that can provide important insights not only into the temporal course, but also into the neurophysiological mechanisms involved in different cognitive processes. Indeed, time-frequency based analysis have the advantage, over the event-related potential (ERP) analysis, to allow linking different frequency bands and their changes over time to different task events and cognitive processes.

Time-frequency based analysis received growing attention just over the last years in the study of cognitive processes and, for this reason, there are still few studies that tackled this issue. One of the findings for which there is general agreement concerns the involvement of theta band (4-7 Hz), especially localized over midfrontal channels, in paradigms of interference (Cavanagh & Frank, 2014; Cavanagh, Zambrano-Vazquez, & Allen, 2012). This frequency band has been proposed to reflect the process of early detection of the interference, which signals the need to exert cognitive control (Cavanagh & Frank, 2014). Moreover, also in the context of proactive and reactive control, theta frequencies have been reported to be implicated in both modes, but leaving open the possibility that distinct frontoparietal networks are engaged in proactive and reactive control (Cooper et al., 2015; Eschmann, Bader, & Mecklinger, 2018), thus highlighting the need of further investigation on this issue.

Moreover, so far different frequency bands have been implicated in different cognitive processes, but, in our view, especially beta frequencies (13-30 Hz) are of particular interest in the process of interference resolution. Evidence from our laboratory suggested that this band may be implied in this process (Ambrosini & Vallesi, 2017) and this fitted well with the growing body of findings demonstrating that beta is not only a “motor” frequency band. Indeed, it has been previously suggested that beta may work as a signal that maintains the “status quo” (Engel & Fries, 2010), and that every change in this state would be reflected in changes of beta activity. As matter of fact, other studies have recently showed implication in beta in the endogenous reactivation of information processing (Spitzer & Haegens, 2017), in decision making (Haegens et al., 2011; Siegel, Engel, & Donner, 2011), in surprise and updating about sensory events (Gould, Nobre, Wyart, & Rushworth, 2012; Meindertsma, Kloosterman, Engel, Wagenmakers, & Donner, 2018). However, conclusive evidence about its involvement in proactive and reactive control is still missing and with our project we also aimed at shedding light on the functional role of beta frequencies in cognitive processes.

Another technique, adopted in the present project, that can clarify the contribution of proactive and reactive control in interference resolution is the analysis of computer mouse trajectories. This approach has been gaining attention over the last few years and has important advantages over the more traditional study of response times (RTs). Indeed, it is particularly suitable for the investigation of interference resolution processes, because it allows to record the attraction from the irrelevant and distracting dimension, providing also information about when and how interference is resolved. Mouse-tracking can indeed capture in real-time the temporal course of cognitive processes while they are in execution (Freeman & Ambady, 2010). This tool records in a continuous way the x- and y-coordinates of the computer mouse with a very high sampling rate (around 60/70 Hz), allowing to catch not only the final result of an action (like in a button press response), but also the online updating and adjusting of the response (Freeman, Dale, & Farmer, 2011). This tool has been previously used in a variety of cognitive domains, for instance, in the study of the language system, where it has been used to report the existence of a parallel processing of competing phonetic representations (Spivey, Grosjean, & Knoblich, 2005), or in the study of the decision-making process, where it has been shown that inter-individual differences in speed of processing of food-related information were associated with dietary self-control failures (Sullivan, Hutcherson, Harris, & Rangel, 2015), and also in the study of social perception of others, where it has been reported that social categories are simultaneously and partially activated while evidence is integrated over time (Freeman & Ambady, 2011).

On the basis of such considerations, mouse kinematics, reflecting our ongoing cognitive processes, can unveil the temporal course of proactive and reactive control in interference resolution, as it will be further pointed out in Chapters 3 and 4. The following section will explain the aims of the different studies presented in this dissertation more in detail.

1.6. Project overview

The leading goal of this project was to shed light on the neural correlates and the temporal dynamics of the cascade of mechanisms exerted by cognitive control to resolve an interference. Despite the large body of existing literature about cognitive control, there are still many open questions. The present dissertation is composed of three different studies, in which we used one or both the tools described above to have a more comprehensive view on the temporal dynamics of interference resolution and the related neural underpinnings.

Undoubtedly, the study of EEG signal can help to tackle this issue, and this is what we aimed at with Study 1 (Chapter 2). Even though much work has been conducted with ERP analysis, the investigation of neural oscillations implicated in cognitive control, and particularly in interference resolution, has been gaining attention only in the last years. As mentioned above, neural oscillations can provide important advantages over ERP analysis, because different frequencies bands and their changes over time can be linked to distinct cognitive processes (Engel & Fries, 2010). Therefore, one of the main goals of Study 1 was to adopt this approach to investigate which brain dynamics are involved in interference resolution, by administering a spatial version of the Stroop task. To answer this question more exhaustively, two samples of participants of different ages (younger and older healthy adults) have been recruited, in order to understand also if the neural oscillations and their temporal course in resolving interference change across the lifespan. Indeed, in agreement with the Cascade of Control model, previous evidence showed that older adults, when performing tasks requiring the resolution of interference, showed more prominent activity in ACC brain regions, as compared to the DLPFC and opposite to what reported for younger adults, suggesting that the earlier steps of the model may be impaired (Milham et al., 2002). In the context of proactive and reactive control, this can be translated as a potential impairment in the exertion of proactive control which, as we reported above, can correspond to the earlier steps of the Cascade of Control model. Indeed, also previous evidence suggested that older adults showed impairments in the active maintenance of task-relevant goals (i.e., proactive control), leading to a preferential use of reactive control to perform tasks (Bugg, 2014; Paxton, Barch, Racine, & Braver, 2007). For these reasons, we also aimed at investigating the age-dependent dissociation between proactive and reactive control in interference resolution. In particular, we wanted to study if the neural correlates of this process were different between younger and older adults, and if there were differences in the temporal dynamics of interference resolutions processes.

However, for a more precise investigation of proactive and reactive control in the Stroop task, the use of the manipulation of the PC has been suggested, in order to elicit different degrees of proactive and reactive control. This consideration led us to the development of Study 2 (Chapter 3). We administered the same version of the spatial Stroop task previously used, but we manipulated the PC at both the list and the item level (i.e., LWPC and ISPC respectively) to elicit proactive and reactive control[1]. Importantly, in this task we also recorded computer mouse trajectories because, as previously specified, the high temporal resolution of this technique would allow to bring important advantages in the study of the temporal dynamics of proactive and reactive control. To our knowledge, this is the second study assessing the specific effects of LWPC and ISPC manipulations in the same participants (see Gonthier et al., 2016). Moreover, despite two recent studies assessed the contribution of ISPC manipulations in a Stroop task by means of mouse-tracking tool (Bundt, Ruitenberg, Abrahamse, & Notebaert, 2018; Ruitenberg, Braem, Du Cheyne, & Notebaert, 2019), no previous study adopted both types of PC manipulations (therefore, eliciting both cognitive control modes), and used a spatial version of the Stroop task. Indeed, we believe that the use of mouse-tracking fits particularly well with the presentation of spatial stimuli, as it is possible to capture the interference due to the overlap of the relevant and irrelevant dimensions (i.e., position and direction of the arrow).

---

[1] Note that, for some authors, our ISPC manipulation is to be considered as context specific (CSPC; see Bugg & Crump, 2012, for a review), because we manipulated the PC according to a feature that is commonly seen as contextual, that is, the position of the stimulus. Nonetheless, we are referring to it as ISPC, because in our paradigm the position of the stimulus overlaps with the response dimension. To try avoiding confusion, we adopted LWPC and ISPC labels to underline that, independently from the contextual feature manipulated, we presented blocks with low, equal, or high PC, and specific items with low, equal or high PC.

However, to study more in depth the anticipatory attentional bias that proactive control may impose before the occurrence of an interference, the analysis of mouse trajectory may be not enough, because it can only capture post-stimulus cognitive processes. Consequently, we developed Study 3 (Chapter 4), where we administered the very same spatial Stroop recording mouse trajectories, but we also recorded EEG activity to have a window on the brain dynamics before stimulus presentation. With this study, we intended to make a comparison with the behavioural findings of Study 2, and to extend the findings of Study 1 about the neural oscillations involved in interference resolution. Nevertheless, it was not possible to administer both LWPC and ISPC manipulations, since we needed to raise the number of trials for the EEG analysis and keeping the same manipulations would have made the task very long. Hence, for Study 3 we focused on LWPC manipulations only. To our knowledge, this is the first study combining EEG and mouse-tracking techniques.

Chapter 2
Brain oscillations in interference resolution

2.1. Introduction

The ability to select relevant information and to ignore the conflicting and irrelevant one is a core aspect of cognitive control, and it allows us to flexibly adapt our behaviour (Miller & Cohen, 2001). Understanding the neural underpinnings of this cognitive function remains challenging. Many experimental designs have been adopted to investigate the selection of task relevant features, but the Stroop paradigm is one of the most widely used to study how we resist to the interference of irrelevant information (MacLeod, 1991; Stroop, 1935). Previous studies suggested that the cognitive processes involved in this task engage the left lateral portion of the PFC, independently of the stimulus domain, as for example the verbal or spatial domain (Vallesi, 2012). We mentioned in Chapter 1 the Cascade of Control model that is based on the case of interference resolution in the Stroop task, and suggests that resolving the interference involves a temporal cascade of selection processes (Banich, 2009). Indeed, this model proposes that the dorsolateral PFC (DLPFC) creates and imposes a top-down attentional set for task-relevant goals, thus applying a bias to specific task-relevant processes and representations, especially needed when other competing but irrelevant information must be suppressed. After setting the attentional bias, posterior regions of dorsal Anterior Cingulate Cortex (dACC) are hypothesized to be involved in processes of responses selection, whereas the more anterior portions are engaged in the evaluation of the output. Notably, as highlighted by the author, the more efficient the control exerted by DLPFC regions is, the less the recruitment of dACC regions is. This is corroborated by evidence showing that older adults, who recruited less the DLPFC, showed increased activation of ACC, meaning that there is probably a failure in the effectiveness of DLPFC control (Milham et al., 2002). A similar pattern of anti-correlation between the activation of these two regions has also been observed in younger adults (e.g., Floden, Vallesi, & Stuss, 2011).

Indeed, how cognitive control change across the lifespan is another important issue to investigate. As social and health conditions improve, also life expectancy increases, and the number of people over 65 years old is rapidly rising (He, Goodkind, & Kowal, 2016). It is well established that healthy aging entails a progressive cognitive decline, the causes of which are still unknown. It has been proposed that a general slowing of processing speed can be responsible for the performance decrease in older adults documented in different tasks (Verhaeghen & De Meersman, 1998). However, other evidence suggested that this slowing cannot be the only answer and that there must be other changes contributing to it (Bugg, DeLosh, Davalos, & Davis, 2007; Forstmann et al., 2011). Indeed, neuroimaging studies reported age-related changes in the brain both anatomically (see Fjell & Walhovd, 2010, for a review) and functionally (Greenwood, 2000), spanning a variety of functions, such as working memory, attention, interference resolution, inhibition of irrelevant information (Gazzaley & D'esposito, 2007; Hasher & Zacks, 1988; Vallesi, Stuss, McIntosh, & Picton, 2009; West, 2004). Moreover, age-related changes in cerebral anatomy and physiology have been proposed to lead to a general reorganization of brain functions, with a reduction in hemispheric specialization (hemispheric asymmetry reduction in older adults –HAROLD– model, see Cabeza, 2002) and a dedifferentiation and/or an over-recruitment of neural resources (scaffolding theory of aging and cognition, see Park & Reuter-Lorenz, 2009; Reuter-Lorenz & Park, 2014), especially concerning the prefrontal cortex. It is important to shed light on the mechanisms that are mainly subjected to these modifications and how they differ from normal functioning, in order to find potential therapies, treatments, or training that can reduce this deterioration.

The aforementioned issues constituted the starting points for the present EEG study, in which we had multiple aims. First of all, we investigated the event-related spectral perturbation (ERSP) of interference resolution and if these spectral dynamics change during adult lifespan. For these reasons, we recruited two samples of participants of different ages and conducted time-frequency analysis, which has the advantage (when compared to the event-related potential method) of providing information about the time course and the involvement of different frequency bands in specific cognitive tasks (Engel & Fries, 2010). Indeed, this analysis allows to extract information about power changes in each frequency under examination and their changes during time with regard to task events (extracting the so-called event-related spectral perturbation), so that different neural oscillations can be linked to many different cognitive processes (Roach & Mathalon, 2008). This approach has been gaining attention over the last years and different studies suggested that oscillatory activity plays a key role in neural communication and other cognitive functions (Fries, 2005; Salinas & Sejnowski, 2001).

Second, we aimed at reconstructing the cortical sources of spectral dynamics to shed light on the contribution of left and right DLPFC in the process of interference resolution, as previous studies suggested the domain-general activation of the left portion (see Vallesi, 2012, for a review). Hence, we employed a spatial version of the Stroop task, since processing of non-verbal information is thought to be lateralized over the right hemisphere (Boulinguez, Ferrois, & Graumer, 2003; Weintraub & Mesulam, 1987). In this way, finding left lateralized spectral correlates for interference resolution using spatial material would allow to draw more compelling conclusions about the domain-independent asymmetry of executive functions.

Concerning the implications of spectral dynamics in cognitive tasks, a general integrative role has been attributed to theta band (4-7 Hz) in the organization of brain activity (Sauseng, Griesmayr, Freunberger, & Klimesch, 2010). More specifically, mid-frontal oscillations in the theta band have been mostly implied in interference resolution and conflict processing, and they have been proposed to reflect the need for cognitive control (Cavanagh & Frank, 2014; Cohen, 2014). In particular, previous studies using colour-word Stroop tasks with manual responses reported an increase in mid-frontal theta power for incongruent conditions (Ergen et al., 2014; Hanslmayr et al., 2008; see also Wang, Li, Zheng, Wang, & Liu, 2014; Zhao et al., 2015). Evidence from other spatial paradigms, such as the Flanker task, also showed increase in mid-frontal theta power for higher cognitive demands when responding to incongruent trials (Nigbur, Ivanova, & Stürmer, 2011; see also Zavala et al., 2013). On the basis of these results, we expected to find evidence for an early temporal involvement of theta band, reflecting a general signal for the need to exert cognitive control, with a specific mid-frontal increase in theta power for incongruent conditions.

Other studies have evidenced the role of beta oscillations (13-30 Hz) in interference resolution. In particular, in a previous study from our laboratory (Ambrosini & Vallesi, 2017), we found that the prefrontal hemispheric asymmetry in beta electrophysiological activity at rest correlated with the participants' ability to control interference in verbal and spatial versions of the Stroop task. Moreover, studies aiming at disentangling conflict associated with stimuli and responses by administering modified versions of the Stroop tasks (i.e., combination of Simon and Stroop task or 2-1 mapping task) showed the involvement of beta band power modulations in response conflict (Wang et al., 2014; Zhao et al., 2015), with a conflict-induced reduction of beta spectral power. Results from another study using intracranial recording revealed greater desynchronization in beta and alpha activity in medial prefrontal cortex for the incongruent condition (Aulická et al., 2014). We thus also expected to find evidence for the involvement of beta frequencies in Stroop performance. Specifically, given the role of theta modulations in signalling the need for cognitive control, we expected beta band modulations to be implicated in later time windows in order to cope with the Stroop interference. In particular, we hypothesized that the cognitive processes implicated in the resolution of Stroop interference, such as the selection of task-relevant representations or appropriate responses, may be translated in the recruitment of beta band, possibly with a left lateralization of prefrontal involvement.

As regards age-related differences in ERSP correlates of cognitive control, we expected to find a general over-recruitment of neural resources in older adults, in line with the scaffolding theory (Park & Reuter-Lorenz, 2009). Moreover, in line with the HAROLD model, we expected to find an age-dependent reduction of the left-lateralized prefrontal asymmetry that has been related to interference resolution and Stroop performance in young participants (see Ambrosini & Vallesi, 2017; see also Vallesi, 2012, for a review).

2.2. Methods

2.2.1. Participants

The initial sample was composed of 24 younger adults (females = 13, mean age = 25.58 years, SD = 4.73 years, range = [18 35] years) and 21 older adults (females = 10, mean age = 72.86 years, SD = 4.55 years, age range = [66 82] years). One younger and one older participant were excluded because they did not complete the task. The final sample was thus composed of 23 younger adults (females = 12, mean age = 25.26 years, SD = 4.55 years, range = [18 35] years) and 20 older adults (females = 9, mean age = 73.2 years, SD = 4.38 years, age range = [66 82] years). There were no gender differences between the two groups ($p > .762$, two-tailed Fisher's exact test). Behavioural data from one female participant from the younger group were not recorded due to technical problems, so she was removed from behavioural and correlation analyses; one male participant from the same group was excluded from electrophysiological and correlation analyses due to technical problems in EEG recording that compromised EEG data quality. All participants met the inclusion criteria to take part to this study, which were being native Italian speakers, right-handed, having normal or corrected-to-normal visual acuity, having no current or major past neurological or psychiatric disorders, and having no cognitive decline or dementia for the older adults. The Edinburgh Handedness Inventory (Oldfield, 1971) was used to measure participants' handedness. Participants were selected in order to match the two age-groups for years of formal education (younger: M = 13.3 years, SD = 4.24 years; older: M = 14.25 years, SD = 4.28 years; $t(40) = .472$, $p = .726$). Older adults were screened for dementia using the Montreal Cognitive Assessment (MoCA) (Nasreddine et al., 2005) (M = 27, SD = .92, range: [26 29]) and only participants with a score ≥ 26 were included. All the participants signed an informed consent before taking part to the study and were reimbursed € 25 for their time. The study was approved by the SISSA Ethical Committee in Trieste.

2.2.2. Design and stimuli

We used a 4-choice version of the spatial Stroop task, previously used by Puccioni and Vallesi (2012)[2], a cognitive conflict task including both stimulus-stimulus and stimulus-response interference. This task was implemented in Presentation® Software (Neurobehavioral System, Inc., Berkeley, CA) as a priming-free task (by avoiding partial and total feature repetitions in first-order trial sequences to prevent any influence on the performance due to these aspects), in order to explore age-related differences in interference resolution, avoiding possible additional confounds. The stimuli were black arrows pointing toward one of the four diagonal directions roughly corresponding to the corners of the screen and appearing in one of the same four corners of an imaginary 9.5x9.5 cm square centered on the center of the screen (upper-left, upper-right, lower-left, lower-right positions). Specifically, the stimuli were presented less than 5 cm above/below and on the left/right from the center of the screen and participants were asked to try maintaining their gaze at the center of the screen during task execution. The stimuli were presented over a light grey background (RGB: 200, 200, 200) with a black fixation cross at the center of the screen. The target lasted for 500 ms, followed by a blank screen for 2000 ms when it was possible to give the response. Subsequently, it was presented an extra blank screen randomly lasting between 250 and 700 ms that constituted the inter-trial-interval (see Figure 2.1). The stimuli were defined as congruent when position and direction of the arrow matched (e.g., an arrow pointing toward upper-right corner and appearing in the upper-right portion of the screen), and as incongruent when they differed (e.g., an arrow pointing toward upper-right corner but appearing in the lower-left portion of the screen). They were equally divided in congruent and

---

[2] This experimental task entails some features in common with tasks used to investigate the Simon effect, in that the spatial position of the response and that of the stimulus (i.e., the task-irrelevant feature) may or may not correspond. However, differently from the Simon task, in our experimental design the task-relevant feature of the stimuli was spatial in nature (i.e., the arrow direction) and presents a dimension overlap with both the response and the task-irrelevant feature (Kornblum & Stevens, 2002). Moreover, Stroop and Simon tasks can be differentiated by assessing the effect of the task-irrelevant information on response time distribution by means of delta plots (see Pratte, Rouder, Morey, & Feng, 2010). We conducted this analysis and we found that the distribution resembles the one commonly seen for Stroop tasks, which has an opposite pattern compared to the one typical for Simon tasks (see Figure A.1 in Appendix).

incongruent conditions and appeared in a pseudorandom order, so that there were no repetitions of the same position or direction on subsequent trials, to minimize any type of priming.

Participants were instructed to ignore the position where the stimulus appeared and to pay attention to the direction the arrow was pointing at, by pressing the corresponding button on a response pad using index and middle fingers of both hands (the buttons were spatially arranged in a configuration that corresponded to the spatial position of the stimuli). The instructions were as follows: "You are going to see some arrows, which will appear one at a time in one of the four quadrants of the screen. We ask you to press the button of the response pad corresponding to the direction indicated by the arrow. You will need to use the index and middle fingers of both hands. Please, try to respond as fast and accurate as possible". The task consisted of a training phase of 16 trials performed until participants reached 10 correct answers, and a test phase separated in three different blocks each one composed of 2 sub-blocks of 64 stimuli each.

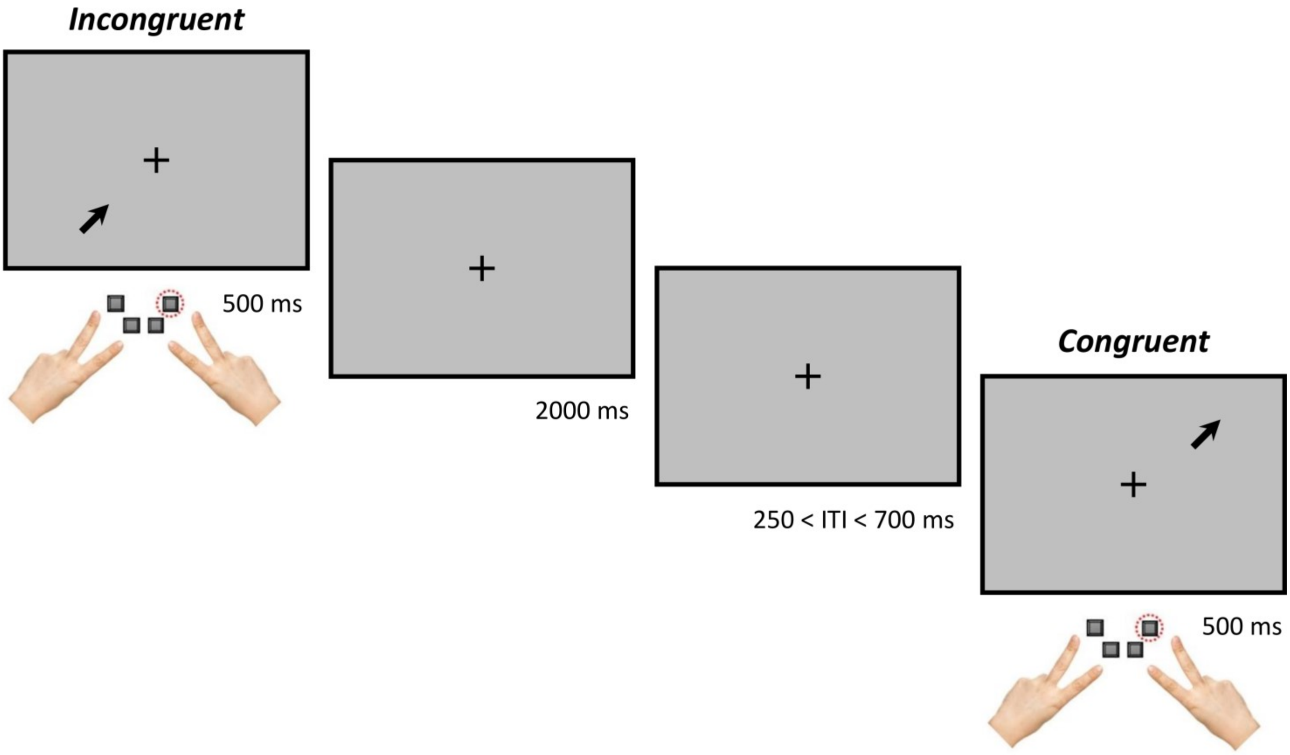

Figure 2.1. Experimental paradigm.

The figure shows an example of the experimental design. Each of the experimental stimuli appeared for 500 ms, followed by a blank screen lasting 2000 ms. The inter-trial-interval appeared as an extra blank screen randomly lasting between 250 and 700 ms. The figure shows an example of incongruent (top left) and congruent (bottom right) trials. Participants were asked to respond by pressing the response button corresponding to the direction indicated by the arrow, while ignoring its spatial position (in the example above, correct responses correspond to the upper-right button and are highlighted by a red dashed circle).

2.2.3. EEG recording

All data were recorded using a Biosemi^{TM} ActiveTwo 128-channel system with sintered Ag/AgCl electrodes. The recording was sampled at 256 Hz and referenced online to the mastoid electrodes. Electrooculographic (EOG) activity was recorded by means of four electrodes placed on right and left external canthi and infra-orbital ridges of each participant. Four additional electrodes were placed on mastoids and peri-auricular areas to record muscular activity. All electrodes were adjusted to maintain their offset below 40 mV and impedance below 10 KΩ.

2.3. Data analysis

2.3.1. Behavioural analysis

Data from error trials and post-error trials (respectively, 3.94% and 3.63% of the experimental trials) were not included in the analysis of response times (RT). RT were log-transformed to improve normality and mitigate the near-multiplicative effects of the general slowing in RT observed in previous aging studies (Cerella, 1990; Faust et al., 1999). Moreover, log-RT above and below two standard deviations (SD) from the mean calculated for each participant and condition were excluded (6.47% of the valid trials). Percentage of accuracy and mean log-RT were analysed using a 2x2 mixed-design ANOVA with trial Congruency (within-subjects) and Age Group (between subjects) as factors. Levene's test confirmed the homogeneity of variances (all $Fs_{(1,40)} < .32$, all $ps > .57$).

2.3.2. Electrophysiological analysis

Offline signal pre-processing was performed using MATLAB (Version R2013b; The MathWorks, Inc., Natick, MA) scripts created ad-hoc based on the functions from the EEGLAB toolbox (version

13.4.4b; Delorme & Makeig, 2004). Raw continuous recordings were filtered offline using a zero-phase Hamming windowed sinc FIR filter (cut-off frequencies: 0.05 and 45 Hz, transition bandwidth: 0.1 and 10 Hz, passband edges: 0.1 and 40 Hz) and subsequently bad channels were detected and removed by means of the clean_rawdata EEGLAB plugin using the Artifact Subspace Reconstruction (ASR; the autocorrelation parameter was set at 0.8, leading to the exclusion of 3.5 channels on average, SD = 4, see Mullen et al., 2013). There was no significant difference in the number of removed channels between younger (M = 3.73, SD = 7.71) and older participants (M = 4.25, SD = 3.19): t(40) = -0.28, p = .78. Data were then segmented into epochs (from -1200 ms to 2700 ms) with respect to the stimulus onset and erroneous trials were excluded from further analyses. Independent component analysis was then applied to correct for eye movements and blinks based on scalp topography, evoked time courses and spectral distribution. Baseline correction from -200 to 0 ms was then used, followed by spherical spline interpolation of bad channels (Perrin, Pernier, Bertrand, & Echallier, 1989). Data were then re-referenced to a common average reference. Detection of artifactual epochs was performed by means of an automatic procedure based on extreme values thresholding (+/- 200 μV) and improbability and kurtosis criteria (SD > 7 for single channel and SD > 3 for global threshold); epochs that violated one or more of these criteria were excluded from further analyses (Delorme, Sejnowski, & Makeig, 2007). The minimum number of epochs used for the analysis was 136 (younger: M = 181 and 172, range = [165 187] and [153 186] for congruent and incongruent trials, respectively; older: M = 176 and 172, range = [170 184] and [136 188] for congruent and incongruent trials, respectively). There was no significant difference between groups and congruency in the number of epochs used for further analysis (F (1,40) = 1.84, p > .18).

We extracted event related spectral perturbation (ERSP) in the frequency range between 4 and 45 Hz (linearly spaced, 1 Hz resolution) using wavelets with a temporal window of approximately 560 ms and corresponding to a linearly increasing number of cycles (from 2 to 22.5 cycles for the 4 and 45 Hz frequencies, respectively); the baseline correction was applied trial by trial using the average power in the time window from 800 to 300 ms before stimulus onset.

Differences in ERSP due to the Stroop effect were tested for statistical significance through the threshold-free cluster-enhancement (TFCE) method, which optimizes the detection of diffuse, low amplitude signal while correcting for multiple comparisons ($p < 0.05$) (Smith & Nichols, 2009). This method was applied on the entire channel-time-frequency space by taking into account all the 128 channels, 200 timepoints covering a time window ranging approximately from -650 ms to 2150 ms (and thus excluding edge artifacts resulting from the wavelet transform and precluding across-trials overlapping of the stimulus-related activity of interest) with a resolution of about 15 ms, and all the 42 frequencies ranging from 4 to 45 Hz. However, in order to facilitate the description of the results, we will refer to the following frequency bands: theta (4-7 Hz), alpha (8-12 Hz), beta1 (13-18 Hz), beta2 (19-24 Hz), beta3 (25-30 Hz), lower gamma (31-45 Hz). This analysis of ERSP at the scalp level was performed to allow for better comparison with previous (e.g., Wang et al., 2014; Zhao et al., 2015) and future studies.

We first assessed the significance of the ERSP Stroop effect in younger and older participants, thus testing for the simple effects of the Congruency factor (incongruent vs. congruent Stroop condition) in each age group. We then assessed whether age significantly modulated the ERSP Stroop effect by contrasting it between younger and older participants. This analysis thus tested for the interaction between Congruency and Group (older vs younger), that is, the effect of primary theoretical interest. Note that we reported the results of the simple effects of the Congruency factor for each age group separately in order to facilitate the interpretation of the interaction between Congruency and Group (older vs younger).

All the results reported in the test were significant at an alpha level of .05 both at the single spatio-temporo-spectral sample level and at the cluster level, thus corresponding to a critical *t* value of ± 2.02 (df = 40).

2.3.3. Distributed source estimation

As detailed in the Introduction (section 2.1), we aimed at shedding light on the contribution of prefrontal functional hemispheric asymmetries in mediating interference resolution processes. To this aim, we estimated the neuronal source of the scalp-based evoked spectral EEG activity using the Brainstorm toolbox (Tadel, Baillet, Mosher, Pantazis, & Leahy, 2011). In particular, we estimated the current strength dynamics of the EEG cortical sources using the depth-weighted minimum norm estimation approach (Baillet et al., 2001) and a boundary element methods (BEM) conductive head model (Gramfort, Papadopoulo, Olivi, & Clerc, 2010; Kybic et al., 2005). The solution space was constrained to the cerebral cortex, which was modelled as a three-dimensional grid of 15002 elementary current dipoles based on the FreeSurfer brain template (FSAverage; see Fischl, Sereno, Tootell, & Dale, 1999). The results were then tested for statistical significance by using again the TFCE method by taking into account all the 15002 vertices, all the 200 original time points, and all the 42 frequencies ranging from 4 to 45 Hz. Therefore, there was no selection of the spatio-temporo-spectral data based on the results of the scalp-level analyses, thus avoiding the circularity problem.

2.3.4. Time-frequency – behaviour correlation analysis

We used Pearson's correlation to test for associations between behavioural and electrophysiological measures. In particular, for each age group, we first computed the correlations between the participants' RT Stroop effect (i.e., the incongruent – congruent difference in RT) and the corresponding ERSP Stroop effect (i.e., the incongruent – congruent difference in the ERSP) in all frequencies, time points, and channels, and assessed their statistical significance using the TFCE method (see section 2.3.2). We then compared the Fisher-transformed correlations in older and younger participants by means of the Fisher's *Z* test and corrected the results for multiple comparisons using the TFCE method. The Fisher's *Z* test is specifically designed to test for statistically significant differences in correlations between two independent groups, thus allowing us to test for age-dependent modulations of the brain-behaviour correlations.

We chose to perform the TFCE mass univariate analyses for the ERSP Stroop effects extracted at the scalp level, instead of those extracted at the source level, because the latter is extremely computationally intensive and time-consuming. In this way, we also hoped to facilitate the comparison between our results and previous and future literature.

2.4. Results

Subject-level behavioural and EEG time-frequency data supporting the conclusions are made available at Open Science Framework (https://osf.io/3wmg4) under a CC-BY 4.0 license, in compliance with the requirements of the funding body (ERC) and the institutional ethics approval.

2.4.1. Behavioural results

Table 2.1 shows descriptive statistics for the behavioural results. On average, participants reported faster RT for congruent trials compared to incongruent trials, as demonstrated by a significant main effect of Congruency ($F_{(1,40)} = 307.49$, $p < .0001$, $\eta^2_p = .88$). There was also a main effect of Group ($F_{(1,40)} = 67.37$, $p < .0001$, $\eta^2_p = .63$) due to older participants showing longer RT than younger controls. The interaction between Congruency and Group was also significant ($F_{(1,40)} = 4.19$, $p = .047$, $\eta^2_p = .09$), meaning that the Stroop effect was higher in the older group as compared to the younger one (see Figure 2.2 A; see also 2.2 C for results on untransformed RTs).

Concerning accuracy (see Figure 2.2 B), the ANOVA revealed a significant main effect of trial Congruency only, so that a higher percentage of correct responses was given for congruent trials ($F_{(1,40)} = 46.23$, $p < .0001$, $\eta^2_p = .54$). Accuracy did not significantly differ between groups ($F_{(1,40)} = 0.21$, $p = .65$, $\eta^2_p < .01$) and the interaction was not significant ($F_{(1,40)} = 0.04$, $p = .83$, $\eta^2_p < .01$). Note that the results did not change when performing non-parametric analyses.

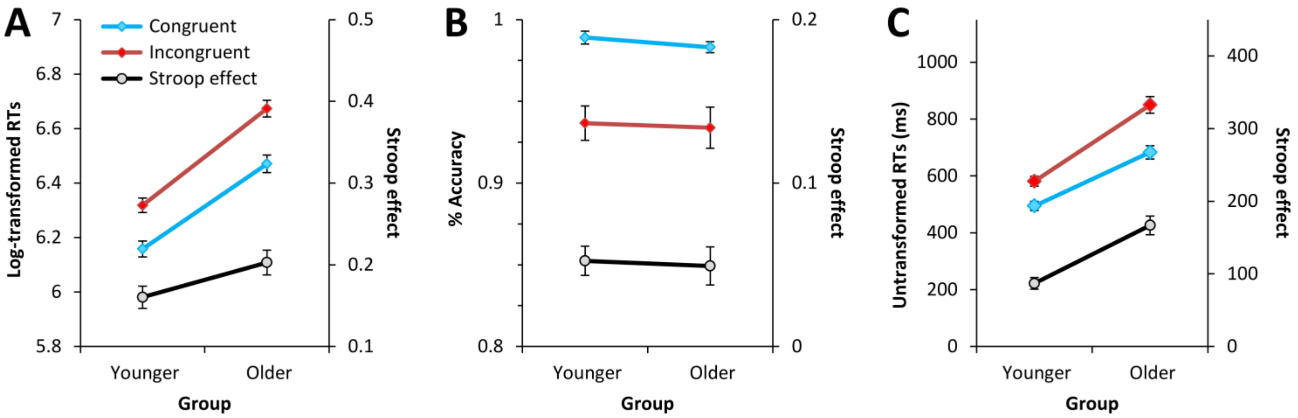

Figure 2.2. Behavioural results.
The figure shows results for log-transformed RT (A), accuracy (B), and untransformed RT (C) as a function of the age Group (x axis) and Congruency factors. The dark red line corresponds to the incongruent trials, and the light blue one to the congruent ones (left y axis). Black lines represent the Stroop effect (i.e., the Incongruent – Congruent difference; right y axis). Error bars indicate standard errors of the mean.

Table 2.1. Descriptive statistics for behavioural results.

	Congruent		**Incongruent**		**Stroop effect**	
	M	*SD*	*M*	*SD*	*M*	*SD*
Log-transformed RT						
Younger	6.158	0.136	6.318	0.126	0.160	0.064
Older	6.470	0.144	6.673	0.138	0.203	0.071
Untransformed RT (ms)						
Younger	494	78	581	81	87	38
Older	683	106	850	131	167	60
Accuracy (%)						
Younger	98.9	1.8	93.7	4.9	5.2	4.2
Older	98.3	1.5	93.4	5.6	4.9	5.5

2.4.2. Scalp-based time-frequency results

The analysis on younger participants revealed a number of significant ERSP Stroop effects mainly involving beta frequencies over parieto-occipital and frontal channels and gamma frequencies over centro-parietal channels in relatively early time windows (see Figure 2.3 A). Specifically, a first cluster showing significant ERSP Stroop effects in the beta2 range was observed over frontal channels, with a slight left lateralization, in a time window approximately ranging from 350 to 950 ms (see Figures 2.3 A and 2.4 A, B). A second cluster involving beta2 frequencies was observed over centro-parietal and parieto-occipital channels, again with a slight left lateralization. However, this posterior effect was temporally and spectrally less specific. Indeed, in this case the ERSP Stroop effect in the beta2 band was earlier and more sustained and it also involved surrounding beta1, beta3, and gamma frequency bands, as well as alpha frequencies over centro-parietal channels in a later time window starting approximately at 1000 ms (see Figure 2.3 A). All these effects were due to a stronger event-related decrease in power for incongruent condition as compared to the congruent one. We also observed a third independent, small cluster involving theta frequencies over left parietal channels in an early time window approximately ranging from 250 to 450 ms. This effect was due to a stronger event-related increase in theta power for congruent as compared to incongruent condition.

The analysis on older participants revealed a pattern of significant ERSP Stroop effects that also involved mainly beta and gamma frequencies, but that was less specific both spatially and temporally (see Figure 2.3 B). Specifically, a first large cluster showing significant ERSP Stroop effects in the beta and gamma frequencies was observed over most of the scalp, with the exclusion of lateral frontal and fronto-temporal channels, in a time window that mainly ranged from 600 to 1400 ms but also included later samples (see Figures 2.3 B and 2.4 C, D). As for younger participants, these effects were due to a stronger event-related decrease in power for the incongruent condition with respect to the congruent one. We also observed a second, partially independent, small cluster involving theta frequencies over bilateral posterior channels in an early time window approximately ranging from 0 to 1200 ms, which also involved alpha frequencies in a later time window (from 750 to 1200 ms). This effect was due to a stronger event-related increase in theta power for the congruent condition as compared to the incongruent one.

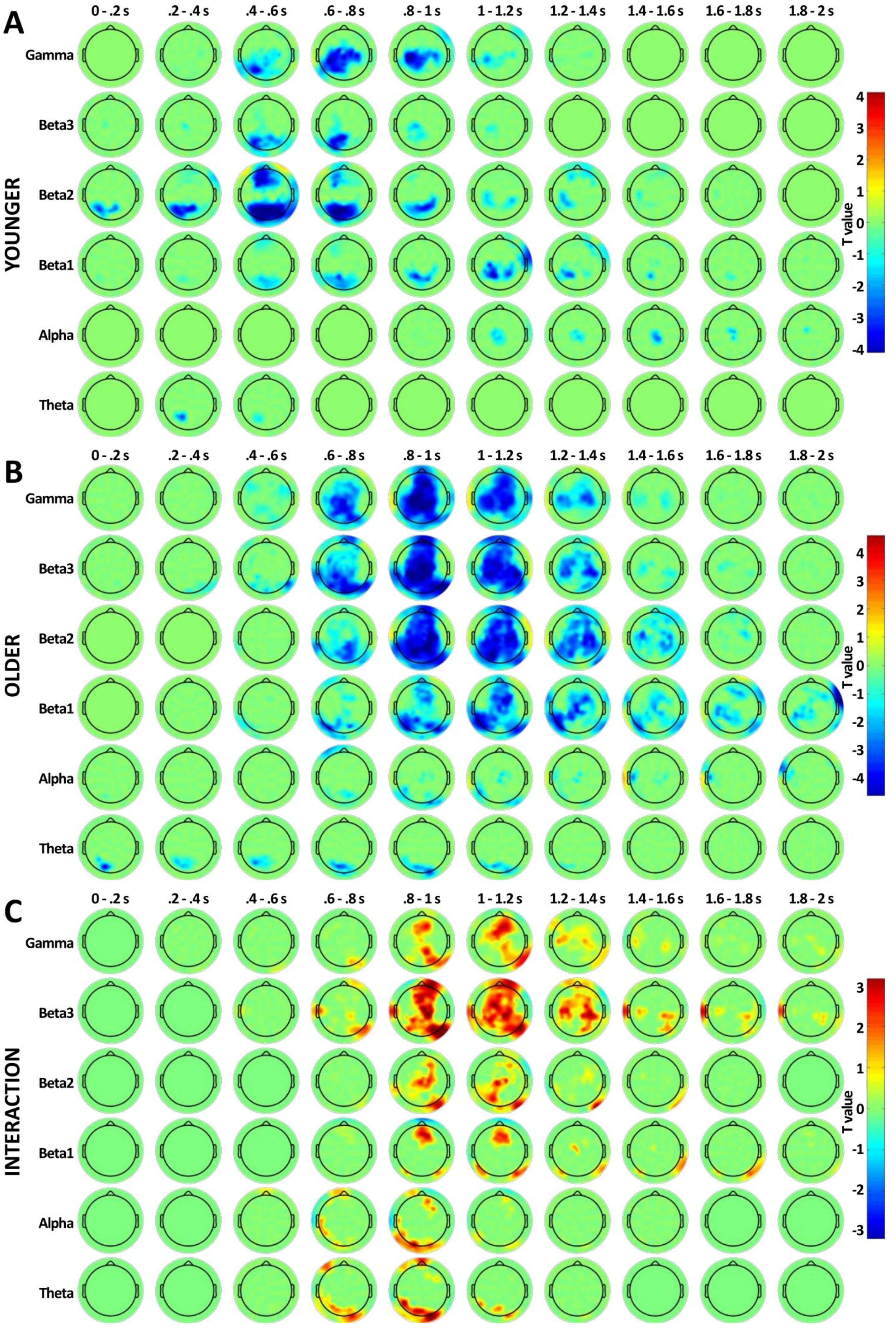
A
B
C
YOUNGER
OLDER
INTERACTION
0 - .2 s
.2 - .4 s
.4 - .6 s
.6 - .8 s
.8 - 1 s
1 - 1.2 s
1.2 - 1.4 s
1.4 - 1.6 s
1.6 - 1.8 s
1.8 - 2 s
Gamma
Beta3
Beta2
Beta1
Alpha
Theta
T value
4
3
2
1
0
-1
-2
-3
-4

Figure 2.3. Results of the scalp-based event-related spectral perturbation (ERSP) analysis.
The figure shows the topoplots for the results of simple effect analysis in younger (A) and older (B) participants, as well as the results of the interaction analysis (C). Each row represents the average of each frequency band, whereas the columns represents the average of EEG activity every 200 ms after stimulus presentation (time 0). The topoplots show the *t values* of the significant results after TFCE. Younger participants' results evidenced a major involvement of higher frequencies range and in particular of beta2. In this band, the activity arose after stimulus presentation from posterior regions and it moved anteriorly showing a left lateralization during the time period preceding the response (400-600 ms). For older participants, higher frequencies bands, from beta1 to gamma, were mostly involved. The activity occurred around the response time (600-800 ms) and involved channels spread all over the scalp. These differences were reflected in the topoplots for the interaction analysis.

These analyses indicate the existence of age-dependent modulations of ERSP Stroop effects, as older participants showed later and more widespread and unspecific spectral correlates of interference resolution processes. This pattern was confirmed by the analysis contrasting the ERSP Stroop effects between younger and older participants, which showed a number of significant age-dependent modulations of ERSP Stroop effects mainly involving higher frequencies (>12 Hz) over parietal and frontal channels and lower frequencies (<12 Hz) over parieto-occipital channels in a time windows ranging from 600 to 1200 ms (see Figure 2.3 C). Overall, this pattern of results closely resembles that observed for the simple effect analysis on older participants. Specifically, a first large cluster showing significant ERSP Stroop effects in the beta and gamma frequencies was observed across a number of electrodes spread over the scalp in a time window that mainly ranged from 600 to 1400 ms but also included later samples (see Figures 2.3 and 2.4 A, B). These effects were characterized by stronger ERSP Stroop effects in older as compared to younger participants. Specifically, this pattern of results was due to the fact that in older participants, as compared to younger ones, the stronger event-related decrease in power for the incongruent condition was more pronounced over central electrodes and, generally, involved a higher number of frequencies over a higher number of channels in a later and more sustained time window. In particular, while the event-related decrease in beta power occurred at around the same time for both age groups and congruency conditions, the decrease in beta power for incongruent as compared to congruent condition was more sustained for older participants. Consequently, the ERSP Stroop effect occurred later ad was more sustained in this age group.

We also observed a second cluster involving theta and alpha frequencies over bilateral posterior channels in an earlier time window approximately ranging from 600 to 1200 ms (see Figures 2.3 and 2.4 C, D). This effect was due to the fact that in older participants, as compared to younger ones, there was a stronger event-related increase in low-frequency power for the congruent condition as compared to the incongruent one.

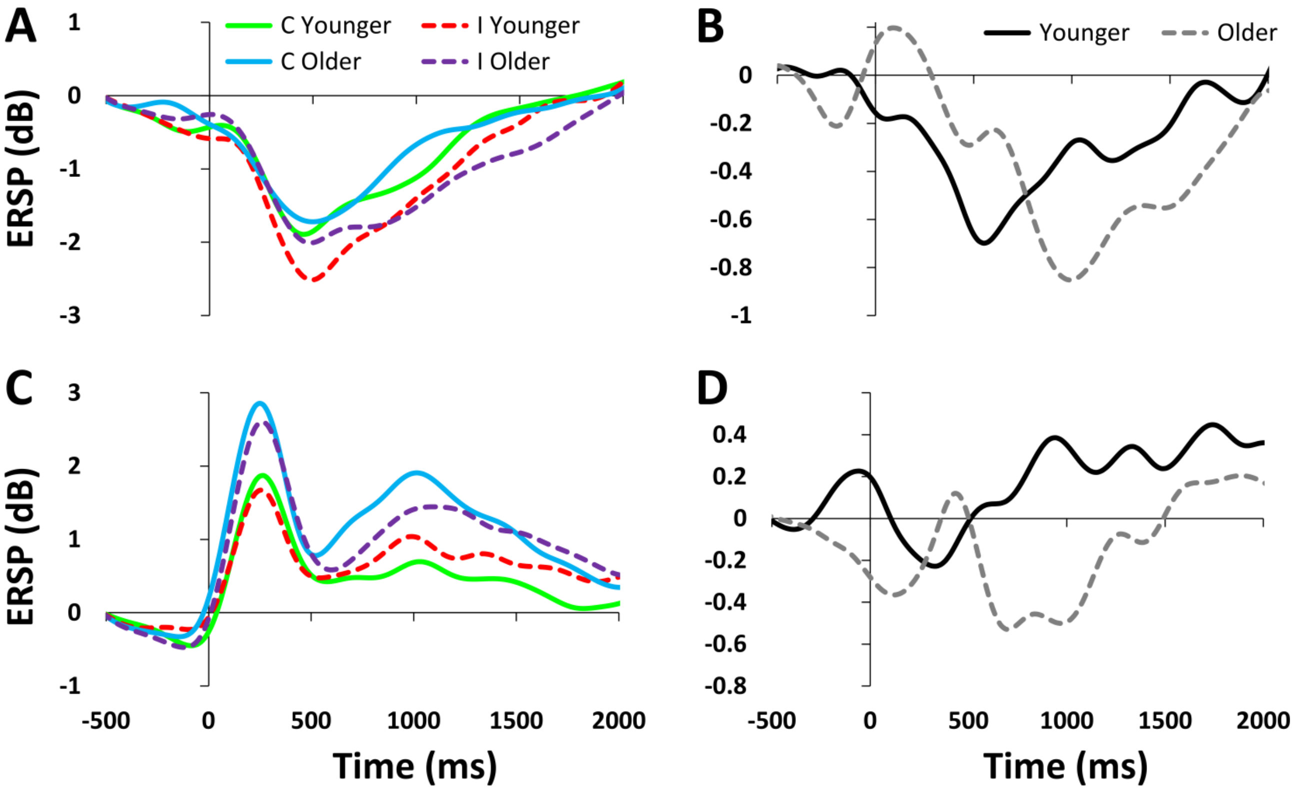

Figure 2.4. Representative results from scalp-based ERSP analysis.
The plots show the ERSP traces for the results of simple effect analysis in younger and older participants for the beta (A) and theta (C) bands, as well as the results of the interaction analysis for the same frequencies (respectively, B and D). The plots in (A) and (B) depicts representative data for a frequency in the beta2 band (20 Hz) extracted from a channel in the mid-frontal cluster (Fz), while the plots in (C) and (D) depicts representative data for a frequency in the theta band (7 Hz) extracted from a channel in the posterior cluster (POz) (see text for details).

To sum up, results from the interaction between Congruency and Group revealed significant effects in all the frequency bands taken into account for this study, which were driven by the ERSP Stroop effects observed in the group of older participants. Overall, higher frequencies, from beta to gamma, seem to be especially involved in interference resolution processes, as summarized in Figure 2.3. Importantly, younger participants mainly engaged frequencies in the beta2 range, with Stroop-dependent modulations starting soon after stimulus presentation on posterior regions and gradually moving over left frontal electrodes, until the time window close to the response. Older participants mainly recruited all the frequencies higher than 12 Hz (from beta1 to gamma bands), and this activity started around the time window of the response engaging electrodes spread over the scalp. For these frequencies and for both groups, incongruent trials yielded a stronger power suppression as compared to the congruent ones.

Regarding the theta band, the scalp-based ERSP analysis showed an unexpected pattern of age-dependent results: a greater increase of power was observed for the congruent condition over posterior channels, while no age-dependent power increase was observed for the incongruent condition over mid-frontal channels, contrary to what we hypothesized (see section 2.1).

2.4.3. Source-based time-frequency results

We computed ERSP data based on the reconstructed cortical sources of electrophysiological activity and performed the same TFCE analysis as for scalp-based ERSP data. The analysis revealed a very high number of significant age-dependent modulations of the ERSP Stroop effects. However, for the sake of conciseness and readability, we reported here only the results for the two spectral bands for which we had strong a-priori hypotheses about their cortical localization, as detailed in the section 2.1: 1) the theta band, for which a large body of evidence suggests the involvement of the medial prefrontal cortex in signalling the need for cognitive control, and 2) the beta2 band, for which we expected to find evidence for the involvement of the DLPFC in mediating interference resolution processes, with a particular interest in assessing possible hemispheric asymmetries.

As regards the theta band, the Group by Congruency interaction was significant in a time window from around 200 ms to 600 ms over bilateral and medial dorsal frontal regions, where cortical sources showed a stronger incongruency-dependent power increase for younger as compared to older participants. This result was mainly due to an earlier and stronger ERSP Stroop effect in younger participants as compared to older ones. Indeed, simple effect analysis showed that younger participants exhibited a significant incongruency-dependent power increase starting from 200 ms mainly involving bilateral dorsolateral and dorsomedial prefrontal regions. By contrast, the same power modulation was almost absent in older participants (Figure 2.5 A)[3].

The results for the beta2 band generally confirmed the impressions derived from the corresponding scalp-based analysis. Indeed, the Group by Congruency interaction was significant in a temporal window from around 600 ms to 2000 ms over bilateral dorsal frontal and parietal regions, where cortical sources showed a stronger incongruency-dependent power decrease for the older group as compared to the younger one. Again, this result was mainly due to a later and more widespread ERSP Stroop effect in older participants as compared to younger ones. Indeed, simple effect analysis showed that younger participants exhibited a significant incongruency-dependent power decrease starting from approximately 300 ms with a clear left prefrontal lateralization involving the middle and superior frontal gyri. By contrast, older participants did not show significant incongruency-dependent power modulations until around 600 ms, which originated in bilateral medial parietal regions and then rapidly spread over extended portions of bilateral dorsal frontal and parietal cortices, lasting even after the power modulation in younger participants disappeared (Figure 2.5 B).

---

[3] We think that this result is not associated to the theta-related effect that we observed in the scalp-based analysis over posterior channels. Indeed, the cortical distribution of the sources showing the significant theta-related effects is hardly consistent with the scalp distribution of the channels showing the significant theta-related effects. Moreover, the scalp-based and the source-based theta effects also have opposite pattern of power increase as regards the experimental conditions, as a greater increase of power was observed for the congruent and incongruent conditions, respectively, in the two analyses.

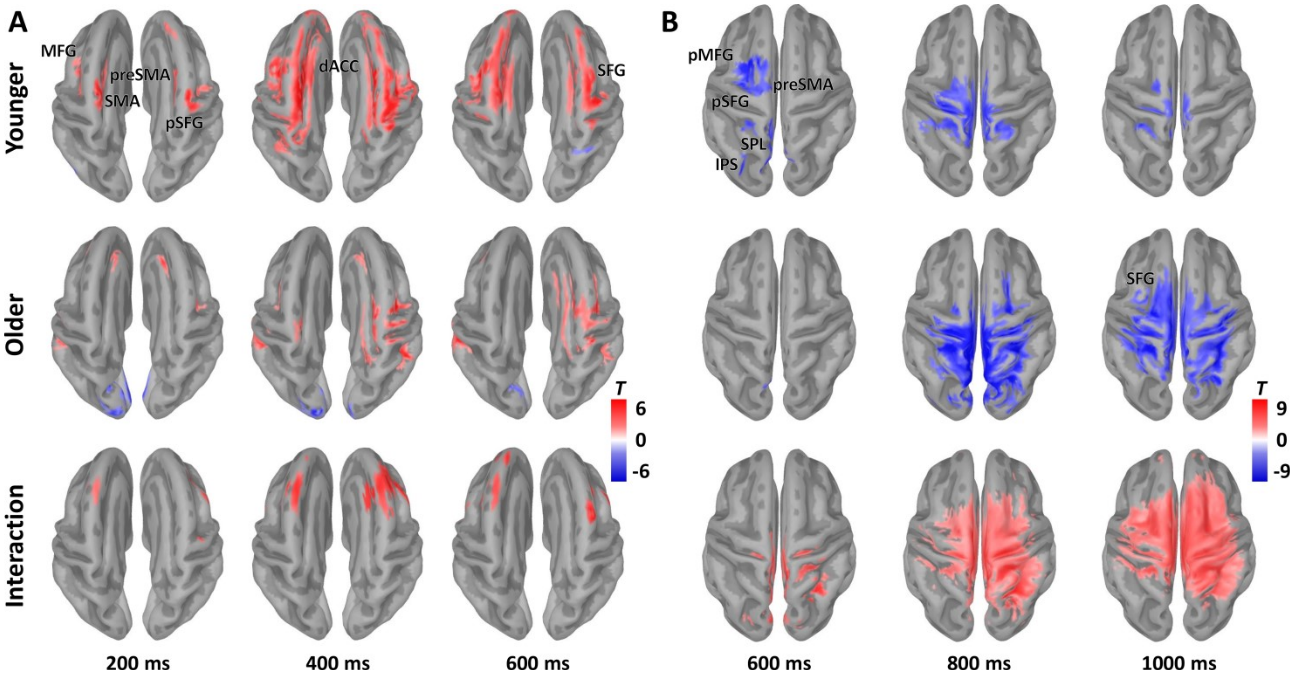

Figure 2.5. Results of the source-based ERSP analysis.

The figure shows the cortical distribution for the results of the source-based analysis contrasting incongruent and congruent conditions in younger and older participants for the theta (A) and beta2 (B) frequencies. For illustrative purposes, results for the 5 Hz (A) and 20 Hz (B) frequencies are shown at three representative time points (columns). The topoplots show the *t* values of the significant results. dACC, dorsal anterior cingulate cortex; IPS, intraparietal sulcus; MFG, middle frontal gyrus; pMFG, posterior part of the middle frontal gyrus; preSMA, pre-supplementary motor area; pSFG, posterior part of the superior frontal gyrus; SFG, superior frontal gyrus; SMA, supplementary motor area.

2.4.4. Brain-behaviour correlations

We assessed the significance of the correlations between RT and ERSP Stroop effects over the entire channel-time-frequency space in each age group. We also investigated whether age significantly modulated these brain-behaviour correlations (interaction analysis testing for age-dependent differences in slope). All the results were corrected for multiple comparisons using TFCE method. Still, the interaction analysis revealed a very high number of significant results involving all the frequency bands and generally indicating opposite patterns of brain-behaviour correlations for younger and older participants, with the former showing positive correlation, so that smaller congruency-dependent power differences were related to a better Stroop performance, and the latter showing negative correlations. We reported here only the clusters that were significant in this interaction analysis and in (at least) one of the simple correlation analyses for each group. Moreover, for the sake of brevity, we reported in the text only the results for the first 1000 ms after stimulus presentation, a time window that includes approximately 90% and 99% of the valid RT for older and younger participants, respectively.

A first cluster showing significant age-dependent modulations of the brain-behaviour correlations involved theta and lower alpha frequencies and was distributed over mid-frontal channels in a time window approximately ranging from 150 to 550 ms (see Figure 2.6). This effect was explained by the fact that, while older participants' ERSP Stroop effects did not significantly explain their behavioural performance, younger participants showed significant positive correlations between RT and ERSP Stroop effects (see Figure 2.7 A). Specifically, younger participants exhibiting a larger behavioural Stroop effect also showed a larger, positive ERSP Stroop effect, that is, greater event-related increases in theta and lower alpha frequencies for the incongruent condition as compared to the congruent one. Similar age-dependent modulations of brain-behaviour correlations – with significant positive correlations between RT and ERSP Stroop effects for younger participants – were found in other partially independent clusters that either involved the same frequencies, but at later time windows and over different scalp locations, or involved beta1 frequencies in an earlier time window (0-300 ms) over left and right centro-temporal channels. Another set of clusters showing a similar age-dependent modulation of the brain-behaviour correlations involved higher frequencies (i.e., >18 Hz) in later time windows (approximately starting from 600 ms) over right parietal and left frontal channels (see Figure 2.6).

Moreover, the analyses also revealed a cluster of significant age-dependent modulations of the brain-behaviour correlations that showed the opposite pattern of results. Indeed, in this cluster, the significant age-dependent modulations were due to the fact that older participants showed significant negative correlations between RT and ERSP Stroop effects, while younger participants showed non-significant correlations (with an opposite trend). This cluster involved beta and gamma frequencies and was distributed over left parieto-temporal channels in a time window starting from 450 ms (see Figures 2.6 and 2.7 A) and, limited to beta1 and beta2 frequencies, over left frontal and central channels in an earlier time window approximately ranging from 350 to 600 ms (see Figure

2.6). Despite the spatio-temporal distribution of these correlations in the beta-gamma frequencies is different from that observed in the scalp-based ERSP analyses described above (cf. Figure 2.3 and 2.6), it should be noted that the ERSP traces corresponding to these correlations show the same pattern, with a larger power suppression for the incongruent as compared to the congruent condition. Moreover, the pattern of correlations for the age-dependent ERSP effect in the beta band (20 Hz) over Fz described above (see section 2.4.2 and Figure 2.4) is the same as that described here (see Figure 2.7 B) in a time window ranging from 750 to 900 ms, with older and younger participants showing, respectively, negative and positive correlations between RT and ERSP Stroop effects (*Z*s > 2.02, *p*s < .05).

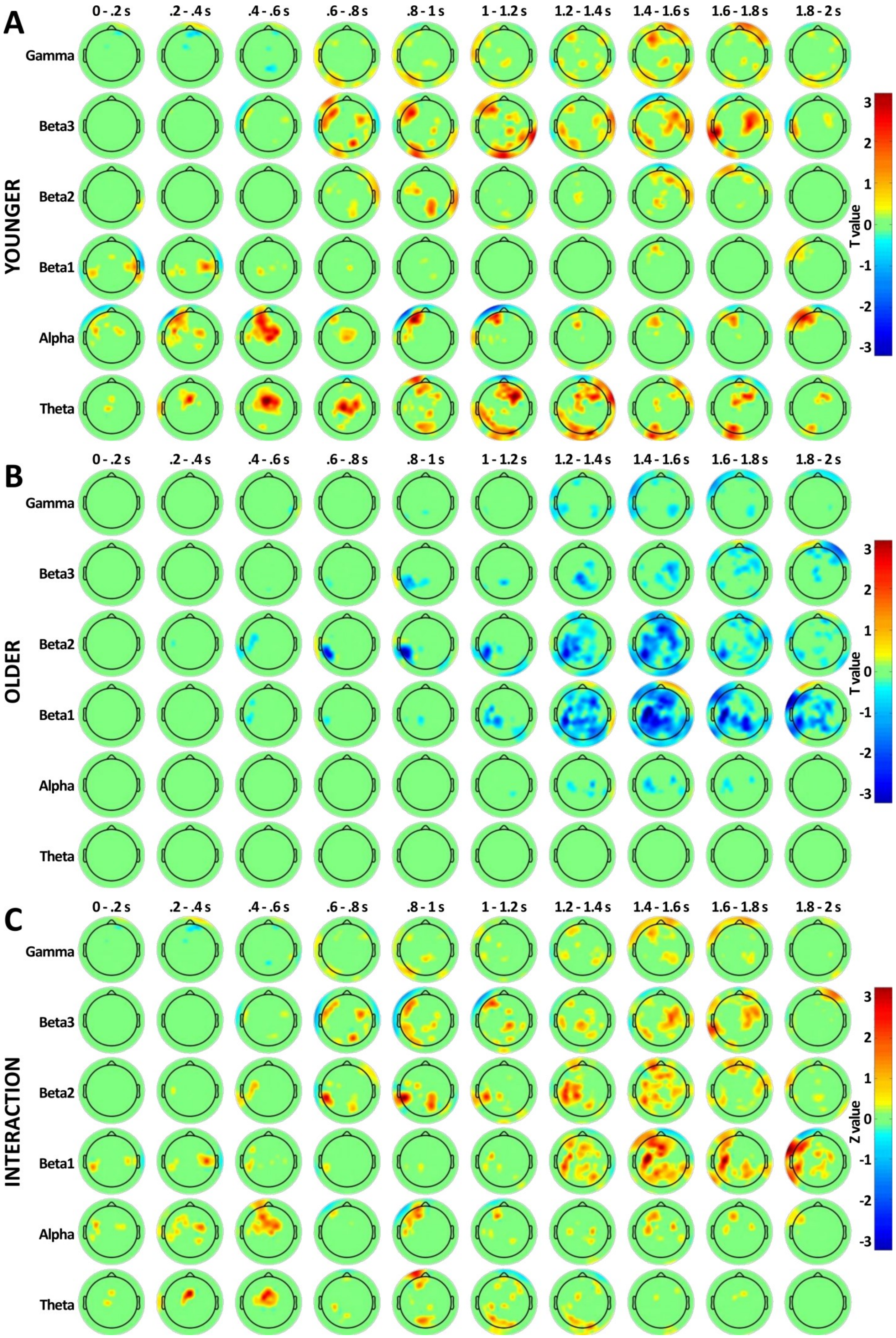
A
YOUNGER
B
OLDER
C
INTERACTION
0 - .2 s
.2 - .4 s
.4 - .6 s
.6 - .8 s
.8 - 1 s
1 - 1.2 s
1.2 - 1.4 s
1.4 - 1.6 s
1.6 - 1.8 s
1.8 - 2 s
Gamma
Beta3
Beta2
Beta1
Alpha
Theta
T value
Z value
3
2
1
0
-1
-2
-3

Figure 2.6. Brain-behaviour correlation results.

The figure shows the topoplots for the results of the brain-behaviour correlation analysis. Specifically, results are shown for the simple effect analysis in younger (A) and older (B) participants, as well as for the interaction analysis (C). Each row represents the average of each frequency band, whereas the columns represent the average of EEG activity every 200 ms after stimulus presentation (time 0). The topoplots show the *t values* of the significant results after TFCE.

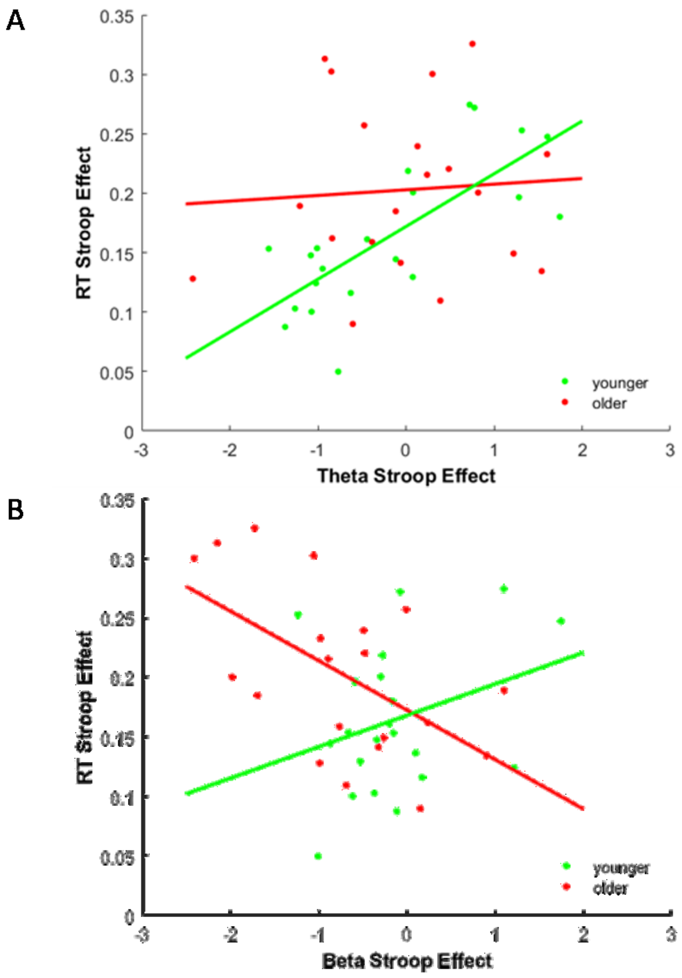

Figure 2.7. Representative results of the brain-behaviour correlation analysis.

The scatterplots show the correlation between the behavioural Stroop effect (*y* axis) and the ERSP Stroop effect for the younger and older groups (light green and red points, respectively; regression lines are also shown in the same colours). The scatterplot in A depicts representative data for a frequency in the theta band (7 Hz) extracted from a channel in the mid-frontal cluster (FCz) at 500 ms, for which the brain behaviour correlation was significantly different between the two age groups (*Z* = 3.46, *p* < .001). The scatterplot in B depicts representative data for a frequency in the beta2 band (20 Hz) extracted from a channel in the left parieto-temporal cluster (near T7) at 850 ms, for which the brain behaviour correlation was significantly different between the two age groups (*Z* = 3.70, *p* < .001) (see text for details).

2.5. Discussion

In this study, we investigated the spectral correlates of interference resolution and their age-related differences. To this purpose, we recorded EEG activity from two age groups and analysed time-frequency dynamics, estimating the underlying neural sources. Furthermore, we also aimed at testing the hypothesis that this cognitive process relies on the left portion of PFC, as suggested by previous studies (Stuss & Alexander, 2007).

Our results revealed a main role of beta2 frequencies (19-24 Hz) and left PFC in younger participants, which may underlie the process of selecting task-relevant representations during interference resolution. We found clear age-related differences, since older participants showed a delayed (600-800 ms) over-recruitment of higher frequencies bands (from beta1 to gamma) with bilateral brain areas involved. The main finding from the correlation analysis concerned a positive correlation between RT and midfrontal theta that was present for the younger participants only and that, according to previous literature, can be considered as a signal for the need for cognitive control (Cavanagh & Frank, 2014).

In terms of behavioural analysis, we found that all participants showed longer RT and lower accuracy in responding to incongruent trials. Moreover, older participants showed a general trend in responding more slowly to both types of trials, but they did not show any difference in accuracy as compared to younger participants. These results are in line with general slowing accounts, which proposed that older adults are slower in responding especially when the task requires to select a stimulus (i.e., ink colour/arrow direction) over a more dominantly represented one (i.e., word reading/arrow position), as in the case of Stroop paradigms (Salthouse, 1996; Verhaeghen & De Meersman, 1998). However, older adults also displayed a stronger Stroop effect for RT when compared to the younger group, which indicated that they are even slower in responding to the incongruent trials and more subjected to cognitive interference. Note that the logarithmic transformation we applied on RT mitigates the near-multiplicative slowing effects commonly observed in aging research (Cerella, 1990; Faust, Balota, Spieler, & Ferraro, 1999). Based on this evidence, together with our electrophysiological results, we suggest that slowing of processing speed is not the only explanation for the age-related difference in Stroop performance.

At the electrophysiological level, we found a major event-related modulation of beta2 (19-24 Hz) frequencies in the younger group, which was localized on prefrontal regions in a relatively early time window (400-600 ms). When we examined the power time series, we found a stronger suppression of these frequencies for incongruent trials compared to congruent ones. By contrast, the pattern for older participants revealed a later, widespread modulation involving all beta (13-30 Hz) and gamma (31-45 Hz) frequencies on most electrodes spread over the scalp. In particular, the ERSP Stroop effect for older adults was evident in a later time window for these frequencies and channels due to a more sustained power suppression for incongruent trials. In line with the dedifferentiation theories of aging (Reuter-Lorenz & Park, 2014), we propose that this pattern of age-related differences may indicate that prefrontal beta2 frequencies would be specifically implicated in interference resolution processing but, at an older age, this specificity is lost, and other frequency bands and cortical regions are additionally recruited.

In the light of recent works posing attention on the cognitive meaning of beta frequencies, we interpreted our beta band activation as a cognitive marker of interference resolution, probably involved in the selection of task-relevant representation (Antzoulatos & Miller, 2016; Spitzer & Haegens, 2017). Previous functional magnetic resonance imaging (fMRI) studies using Stroop paradigms reported evidence compatible with this hypothesis suggesting that conflict resolution is achieved thorough a mechanism involving the amplification of task-relevant representations (Banich, 2009; Egner & Hirsch, 2005). Indeed, according to our source results, the incongruency-dependent beta2 power modulations seem to be generated especially from posterior portions of the left middle and superior frontal gyri (pMFG, pSFG) engaged after stimulus presentation. This is in agreement with the model proposed by Banich (2009) where the middle portion of DLPFC is recruited to bias the selection of the relevant representations. Moreover, our results from younger participants confirmed previous findings suggesting that left prefrontal cortex mediates interference resolution through the process of selection of task-relevant rules (Derrfuss, Brass, Neumann, & von Cramon, 2005; Stuss, 2011; Stuss & Alexander, 2007; Vallesi, 2012). They are also in line with those of a previous study linking beta band activity on MFG, and in particular its left lateralization, with Stroop performance (Ambrosini & Vallesi, 2017). Indeed, the authors reported that a stronger left lateralization of prefrontal beta spectral activity at rest correlated with a smaller Stroop effect and better capacity to resist to the interference.

Albeit we cannot exclude that motor processes contributed to explain our results involving beta band, we think that they could not be just explained as mere correlates of motor outcomes. First, we found the power suppression mainly on the left hemisphere, despite the task required a bimanual response, and the results from the source estimation did not show involvement of the primary hand motor areas. Second, despite we did not perform response-locked ERSP analyses, the pattern of the event-related decrease in high frequency power is not compatible with the pattern of RT. Indeed, despite older participants' RT were slower in both conditions, and especially in the incongruent one (see Figure 2.2), the maximum decrease in beta power was observed at around the same time for both age groups and for both congruent and incongruent trials. Rather, the decrease in beta power for incongruent as compared to congruent condition was more sustained for older participants, causing the ERSP Stroop effect to occur later in this age group (see Figure 2.4 A, B). Third, even if we assume that the temporal differences in the ERSP Stroop effects between the two age groups could be explained by the RT slowing shown by older participants, this can hardly explain the age-dependent spatial and spectral over-recruitment we found. Fourth, the suppression of beta (15-30 Hz) power that is usually observed before and during the execution of voluntary movements should be: 1) accompanied by a similar suppression of mu (8-14 Hz) power and 2) followed by the so-called beta rebound, a post-movement increase in beta power (Jurkiewicz, Gaetz, Bostan, & Cheyne, 2006). However, no beta rebound was evident in our data (see Figure 2.4 A) and the frequencies in the mu band showed an event-related increase in power, rather than suppression, especially in younger participants (see Figure 2.3). This is also in line with evidence suggesting that beta frequencies are not only involved in low-level motor mechanisms, but they can represent an online mechanism of response selection (Van Wijk, Daffertshofer, Roach, & Praamstra, 2008).

Indeed, concerning the results for older adults, we found an over-recruitment of beta and gamma bands. Specifically, the source-based ERSP analysis revealed that older participants showed a more widespread ERSP Stroop effect in the beta2 frequencies, as compared to younger ones, which involved extended portions of bilateral dorsal frontal and parietal cortices without any sign of hemispheric asymmetry. This result is consistent with other studies reporting an age-related overactivation and reduction in hemispheric specialization, or a general dedifferentiation of neural processing (Cabeza, 2002; Goh, 2011; Park & Reuter-Lorenz, 2009; Reuter-Lorenz & Park, 2014). To specifically select task-relevant information and ignore irrelevant and dominantly represented one, as required in the Stroop task, is a demanding function. Therefore, it is possible that, with aging, a restricted spectrum of frequencies (such as beta2 for younger participants) may be no longer enough to carry out this function, and that it may be necessary to recruit more electrophysiological resources in terms of both frequencies and neural sources. Moreover, older participants not only showed a spectral and spatial over-recruitment of neural resources, but also a more sustained power suppression for incongruent trials. Again, these results seem to be in line with theories suggesting that aging is related to a so-called dedifferentiation (Reuter-Lorenz & Park, 2010, 2014). Finally, the recruitment of medial portions of the frontal cortex (i.e., dACC) in older participants is also consistent with this idea, as well as with the predictions of the Cascade of Control model (Banich, 2009) and with findings of older adults showing increased activity in the cingulate cortex during a Stroop task (Milham et al., 2002). Indeed, some authors interpreted similar results also in vein of the DMC model (Braver, 2012; Braver et al., 2007), proposing that the impairments reported in older adults may be due to a decline in the ability of maintaining task-goals in a sustained manner (i.e., proactive control), which in turn causes a main use of on-demand control mechanisms (i.e., reactive control; Paxton et al., 2007). In light of all these findings, our results can be considered as further evidence that also oscillatory dynamics are sensitive to age and may reflect the changes in the use of different cognitive control modes.

The source-based time-frequency analysis also showed age-dependent differences in theta ERSP Stroop effects over dorsomedial and dorsolateral prefrontal cortices for younger as compared to older participants, for whom this effect was virtually absent. Even if this result was not reflected in the scalp-based analysis, it indicates an age-dependent impairment of the theta-related mechanism signalling the need of cognitive control, that is, an early process that, based on the current contextual information, signals that cognitive control processes are needed to cope with the Stroop interference. This interpretation is in line with a large body of findings suggesting that midfrontal theta activity may be a marker that signals the need for cognitive control (Cavanagh & Frank, 2014; Cohen, 2014; Nigbur et al., 2011; Sauseng et al., 2010). Moreover, we also found an age-dependent difference in the correlation between the Stroop effect in RT and the one in theta power over midfrontal regions as soon as 150 ms after stimulus presentation, which emerged from interaction results but was due to younger participants only. Indeed, younger participants exhibiting a larger behavioural Stroop effect also showed a larger, positive ERSP Stroop effect. Indeed, for this group we found greater event-related increases in theta (and lower alpha) frequencies for the incongruent condition as compared to the congruent one, and this correlation was significantly different from the non-significant one observed in older participants (Figure 2.7 A). Given the proposed role of midfrontal theta as a marker for the need of cognitive control (Cavanagh & Frank, 2014; Cohen, 2014), our results for the theta frequencies would suggest that this function may change during the adult lifespan. Finally, these results are in line with recent findings showing that older adults are less capable to detect interference than the younger ones, as evidenced by a decrease in mid-frontal theta power effects, and thus lack early interference detection signals (Ferreira, Maraver, Hanslmayr, & Bajo, 2019).

2.6. Conclusions

To the best of our knowledge, this is the first study investigating oscillatory dynamics in spatial conflict processing with groups of different ages. Our results highlighted that, during the adult lifespan, neural oscillations show age differences mainly reflected in the impairment of theta-related cognitive processes signalling the need of control and an over-recruitment over frequencies and brain areas. This evidence can be in line also with studies showing age-related decline in the earlier cognitive mechanisms needed to solve interference. Indeed, we hypothesized that these age-dependent differences may contribute to the decline commonly observed in cognitive aging. Of course, this interpretation should be corroborated with a longitudinal approach. Future studies should also address the issue of causal involvement of specific neural correlates in interference resolution process, for example, through neurostimulation techniques. Shedding light on these mechanisms would also help designing neuromodulation therapies for clinical population and reducing the cognitive decline observed in healthy aging.

Chapter 3
Tracking proactive and reactive control in interference resolution

3.1. Introduction

As highlighted in previous sections, cognitive control is one of the most important abilities that characterize human beings, contributing to our capacity of adapting behaviours in a context-dependent fashion (Miller & Cohen, 2001). Cognitive control plays a key role in all the high-order cognitive processes, such as decision-making, planning, and problem solving, among others, and this makes it important to understand how this ability is exerted and how it is modulated according to task demands. Despite the large interest in studying cognitive control, a unifying framework of how it works, and what are the underlying mechanisms involved in it, is still matter of debate. In Chapter 1 (see section 1.3), we introduced the DMC model (Braver, 2012; Braver et al., 2007), proposing that cognitive control may work through two different modes, the proactive and the reactive control. Even though the model suggests that these two modes entail different temporal dynamics, because proactive control works anticipating the interference and reactive control works in an on-demand manner, the precise mechanisms involved by these two modes to solve interference are still not clear. For this reason, in the present study we aimed at tackling this issue, focussing on how the different temporal dynamics of proactive and reactive control can influence the cascade of processes needed to solve interference. As previously stated, the Stroop task (Stroop, 1935) is one of the preferred and most suitable paradigms to investigate interference resolution processing.

Moreover, as we have previously mentioned in Chapter 1 (see section 1.4), different studies showed that cognitive control can be modulated through the manipulation of the proportion of congruent and incongruent trials (proportion congruency, PC; Logan & Zbrodoff, 1979). Importantly, PC can be manipulated at different levels (i.e., list-wide and item-specific levels) and these manipulations are hypothesized to elicit different mechanisms underlying cognitive control. On one hand, for the list-wide manipulation (LWPC), cognitive interference (i.e., the Stroop effect) is reduced when the majority of the trials in a block are incongruent compared to mostly congruent blocks or blocks with an equal number of congruent and incongruent trials; on the other hand, for the item-specific manipulation (ISPC), cognitive interference is reduced for items presented mainly as incongruent within a single block, despite an equal total percentage of congruent and incongruent trials (Gonthier et al., 2016; Jacoby et al., 2003; Lindsay & Jacoby, 1994). These findings are also in line with theories proposing that cognitive control may work through two different components, as hypothesized in the DMC model proposed by Braver (2012; 2007). Indeed, proactive control works as a sustained and early attentional bias toward the relevant information capable to anticipate the interference, whereas reactive control acts as a later attentional mechanism that is recruited after the interference occurred. Therefore, on one hand, proactive control is the mechanism mainly involved in resolving the interference of LWPC manipulation, because participants are able to rely on an anticipatory and sustained attentional bias depending on the PC of a given block; on the other hand, reactive control plays a crucial role in resolving the interference of ISPC manipulation, where participants are not able to prepare in advance because congruent and incongruent trials are equally probable (see Bugg & Crump, 2012, for a review). In line with the DMC model (Braver, 2012; Braver et al., 2007), previous studies using different Stroop paradigms suggested that LWPC- and ISPC-dependent effects reflect distinct components of cognitive control (Bugg, Jacoby, et al., 2011; Bugg, McDaniel, et al., 2011), but only one study assessed the contribution of LWPC and ISPC effects in the same participants (Gonthier et al., 2016). In this study, the authors used a picture-word Stroop task and they found that proactive and reactive control processes are dissociable and lead to different behavioural signatures, suggesting that they constitute independent mechanisms.

However, none of the previous studies investigated the different temporal dynamics enclosed in proactive and reactive control. Indeed, response times in key pressing or vocal responses are only the final output of cognitive processes and they do not allow making inferences on how these processes evolve over time. Therefore, here we aim at tackling this issue by investigating the temporal dynamics and real-time effects of proactive and reactive controls in the development and updating of decision and response processes. For this purpose, we implemented a similar spatial version of the Stroop task seen for the first study (see section 2.2.2) in the MouseTracker Software (Freeman & Ambady, 2010), manipulating the PC both at the list and at the item levels. The use of this software allows to record mouse trajectories on x- and y-coordinates of the computer screen with high temporal precision, and it can be considered as a real-time estimation of the continuous evolving of the decision process and updating of response output (Hehman, Stolier, & Freeman, 2015). Thus, in the study of interference resolution, this tool provides useful insights about the response development in front of distracting information and alternative responses, and it can help in shedding light on the temporal dynamics of interference resolution. For example, one of the most used measures (i.e., the point of the maximum deviation from the ideal trajectory, MD) reflects the deviation from the optimal trajectory and, thus, the magnitude of the attraction toward the task-irrelevant response and the temporal dynamics of conflict resolution (Freeman & Ambady, 2010). Only few works have used mouse trajectories to study interference resolution in conflict paradigms. In the context of Stroop tasks, Incera and McLennan (2016) used this technique in a colour-word version administered to monolingual and bilingual participants. The authors not only demonstrated that the Stroop effect was present in mouse trajectories measures, but also, by means of the analysis of the movement initiation times and the x-coordinate over time, they were able to demonstrate that bilinguals took longer to initiate the movement, but moved faster toward the correct response. To our knowledge, only two other previous studies analysed mouse trajectories adopting a PC manipulation in a Stroop task (with a colour-word version), but the PC was manipulated only at the item-level (Bundt et al., 2018; Ruitenberg et al., 2019). Both studies demonstrated an effect of the ISPC manipulation, showing that the Stroop effect was smaller for low-PC blocks.

3.2. Rational and hypotheses

Our aim was thus to investigate whether, and to what extent, LWPC and ISPC manipulations can modulate the involvement and related temporal dynamics of proactive and reactive cognitive control in the spatial Stroop task. Generally, based on the existing body of evidence reviewed above, we expected to find a reduced cognitive interference (i.e., Stroop effect) on mouse trajectories in low-PC conditions (i.e., LW25PC, IS25PC) as compared to high-PC conditions (i.e., LW75PC, IS75PC). However, despite previous evidence suggested that proactive and reactive control are two dissociable and independent mechanisms (Gonthier et al., 2016), further investigation is still needed to verify their specific contribution in interference resolution. For this reason, we assessed the specific contribution of these two processes by manipulating parametrically both LWPC and ISPC. In particular, using linear mixed effects analyses to model as continuous variables both list-wide and item-specific PC manipulations (and thus the degree of proactive and reactive control) allows us to evaluate the specific, unique effect of each control mode above and beyond the other one. This would not be possible by considering PC manipulations as categorical variables and assessing their effects by using standard General Linear Model (GLM) analyses, as done in existing studies (Bugg & Chanani, 2011; Gonthier et al., 2016; Jacoby et al., 2003).

Indeed, even considering the PC of list-wide and item-specific manipulations to define the experimental conditions (e.g., 25% of congruent trials in LW25PC), they are still characterized by PC values at both the list-wide and the item levels. For example, in our study we manipulated the PC at the list-wide level to have 25% of congruent trials in a block (LW25PC condition), but this was achieved by manipulating the PC at the item level, so that all the items were presented in the 25% of cases as congruent or, stated differently, all the items had an ISPC of 25%. Similarly, in the LW50PC condition the list-wide PC was manipulated to have 50% of congruent trials by having all the items in that block with an ISPC of 50%. In these cases, LWPC and ISPC coincide and it is not possible to disentangle their specific effect in this condition. On the contrary, the items taken into account for the IS25PC condition had an ISPC of 25%, but they were presented in an experimental block that also included other items with an ISPC of 75% (IS75PC condition) in order to maintain the list-wide PC at 50%. Therefore, our IS25PC is characterized not only by an ISPC of 25%, but also by an LWPC of 50% (see Table 3.1 for a summary of PC manipulations).

Table 3.1. Summary of PC manipulations.

			DIRECTIONS				ISPC	LWPC
			↖	↗	↘	↙		
LW50PC (LW: 50%, IS: 50%)	POSITIONS	🟩☐ ☐☐	**18**	6	6	6	**18**/(**18**+6+6+6)=**50%**	(**18**x4)/ [(**18**+6+6+6)x4]= **50%**
		☐🟩 ☐☐	6	**18**	6	6	**18**/(**18**+6+6+6)=**50%**	
		☐☐ ☐🟩	6	6	**18**	6	**18**/(**18**+6+6+6)=**50%**	
		☐☐ 🟩☐	6	6	6	**18**	**18**/(**18**+6+6+6)=**50%**	
LW75PC (LW: 75%, IS: 75%)	POSITIONS	🟩☐ ☐☐	**36**	4	4	4	**36**/(**36**+4+4+4)=**75%**	(**36**x4)/ [(**36**+4+4+4)x4]= **75%**
		☐🟩 ☐☐	4	**36**	4	4	**36**/(**36**+4+4+4)=**75%**	
		☐☐ ☐🟩	4	4	**36**	4	**36**/(**36**+4+4+4)=**75%**	
		☐☐ 🟩☐	4	4	4	**36**	**36**/(**36**+4+4+4)=**75%**	
LW25PC (LW: 25%, IS: 25%)	POSITIONS	🟩☐ ☐☐	**18**	18	18	18	**18**/(**18**+18+18+18)=**25%**	(**18**x4)/ [(**18**+18+18+18)x4]= **25%**
		☐🟩 ☐☐	18	**18**	18	18	**18**/(**18**+18+18+18)=**25%**	
		☐☐ ☐🟩	18	18	**18**	18	**18**/(**18**+18+18+18)=**25%**	
		☐☐ 🟩☐	18	18	18	**18**	**18**/(**18**+18+18+18)=**25%**	
IS25PC (LW: 50%, IS: 25%) **IS75PC** (LW: 50%, IS: 75%)	POSITIONS	🟩☐ ☐☐	**54**	6	6	6	**54**/(**54**+6+6+6)=**75%**	(**54**x2+18x2)/ [(**54**+6+6+6)x2+ (18+18+18+18)x2]= **50%**
		☐🟩 ☐☐	18	**18**	18	18	**18**/(**18**+18+18+18)=**25%**	
		☐☐ ☐🟩	6	6	**54**	6	**54**/(**54**+6+6+6)=**75%**	
		☐☐ 🟩☐	18	18	18	**18**	**18**/(**18**+18+18+18)=**25%**	

Notes. The table represents PC manipulations for each experimental condition. On the left, the type of experimental block is reported (i.e., LW50PC, LW75PC, LW25PC, IS25/75PC), with their PC at the list and item level (LW and IS, respectively) shown in parenthesis. Next to them, the position where the arrow appeared – corresponding to the dimension on which the PC was manipulated – is highlighted in green. The numbers in the cells correspond to the number of presentations for each combination of direction (reported above as green arrows) and position. IS25PC and IS75PC are presented in the same block to allow a LWPC of 50% (the positions on which PC is manipulated are counterbalanced across participants, even if not shown in the table). Finally, PC is calculated as the number of congruent trials (in bold), divided by the total number of trials. The columns ISPC and LWPC report the PC calculation for each position row and for the entire block, respectively. For example: in LW50PC condition, the first row corresponds to the upper-left position of the screen (square highlighted in green). For this condition, the first arrow pointing in the upper-left corner is presented 18 times and it is congruent to the position. The other three arrows are presented 6 times each and, in this way, congruent and incongruent items are equally probable with a PC at the item level of 50% and a global PC at the block level of 50%. See section 3.3.2 for further details.

In this scenario, traditional GLM analyses that consider the PC manipulations as categorical variables could still be used in trying to evaluate the specific effects of LWPC and ISPC manipulations, but this requires performing different, independent contrasts, as done in the study of Gonthier and colleagues (2016), which is a sub-optimal approach. Instead, with our linear mixed effects approach, both LWPC and ISPC are modelled as continuous regressors, which allows quantifying in a fine-grained way their specific contribution, as well as their possible interaction, in explaining participants' performance and, thus, effectively testing alternative hypotheses about the impact of proactive and reactive control.

In particular, we hypothesized four possible scenarios. First, it is possible that only the LWPC manipulation is effective, thus indicating the specific and sole effect of proactive control. In this case, our analytical approach would reveal a non-null slope for the LWPC regressor only; in other terms, the participants' performance would best be explained by a regression plane as shown in Figure 3.1 A. A second possibility is that only the ISPC manipulation results effective, thus indicating the specific and sole effect of reactive control. In this case, our analytical approach would reveal a non-null slope for the ISPC regressor only, as reflected by the regression plane shown in Figure 3.1 B. Third, it is possible that both the LWPC and ISPC manipulations modulate participants' performance with independent, additive effects, meaning that both proactive and reactive control modes have a specific effect in affecting participants' interference resolution ability. In this case, our analytical approach would reveal non-null slopes for both LWPC and ISPC regressors, with a non-significant interaction term, as reflected by the regression plane shown in Figure 3.1 C. Lastly, LWPC and ISPC could both modulate participants' performance with multiplicative, interacting effects. In this case, the effect of proactive control would depend on the degree of reactive control or, in other words, the slope of the LWPC effect would be different for different values of the ISPC regressor, as reflected by a non-rigid regression plane as that shown in Figure 3.1 D. Specifically, we expected the third scenario to be true, where proactive and reactive control specifically impact the temporal course and kinematic parameters of the mouse responses, as assessed by using the MouseTracker software. We expected participants to be able to use the LWPC information to anticipate the interference when responding to incongruent trials, because they can rely on proactive control that imposes an early attentional bias toward task-relevant information. Indeed, we hypothesized that when proactive control is engaged, the effect of the interference is smaller (i.e., smallest Stroop effect) and the trajectories are corrected faster. We expected also to find an effect of reactive control for which also the ISPC information can be used by participants to reactively modulate their performance (i.e., smallest Stroop effect for IS25PC). In sum, we expected to find a modulation of the Stroop effect magnitude as function of both PC manipulations.

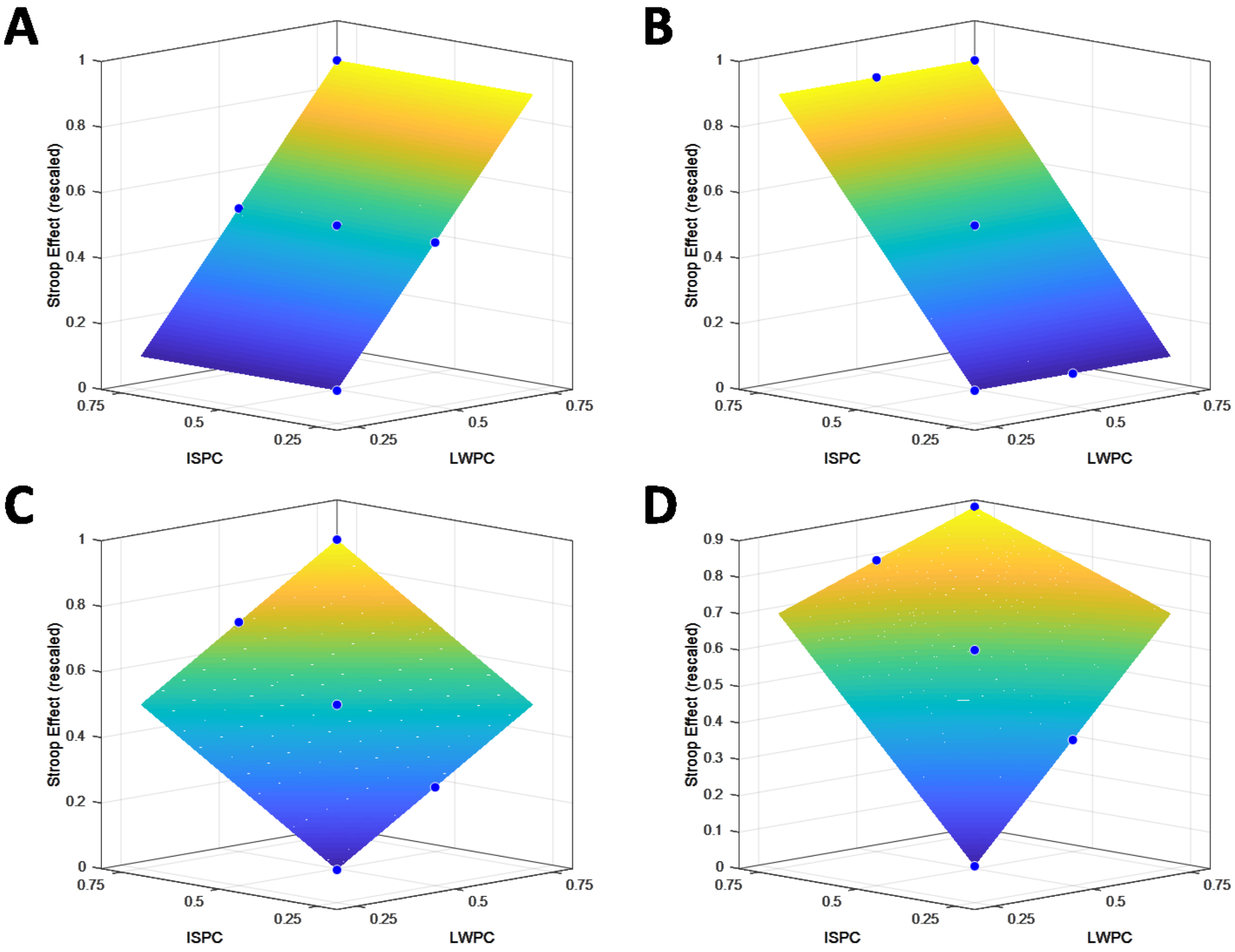

Figure 3.1. Hypothetical scenarios

The figure represents a visual example of the four hypotheses that we described in section 3.2. The Stroop effect in the five experimental conditions (blue dots) is plotted on the vertical axis, while the proportion of congruent trials due to the ISPC and LWPC manipulations define the horizontal axes. A fitting plane is also shown explaining the Stroop effect as a function of both ISPC and LWPC, as well as their interaction, according to the equation Stroop Effect = a + b1*ISPC + b2*LWPC + b3*LWPC:ISPC. The amount of the predicted Stroop effect is color-coded, with cold and warm colours representing, respectively, smaller and larger Stroop effects. Figure A reflects the hypothetical scenario where only the LWPC manipulation is effective in modulating the interference, showing that the Stroop effect increases as function of the LWPC only. In this case, the Stroop effect is the same across the three conditions with the same LWPC of .5, that is, IS25PC, LW25PC and IS75PC, even if they have different ISPC values (respectively, .25, .5 and .75).

Figure B represents the opposite scenario, in which only ISPC is effective in modulating the Stroop effect. In this case, the Stroop effect is the same between IS25PC and LW25PC conditions, which have the same ISPC value (.25) but different LWPC values (.5 and .25, respectively), as well as between IS75PC and LW75PC, which have the same ISPC value (.75) but different LWPC values (.5 and .75, respectively). Figure C represents the scenario where both LWPC and ISPC manipulations lead to independent and additive effects in modulating interference. In this case, the Stroop effect is modulated by both LWPC and ISPC. Figure D represents the scenario where LWPC and ISPC manipulations interact in modulating the interference with multiplicative effects. This is indeed the only case in which the relation between the Stroop effect and LWPC and ISPC is non-linear, as evidenced by the non-rigid fitting plane. Note that, for the sake of simplicity, in these last two scenarios the effects of LWPC and ISPC manipulations are assumed to have the same weight in modulating the Stroop effect.

3.3. Methods

3.3.1. Participants

We recruited 48 healthy young participants (females = 35, mean age = 28.23 years, range = [21 41]), all Italian native-speakers. An a priori sensitivity power analysis conducted on G*Power software (Faul, Erdfelder, Buchner, & Lang, 2009) revealed that 46 participants were needed to detect a within-subjects significant difference (α = 0.05) corresponding to a medium effect size (Cohen's d) of .3 with a statistical power (1-β) of 0.80, assuming a between-measures correlation of .75.A modified version of the Edinburgh Handedness Inventory (Oldfield, 1971) was used to measure participants' handedness (average handedness score = 75.83, SD = 35.71). An additional item was included assessing the preferred hand when using the computer mouse and left-handed participants who always used the right hand to control the computer mouse were included in the study. All the participants signed an informed consent before taking part to the study. All the experimental methods had ethical approval from the Research Ethics Committee of the School of Psychology of the University of Padua (prot. N. 2717) and was conducted in accordance with the guidelines of the Declaration of Helsinki (World Medical Association, 2013).

3.3.2. Design and stimuli

We implemented in the MouseTracker Software (Freeman & Ambady, 2010) the 4-choice spatial Stroop task previously used in Study 1 of this dissertation, with some differences (see Figure 3.2 and cf. section 2.2.2). We recorded the data through a 16-inch laptop monitor with a resolution of 1024 x 768 pixels, corresponding to a 4:3 ratio. Stimuli were presented on a grey background (RGB: 200, 200, 200) within an imaginary frame of 768 x 768 pixels that was horizontally centered on the screen. At the beginning of each trial, a small grey square (31 x 31 pixels; RGB: 165, 165, 165) was presented at the center of the screen; this square constituted the starting point for the mouse movement. When participants clicked on this square, it disappeared and, at the same time, four white response squares (92 x 92 pixels) were presented at the four corners of the frame (upper-left, upper-right, lower-left, lower-right). In one of them an arrow (the experimental stimulus) appeared pointing toward one of the same four directions. Equally to Study 1, stimuli were either congruent or incongruent based on the congruence between the position and the direction of the arrow.

The onset of the response squares and the experimental stimulus signalled the beginning of the trial. Participants were asked to move the mouse cursor and to click on the response square indicated by the direction of the arrow, independently from the position where it appeared. The choice to include white squared frameworks where arrows could appear allows to limit the area where participants could click to respond, facilitating data analysis. Participants were allowed to complete their response within 2500 ms; if they failed, a timeout message was provided after stimulus presentation (i.e., a red “timeout” text at the center of the screen). Moreover, participants were given 750 ms to start moving from the starting square after having clicked on it; if they failed to do so, another timeout message was immediately presented asking them to try starting the movement faster on subsequent trials. When participants clicked on the chosen response square, a blank screen was presented, signalling the end of the trial, and after 250 ms it was followed by the presentation of the grey starting square. After having made their response, participants were instructed to go back and click on the starting square to start the next trial. They were allowed to do so at their own pace, that is, the trial progression was self-paced with a minimum inter-trial interval of 250 ms (plus the time needed to move the mouse cursor back over the starting square and click on it). The stimuli were presented in a pseudorandom order so to avoid all types of repetitions and minimize both positive and negative priming confounds, as done for Study 1.

Moreover, for this study we manipulated the PC at both the item-specific and the list-wide levels in different blocks. The task was indeed composed by nine different experimental blocks, each consisting of either 74 or 98 trials, as well as by four training blocks (one for each type of manipulation) consisting of either 16 or 24 trials. In particular, there were three conditions in which PC was manipulated at the list level (LWPC): 1) one condition in which congruent trials were presented in 75% of cases (LW75PC), consisting of two blocks of 98 trials preceded by a training block of 24 trials; 2) one condition in which congruent trials were presented in 25% of cases (LW25PC), consisting of two blocks of 98 trials preceded by a training block of 24 trials; 3) one condition in which congruent trials were presented in 50% of cases (LW50PC), consisting of two blocks of 74 trials preceded by a training block of 16 trials. There was also a fourth condition (consisting of three blocks of 98 trials preceded by a training block of 24 trials) in which the LWPC was maintained at 50%, while the PC for specific items (ISPC) was manipulated so that, for two of the four positions, the arrows were presented in 75% of cases as congruent (IS75PC trials), whereas for the other two positions the arrows were presented in 25% of cases as congruent (IS25PC trials). Furthermore, the IS75PC and IS25PC conditions were counterbalanced for item positions across participants, so that for half of the participants IS75PC and IS25PC stimuli appeared, respectively, at the upper-left and bottom-right positions, while for the other half the opposite mapping was applied. The order of presentation of the four conditions was counterbalanced across participants but blocks with the same PC were always presented in succession. Participants were allowed to take a break at the end of each block.

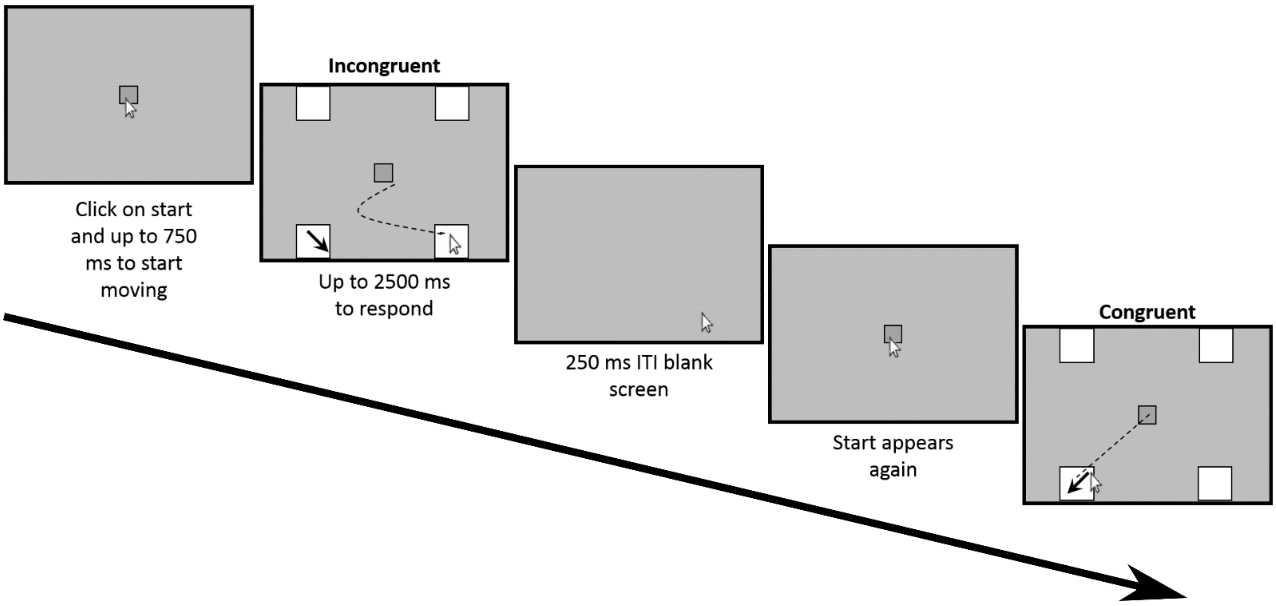

Figure 3.2. Example of MouseTracker experimental paradigm

The trial began with a grey square at the center of the screen (start), where participants needed to click in order to make the arrows appear. After they clicked, four white squares (response alternatives) appeared in the four corners of the screen (i.e., upper-left, upper-right, lower-right, and lower-left positions) and in one of them an arrow pointing at one of the same four directions was presented. Participants had to start moving within 750 ms and they had up to 2500 ms to respond by performing a reach-to-click movement of the mouse cursor to the response alternative indicated by the direction of the arrow. The squares and arrow disappeared when the response was given, and an additional blank screen was presented for 250 ms as inter-trial interval (ITI). After this time, the start square appeared again, and the participants could come back to the center of the screen and click the square to make the following trial appearing. In this figure, the first trial is an example of incongruent trial, whereas the second one is an example of congruent trial with their typical mouse response trajectory in dashed line.

3.4. Data analysis

3.4.1. MouseTracker measures

The MouseTracker software allows to record in real-time x- and y-coordinates of the computer mouse (with a 16-ms temporal resolution with a monitor refresh rate of 60 Hz). Indeed, one second contained around 60 pairs of x- and y-coordinates (in pixels), which makes this tool very flexible, allowing the extraction of different kind of measures (Freeman & Ambady, 2010). Before analysing mouse trajectories measures, it is necessary to apply some pre-processing, which we conducted in Matlab (version 2017b; The Mathworks, Inc. Natick, MA). In order to compare and average trajectories, they were remapped into a standard coordinate space with the lower-left corner at the coordinates [-1.5, 0] and the upper-right corner at the coordinates [1.5, 1]. Then, these normalized trajectories were flipped and/or rotated by 90°, in order to be directed toward the upper-right corner and having the interfering response alternative at the upper-left corner (Freeman & Ambady, 2010). From the recorded data, it is possible to extract different measures both at the trial-level (one summary value for each trial) and at the time-level (time-resolved values reflecting the online evolution and updating of the mouse response for each trial). Since the trajectories may have different lengths, before computing time-resolved measures, a time normalization was applied with a linear interpolation of 101 time-steps to allow 100 time-normalized equal spaces.

In order to compute trial-level measures, the recorded data for x- and y-coordinates for each time sample were smoothed using a linear Savitzky-Golay filter (span: 25 ms) to eliminate measurement noise and interpolated to 1-ms resolution. We then calculated the time course of the instantaneous velocity of the trajectories, as well as that of the Euclidean distance from the target and from the starting point. Based on these data, we computed a number of the trial-level measures: the Response Time (RT), that is the time elapsed between the click on the start and the final click on the response square; the Initiation Time (IT), which is the time of the response initiation, defined as the point when the cursor was moving more than 10 cm/s from at least 50 ms; the Movement Time (MT), defined as the time elapsed from the IT to the end of the response; the Maximum Deviation (MD), calculated as the maximal perpendicular distance of the recorded trajectory from the optimal trajectory (i.e., a straight trajectory connecting the starting point and the center of the target response square); the Maximum Deviation Time (MDTime), the time at which the MD is reached; the x-coordinate at the MD (MDx); the distance from the starting point at the MD (MDd); the Area Under the Curve (AUC), that is the geometric area between the recorded trajectory and the optimal one; the Travelled Distance (TravD), which is the total length of the trajectory; the number of x flips (XFlip), that corresponds to the number of reversal of the trajectory on the horizontal axis; the number of velocity flips (VelFlip), which is the number of changes in velocity during the response; the initial direction of the trajectory (StartAngle), calculated as the angle between the starting point and the trajectory point at 50 ms after the response initiation; the point of Maximal Velocity (MaxVel); the Time of the Maximal Velocity (MaxVelTime); the Minimum x-coordinate (Xmin), that is, the x coordinate of the leftmost point of the recorded coordinate. Beside the standard measure of RT (and related measures of MT and IT), these measures reflect different aspects of the dynamics of interference resolution processes, including the degree of interference from the alternative response option, meaning the degree of spatial attraction of the mouse trajectory toward the irrelevant dimension (e.g., MD and related measures, AUC, and Xmin), and the smoothness and spatial complexity of the mouse trajectory (e.g., TravD, XFlip, VelFlip, and MaxVel), as well as how the interference resolution processes evolve over time (e.g., StartAngle, MDTime, and MaxVelTime).

Concerning the time-level measures, we extracted the normalized time course of the x coordinate, the distance from the target, and the velocity.

3.4.2. Statistical analysis

We conducted the statistical analysis on R (R Core Team, 2016). When needed, we transformed our trial-level dependent variables to improve normality and mitigate the influence of skewed data. In particular, we applied logarithmic transformation for the MD, MDTime, AUC, TravD, MaxVel, and MaxVelTime; we used the inverse transformation for the RT, MT, and IT; and we used the BoxCox transformation (Box & Cox, 1964) to adjust the tails of the Xmin.

For each of the *trial-level* dependent variables, we performed linear mixed-effects modelling by using the function *lmer* from the *lme4* package (Bates, Maechler, Bolker, & Walker, 2014; version 1.1-17). This is a robust approach for the analysis of repeated measures designs. Indeed, it allows to take into account the variability across participants, because the analyses are conducted at the trial level, providing flexibility in assessing random and fixed effects both at within- and between-subjects levels (Baayen, Davidson, & Bates, 2008). Moreover, this approach allowed us to model the impact of the LWPC and ISPC manipulations at the same time and in a continuous way. In particular, the PC values at both the list- and the item-level (i.e., 25, 50 and

75%) were rescaled and centered respectively at -2.5, 0 and 2.5. In this way all the blocks entailed both LWPC and ISPC manipulations. For example, the LW25PC blocks had a list-level PC of 25% but at the same time, because of this manipulation, these blocks also entailed an item-level PC of 25%. Similarly, the IS25PC or IS75PC blocks also had list-level PC of 50%. Moreover, to facilitate model convergence, we also scaled and centered the regressor vector the ordinal number of trials (cTrialT), which accounted for potential effects of fatigue or progressive learning of the task.

The final model included as fixed effects cTrialT, the interaction between the LWPC manipulation and the ISPC manipulation and the Congruency type (Congruent and Incongruent). As random effects, we allowed by-subject random slopes for the interaction between LWPC, ISPC and Congruency. Lastly, we re-fitted the final model after excluding observations with absolute standard residuals greater than 3 (never more than 3% of observations were eliminated). The statistical significance of the coefficients for each regressor was calculated by means of *lmerTest* package (Kuznetsova, Brockhoff, & Christensen, 2017; version 3.0-1) that provides p-values using the Satterthwaite's method to estimate degrees of freedom.

Similarly, the same model and procedure were adopted for the *time-level* measures, with the only difference that these measures were normalized in 101 time points and we fitted a model for each one of these time points. Again, the final model was fitted after excluding observations with absolute standard residuals greater than 3 (never more than 3.5% of observations were eliminated). All the *t-values* obtained from *lmer* were corrected for multiple comparisons through Bonferroni correction in order to limit the inflation of Type-I errors due to multiple comparisons. Moreover, for these measures, we reported only the time bins that showed a significant effect for more than 5 consecutive time points.

3.5. Results

Figure 3.3 shows the general pattern of results at first glance. The figure represents the average of the trajectories for incongruent trials (warm colours) and congruent trials (cold colours) in all the blocks. Trajectories for congruent trials were mainly straight lines, almost overlapping to each other, whereas the trajectories for incongruent trials showed a linear increase in the magnitude of the spatial attraction of the irrelevant dimension (note that the interfering response alternative was located in the upper-left corner after the spatial remapping; see section 3.4.1). Indeed, the maximum interference was present for the condition requiring less amount of control (i.e., LW75PC).

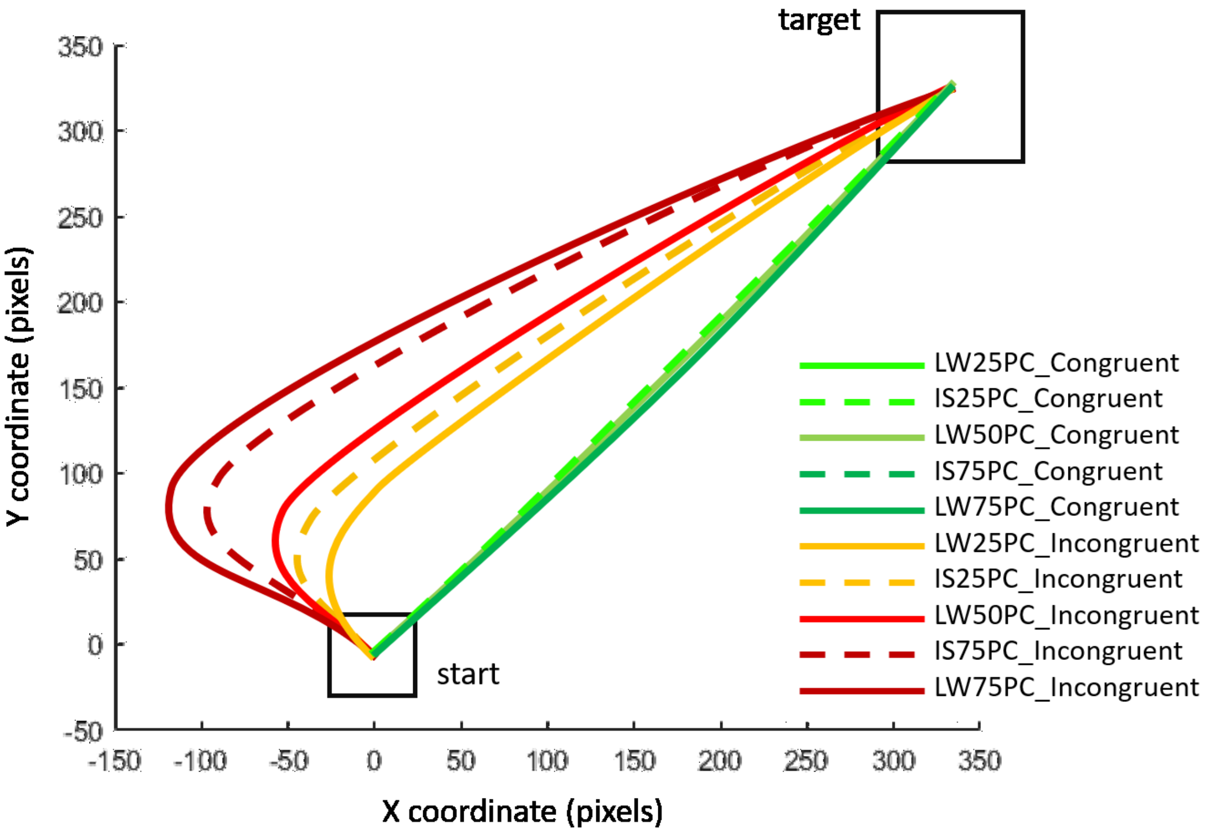

Figure 3.3. Average of trajectories of congruent and incongruent trials for all blocks.

The figure represents the upper-right portion of the screen, with the average of trajectories for congruent (cold, green colours) and incongruent (warm, red colours) trials in all the blocks. On the x and y axes there are the x- and y- coordinate in pixels of the MouseTracker space. Here, all the trajectories are remapped in order to have the target on the upper-right corner and the irrelevant dimension on the upper-left. The start square is at the center of the screen. Congruent trajectories followed a straight line toward the target, whereas it is possible to notice a gradual increase in the magnitude of the interference (i.e., spatial attraction of the irrelevant dimension) for the incongruent trajectories. In particular, the innermost and solid line (in orange) corresponds to the trajectory for the LW25PC, the dashed orange line corresponds to the one of the IS25PC, the solid red line in the middle corresponds to the LW50PC, the dashed dark red line to the IS75PC and the outermost solid dark red line to the LW75PC.

The following results for the *trial-level* measures are summarized focussing on the effects of main theoretical interest, that is, the effect of Congruency, the interaction between LWPC and Congruency, the interaction between ISPC and Congruency and the three-way interaction LWPC by ISPC by Congruency. For a detailed description of the results for each of the dependent variables and for a complete table of all the effects see Appendix B. Overall, the analysis showed the same pattern of results for all the measures taken into consideration. In particular, regarding the effects that are of primary relevance for our hypotheses, the main effect of Congruency was constant for all the measures, except the IT. This indicated that, on average, there was a significant cost in responding to incongruent trials (i.e., the Stroop effect), where mouse trajectories were more attracted toward the irrelevant dimension, were less smooth, more spatially complex, and took more time to be completed, with a specific temporal evolution of the interference resolution processes. LWPC by Congruency and ISPC by Congruency interactions were both significant for all the measures except IT, Start Angle, and MDd, showing that both PC manipulations were effective in modulating participants' Stroop effect. In particular, the participants' Stroop effects were smaller for conditions with lower PC values at both the list-wide and the item-specific level. Importantly, significant three-way interactions were found for eight out of the twelve measures, thus suggesting that the effects of LWPC and ISPC manipulations - and thus proactive and reactive control processes respectively - are non-additive and interact with each other in a complex way, affecting participants' interference resolution abilities (see Figure 3.4). Table 3.2 provides the Estimates, Standard Error (SE), degree of freedom (df), *t* and *p values* for all the parameters fitted in the final models and for one representative measure at the *trial-level*: Xmin.

Table 3.2. Results of the analysis for the representative measure of Xmin

	Xmin				
EFFECT	Estimate	SE	df	t values	*p* values
Intercept	8.69	0.05	47.06	169.46	0.000
Trial Tot	0.02	0.01	1364.06	2.55	0.011
LWPC	0.04	0.01	59.94	2.96	0.004
ISPC	0.05	0.01	230.33	5.88	0.000
Congruency	-2.37	0.09	46.97	-25.58	0.000
LWPC*ISPC	-0.02	0.01	53.91	-4.52	0.000
LWPC*Congruency	-0.21	0.03	46.48	-7.27	0.000
ISPC*Congruency	-0.18	0.02	53.78	-11.85	0.000
LWPC*ISPC*Congruency	0.03	0.01	50.76	3.34	0.002

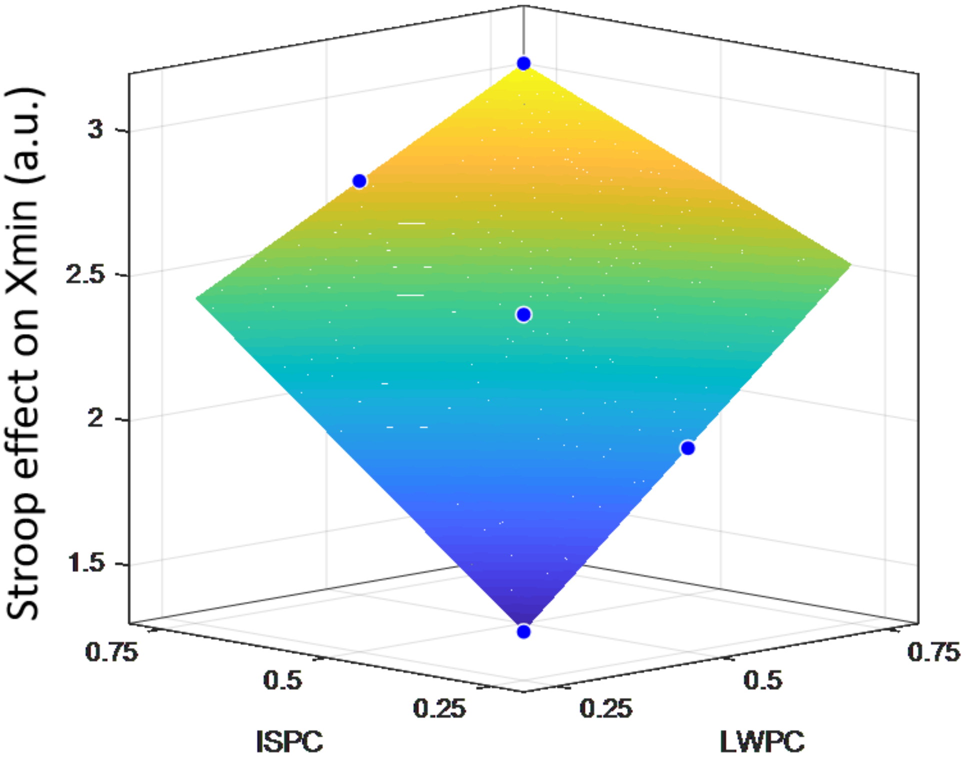

Figure 3.4. Effects of Xmin

The figure shows the Stroop effect for the Xmin measure on the vertical axis, for all the five experimental conditions (blue dots). Xmin is represented in arbitrary units (a.u.), as it was transformed through BoxCox transformation (Box & Cox, 1964). Proportions of congruent trials for ISPC and LWPC define the horizontal axes. A fitting plane explaining the Stroop effect is also shown, where cold and warm colours represent smaller and larger Stroop effects, respectively. The fitting plane is non-rigid, reflecting the interaction between LWPC and ISPC manipulation effects in modulating the interference for Xmin. This pattern was found for eight out of twelve measures (see text) and corresponded to our fourth hypothetical scenario described above (see section 3.2).

The following results for the *time-level* measures are also summarized focussing on the same effects of main theoretical interest described for the *trial-level* measures.

All the measures showed significant effects of the main effect of Congruency, as well as the two-way interactions ISPC by Congruency and LWPC by Congruency. However, there were no significant three-way interactions, in line with our third hypothetical scenario (see Figure 3.5).

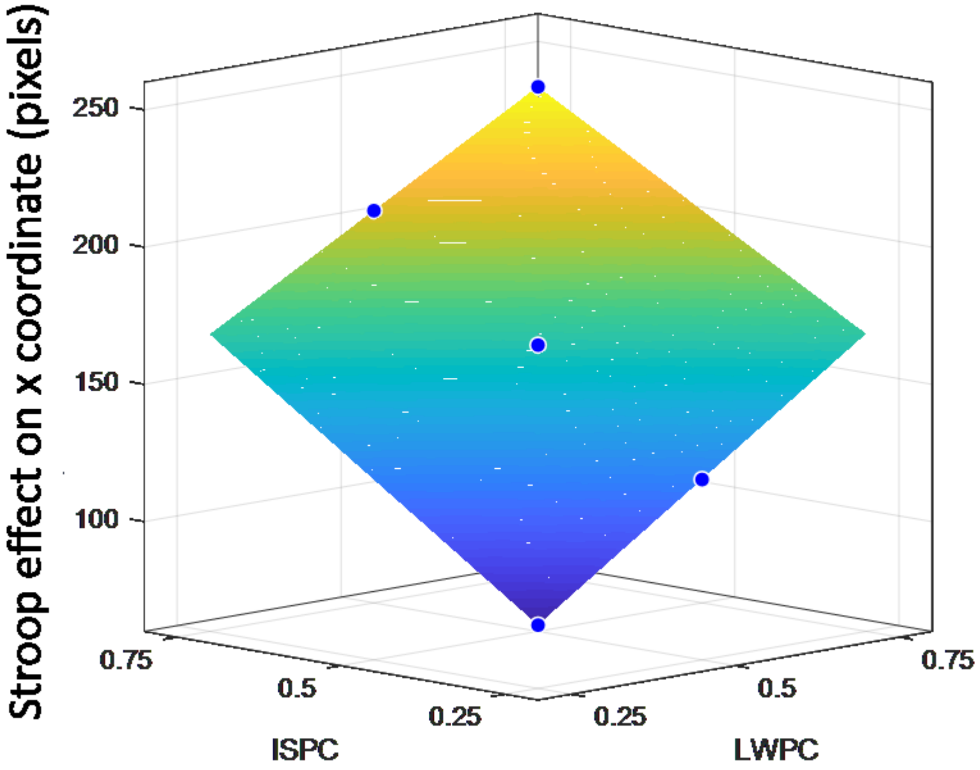

Figure 3.5. Effects of one representative time point of the x coordinate

The figure shows the Stroop effect for one representative time point of the x coordinate (in pixels) on the vertical axis, for all the five experimental conditions (blue dots). Proportions of congruent trials for ISPC and LWPC define the horizontal axes. The amount of Stroop effect is color-coded, with cold and warm colours representing smaller and larger Stroop effects, respectively. The fitting plane shows that both LWPC and ISPC manipulations led to independent and additive effects in modulating the interference. This pattern was found for all the three time-level measures and for four out of twelve trial-level measures (see text), corresponding to third hypothetical scenario described above (see section 3.2).

In particular, for the x-coordinate we found a significant effect of Congruency in the time bin from 19 to 78, due to the leftward shift of the trajectories for incongruent trials. LWPC by Congruency and ISPC by Congruency had similar patterns of results, for which the Stroop effects showed a linear increase in the magnitude of the interference from the low-PC to the high-PC conditions. Specifically, the leftward deviations of the trajectories for the incongruent trials were smaller in the low-PC condition, both for the LWPC and ISPC manipulations. The LWPC by Congruency effects were significant in a time window comprising the time bins from 36 to 61, whereas the ISPC by Congruency significant effects involved the time bins from 25 to 63. At first sight, these results seem to suggest that the modulatory effect of the reactive control on Stroop performance, as evidenced by the significant ISPC by Congruency interaction, preceded that due to proactive control, evidenced by the significant LWPC by Congruency interaction. However, this apparent difference in the time course of these two effects was in fact caused by the fact that the ISPC by Congruency effect was numerically stronger than the LWPC by Congruency one. Moreover, the maximum effect for the two interactions was observed at almost the same time bin (i.e., 49 and 48 for the ISPC by Congruency and LWPC by Congruency interactions, respectively), highlighting the similarity in the time course of these effects (see Figure 3.6).

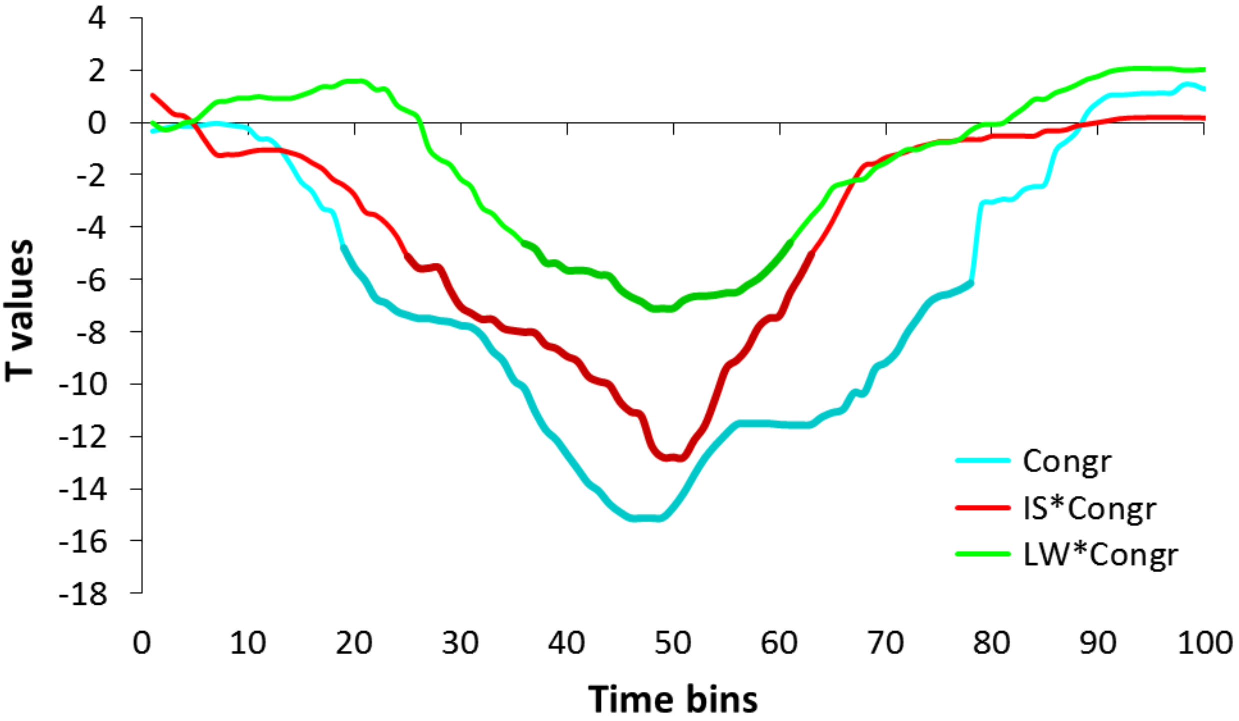

Figure 3.6. Results of time-level analysis on x coordinate

The figure shows the time course of t values (y-axis) for the effects of main theoretical interest: Congruency (Congr in blue), ISPC by Congruency interaction (IS*Congr, in red) and LWPC by Congruency Interaction

(LW*Congr, in green). X axis represents the time bins. Darker and thicker portions of the lines indicate time window of statistical significance (corrected for multiple comparisons by means of the Bonferroni method).

Concerning the distance from the target, there was a significant main effect of Congruency for the time bins from 25 to 89, confirming that participants' trajectories ended up farther away from the target for the incongruent as compared to congruent trials. For the LWPC by Congruency and ISPC by Congruency, we found similar pattern as previously found for the x-coordinate. In particular, the two interactions showed the same linear increase in magnitude of the Stroop effect as function of the PC. Indeed, the distance from the target for the incongruent trials was significantly higher for the high-PC manipulations. LWPC by Congruency showed a significant effect for the time bins from 37 to 78, whereas the ISPC by Congruency for the bins 29 to 85. Again, the apparent difference in the time course of these two effects was in fact caused by the fact that the ISPC by Congruency effect was numerically stronger than the LWPC by Congruency one and the maximum effect for the two interactions was observed at almost the same time bin (i.e., 49 and 48 for the ISPC by Congruency and LWPC by Congruency interactions, respectively), further supporting the conclusion that the two effects had similar temporal dynamics (see Figure 3.7).

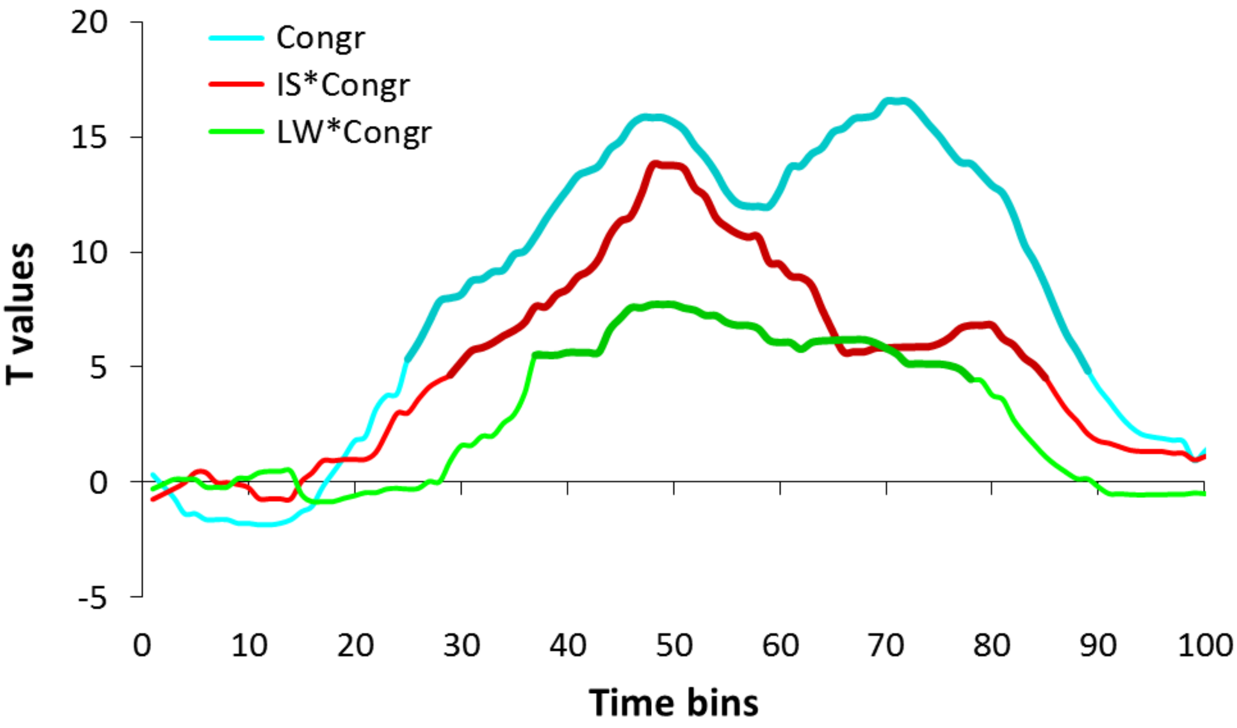

Figure 3.7. Results of time-level analysis on distance from the target

The figure shows the time course of t values (y-axis) for the effects of main theoretical interest: Congruency (Congr in blue), ISPC by Congruency interaction (IS*Congr, in red) and LWPC by Congruency Interaction (LW*Congr, in green). X axis represents the time bins. Darker and thicker portions of the lines indicate time window of statistical significance (corrected for multiple comparisons by means of the Bonferroni method).

Finally, the velocity showed a significant main effect of Congruency for four time windows: the first one (time bins from 18 to 35) reflected the greater velocity for incongruent than congruent trials during the initial acceleration phase when the trial began; the second one (time bins from 40 to 46) reflected a decrease in velocity for the incongruent trials due to the need to adjust the trajectories following the erroneous deviation toward the interfering, alternative response option; the third (time bins from 51 to 67) and the fourth one (time bins from 76 to 92) represented the greater velocity for incongruent than congruent trials during a new increase in velocity to give the correct response and counteract the erroneous deviation in the trajectory. Concerning the two interactions, both showed that the Stroop effect was modulated as function of the PC in a similar way as shown for the other time-resolved effects, with lower Stroop effects for lower PC values, but the LWPC by Congruency one was significant in the time bins from 28 and 35 and from 61 to 66, which correspond respectively to the initial deviation of the trajectories toward the interfering response option and the first rebound increase in velocity for the incongruent trials, whereas the ISPC by Congruency was significant in the time bins from 40 to 46 and from 54 to 67, which correspond, respectively, to the decrease and first rebound increase in velocity for the incongruent trials. Again, the ISPC by Congruency effect was numerically stronger than the LWPC by Congruency one, but they had very similar temporal dynamics (see Figure 3.8).

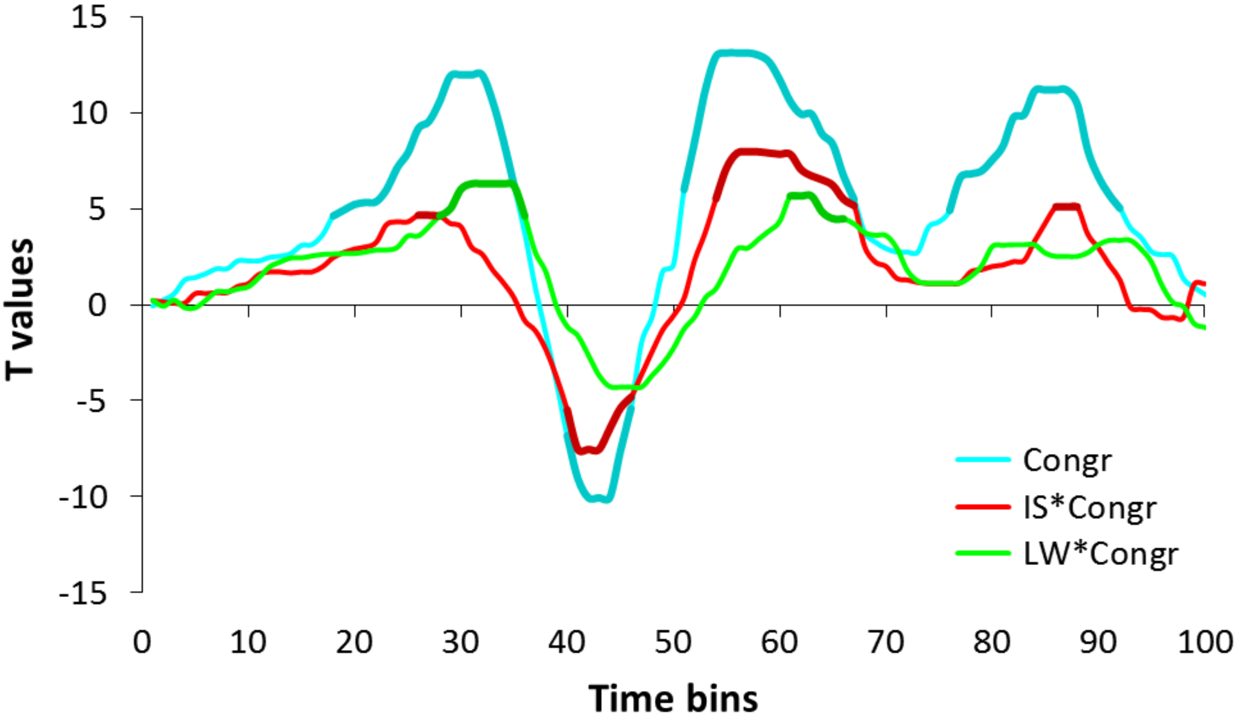

Figure 3.8. Results of time-level analysis on velocity

The figure shows the time course of t values (y-axis) for the effects of main theoretical interest: Congruency (Congr in blue), ISPC by Congruency interaction (IS*Congr, in red) and LWPC by Congruency Interaction (LW*Congr, in green). X axis represents the time bins. Darker and thicker portions of the lines indicate time window of statistical significance (corrected for multiple comparisons by means of the Bonferroni method).

3.6. Discussion

The analysis of mouse trajectories has been gaining attention over the last few years, since it can be considered as a window on our ongoing cognitive processes while they are exerted and updated. Although previous literature already reported the presence of the Stroop effect in measures derived from mouse trajectories (Bundt et al., 2018; Incera & McLennan, 2016; Ruitenberg et al., 2019), to the best of our knowledge, this is the first study demonstrating its presence in a spatial version of the Stroop task. In the present study, we had the aim of shedding light on the temporal dynamics of proactive and reactive control in interference resolution. According to the DMC model proposed by Braver (2012; 2007), through proactive control it is possible to anticipate the interference, imposing an early attentional bias toward the relevant information, whereas reactive control comes into play as a late correction mechanism after the occurrence of the interference. It has been suggested that these two mechanisms of cognitive control may be elicited by different types of PC manipulations, influencing the magnitude of the interference (Bugg & Crump, 2012; Logan & Zbrodoff, 1979). In particular, PC can be manipulated at the list-wide level (LWPC) or at the item-specific level (ISPC), with the constant finding that interference is mainly reduced in low-PC conditions. Even if participants are unaware of the manipulations, it has been proposed that modulating the PC at the list level allows to impose an early attentional bias toward the relevant information, hence engaging proactive control especially in the low-PC conditions (Bugg, McDaniel, et al., 2011; Gonthier et al., 2016). Instead, with the manipulation at the item-level, it is not possible to efficiently predict the occurrence of an interference (i.e., congruent or incongruent trials), so engaging reactive control (Bugg, Jacoby, et al., 2011; Gonthier et al., 2016).

Previous literature mainly investigated LWPC and ISPC separately, with only one study assessing independent measures of their effects in the same participants (Gonthier et al., 2016). Indeed, the present study can bring an important contribution to the field, since we not only assessed the effects of LWPC and ISPC in the same participants, but we also investigated the temporal dynamics underlying proactive and reactive control with a new and flexible technique. This tool allowed us to obtain two different types of measures: at the trial-level, where we extracted one summary value for each trial, and the time-level, where we recorded the evolution and the updating of the response for each trial. We analysed these data with mixed-effects models to evaluate the contribution of one manipulation beyond the other, modelling ISPC and LWPC impacts in a continuous way.

Our findings demonstrated that the Stroop interference was present as costs in responding to the incongruent trials, translated in a greater attraction toward the irrelevant information, less smooth trajectories, and longer time to complete the response due to the need to update and adjust the trajectories. More importantly, our findings also showed that the magnitude of the interference varied as a function of the PC manipulations. First of all, from the qualitative analysis of the average of mouse trajectories, it was possible to have a first idea that the manipulations adopted were effective in modulating the Stroop effect, showing a gradual increase in the magnitude of the interference as a function of the PC (both LWPC and ISPC; see Figure 3.3). This pattern was constant across all the trial-level measures that we analysed. Indeed, we were able to extract fifteen measures that provided a reach body of information on the temporal dynamics of the interference resolution process, which is not possible to obtain using only the standard response times. In particular, our approach allowed to shed light on different aspects of this process: the amount of interference, given by the degree of the spatial attraction due to the irrelevant dimension; the degree of certainty over a response option, given by the smoothness of the mouse trajectories; and how fast the resolution of the interference was.

More in details, our fourth hypothetical scenario best fitted the pattern of results for most of our trial-level measures, showing multiplicative and interacting effects of the PC in modulating interference resolution process (i.e., for low PC both at the list and item-level interference is smaller). However, for four out of the fifteen trial-level measures (i.e., MD, MDTime, AUC, MaxVel), the third scenario was true, where LWPC and ISPC manipulations, and so proactive and reactive control, both had specific effects in modulating the interference even after having partialled out the effect of one from the other. Similarly, also for the three time-level measures, we found a similar pattern of results and no three-way interaction. In particular, the deviations in the trajectories for the incongruent trials were smaller (i.e., x-coordinate and distance from the target) and the trajectories were corrected faster (i.e., velocity) in both low-PC conditions, showing similar temporal patterns.

Therefore, the analysis of mouse trajectories revealed to be a relatively novel method that allows to capture the underlying temporal dynamics of proactive and reactive control. Taken together, our results show that the LWPC manipulation that we used was effective in modulating the degree of proactive control with a reliable effect on the Stroop performance, over and above the effect due to reactive control driven by the ISPC manipulation. Indeed, by means of mixed effects models, it was possible to control for, and disentangle, the differential contribution of each manipulation. In other words, we were able to control for the confound that, in our paradigm, ISPC manipulation was intrinsic in the LWPC one (e.g., the PC at the block level is manipulated in order to globally have 25% of congruent trials, meaning that each of the four possible congruent items is presented in the 25% of cases; see Table 3.1). Therefore, our results indicate the existence of a specific effect of the proactive control on Stroop performance, specifically driven by the global LWPC manipulation after partialling out the effect due to the local ISPC manipulation within LWPC blocks.

Importantly from a theoretical standpoint, this is in contrast with accounts and previous studies proposing that LWPC effects are entirely due to the ISPC manipulations and that questioned the involvement of proactive control in such blocks (Blais & Bunge, 2010; Bugg et al., 2008). However, as we already mentioned in section 1.4, other studies showed the involvement of proactive control in LWPC blocks by including an additional set of items, that are presented congruent or incongruent with equal probability (i.e., unbiased items; Bugg & Chanani, 2011; Gonthier et al., 2016). Indeed, the authors reported a reduction in interference also for these unbiased items, and they explained this effect by the use of proactive control, that (through the imposition of an early attentional bias toward the relevant information) transfers this advantage also to the unbiased items. However, our findings suggest that the inclusion of additional unbiased items (that would have been particularly difficult with our set of stimuli, because including one or more unbiased items would have led to spatial asymmetries in PC manipulation) may not be the only way to disentangle the contribution of LWPC and ISPC effects.

Overall, our results are in line with our expectations and with findings of previous literature (Bugg & Crump, 2012; Bundt et al., 2018; Gonthier et al., 2016). We found that, when PC was modulated at the list-level with a low-PC, participants were able to rely on proactive control imposing an early attentional bias that allowed them to cope better with interference. This was evident in a variety of measures and was translated in smaller attractions toward the irrelevant information, faster corrections toward the correct responses and faster movements. Going back to Cascade of Control model (Banich, 2009; see section 1.2), that puts a specific focus on the steps involved in Stroop interference, we propose that proactive control may correspond to the first step: the bias toward the task relevant processes. Indeed, through the imposition of the early and top-down attentional bias, proactive control may be involved in the strengthening of the weights to elaborate arrow direction. At a first glance, it is possible to have an idea of this early effect by the visual inspection of the trajectories for incongruent trials in all the manipulations (see Figure 3.3). Indeed, the incongruent trajectories for the low LWPC block (i.e., LW25PC) showed the least attraction toward the distracting information. Moreover, also the results reported from the analysis of the velocity showed earlier effects for the LWPC manipulation, as compared to the ISPC one, with a smaller initial attraction toward the distracting information in the incongruent trials of the LW25PC block.

However, our findings showed that also when PC was modulated at the item-level with a low PC, participants showed a similar pattern of results. This means that even though it was not possible to anticipate the interference (congruent and incongruent trials were equally probable), reactive control may have worked similarly to proactive control, extracting PC information and boosting the bias toward the relevant dimension soon after stimulus appearance. This interpretation is also in line with the results of the time-level analyses on the x-coordinate and the distance to target measures, which showed an early effect of the ISPC manipulation, as well as with the additional results showing that the time courses of the proactive and reactive effects were very similar. Indeed, we suggest that also reactive control may correspond to the first step of the Cascade of Control model (Banich, 2009), with the only difference that the weights for arrow’s direction elaboration cannot be strengthened before the presentation of the stimulus. The hypothesis that reactive control may be faster than previously thought is also in line with other studies investigating item-specific effects on interference resolution (i.e., smaller Stroop interference for low-PC condition also when using ISPC manipulation). Indeed, this effect has been interpreted as an evidence that also reactive control may be able to impose a rapid attentional bias to cope with the interference (i.e., stimuli-attention association; see Bugg & Crump, 2012, for a review). This interpretation would explain the smaller cost in responding to low-PC items, even though in ISPC blocks it is not possible to effectively rely on the anticipation of the interference.

3.7. Conclusions

To sum up, our findings suggested that manipulating the PC at the list and the item level can engage different cognitive control modes that differently influence interference resolution. With the new approach of mouse-tracking analysis, we showed that both low-PC manipulations, at the list and item-level, allowed to cope better with the interference, generally reporting smallest Stroop effect, less attraction toward the irrelevant dimension and faster update of the responses. Importantly, our results showed the existence of specific proactive control effects in LWPC blocks that are not driven by the sum of ISPC manipulations, supporting the idea that global LWPC manipulations modulate the participants’ reliance on proactive control to copy with Stroop interference. However, our findings also suggest that proactive and reactive control may have similar temporal dynamics and that they may work in a similar way. Nonetheless, it is still possible that their functional difference relies on the time before stimulus presentation and on the strength of the bias that is possible to prepare before the occurrence of an interference. To further investigate this issue, we implemented an extension of the present study adding the recording of EEG, that allows to have a window on the neurophysiological activity also before the presentation of the stimuli.

Chapter 4
Neural and kinematic dynamics of interference resolution

4.1. Introduction

As we discussed in previous chapters, adapting our behaviour according to contexts and internal goals is one of the most fascinating aspects of human cognition. However, still little is known about the mechanisms through which we are able to implement this ability. We have previously introduced the DMC model (Braver, 2012), suggesting that cognitive control may work by anticipating the interference (i.e., proactive control), or as a mechanism engaged after its detection (i.e., reactive control). We have also reported how previous studies using different versions of the Stroop tasks demonstrated that by manipulating the PC at the global, list-wide level it is possible to modulate task demands and the employment of proactive control, whereas by manipulating PC at the local, item-specific level it is possible to elicit reactive control (Bugg & Chanani, 2011; Bugg & Crump, 2012; Bugg, et al., 2011; Logan & Zbrodoff, 1979). Generally, these findings showed that the Stroop effect (and interference) is reduced in low-PC conditions. However, these two manipulations have been mainly studied separately, with only one study investigating their independent effects in the same participants (Gonthier et al., 2016). Moreover, an important aspect of the dissociation between proactive and reactive control regards the different temporal dynamics with which they solve the interference.

These reasons led us to the design Study 2 presented in Chapter 3, where we studied computer mouse trajectories to capture the online temporal development and updating of the responses. Our results showed that both the LWPC and ISPC manipulations were effective in modulating the interference, leading to smaller Stroop effects in the low-PC conditions. Moreover, also the time course of trajectories' development and the control effects were very similar between the two types of manipulations. Therefore, we suggested that proactive and reactive control, that are hypothesized to be engaged in LWPC and ISPC manipulations respectively, may work very similarly. These findings suggested that these two manipulations may only differ in the amount of evidence that participants can collect about how likely distracting information (or interference) may occur. It follows that the more it is possible to expect an interference in advance, the earlier the attentional bias toward the relevant information can be imposed. To shed light on this temporal aspect, we used another helpful tool in the study of cognitive processes: EEG. Indeed, in the present study we aimed at extending our previous findings by adding EEG recording. Despite the analysis of the mouse trajectories provided some insights on the temporal dynamics of interference resolution process, EEG recording would allow to have a clearer picture of the neural dynamics responsible for cognitive control in the temporal window before stimulus onset, constituting a more direct window on the anticipatory bias that can be imposed.

Moreover, with the present study we also aimed at making a comparison with Study 1 presented in Chapter 2, in order to understand if the brain oscillations that we found involved in interference resolution process are influenced by the manipulation of PC. Some studies tried to shed light on the temporal course of interference resolution and how it is modulated by PC manipulations by investigating ERP components (see Appelbaum, Boehler, Davis, Won, & Woldorff, 2014; Colás, Capilla, & Chica, 2018; Jiang, van Gaal, Bailey, Chen, & Zhang, 2013; West, Bailey, Tiernan, Boonsuk, & Gilbert, 2012). However, still few works have been conducted focussing on event-related spectral perturbations (ERSP), despite the advantages of this technique. Indeed, decomposing EEG signal in its time and frequency properties can greatly help in understanding the functional role and neural mechanisms of cognitive control processes, as it has been suggested that different frequencies may play different roles in cognitive processes (Fries, 2005). As previously mentioned, theta band over midfrontal regions is the mostly reported signature of cognitive control, especially in paradigms involving conflicts and interference resolution. In particular, it has been proposed that it may correspond to an early signal of the need to exert cognitive control (Cavanagh & Frank, 2014), and the findings of our first study provided some additional support for this idea. Furthermore, beta band has been recently proposed to have a more important function in cognitive processes than previously thought. For example, previous literature suggested that these frequencies may have different cognitive roles, such as in maintaining the “status quo” (Engel & Fries, 2010), in the endogenous reactivation of contents representations (Spitzer & Haegens, 2017), and that their suppression may be linked to surprise about sensory events (Meindertsma et al., 2018), which is in line with the two previous evidence. Moreover, also evidence from our laboratory is in line with these findings, pointing toward a role for beta band in the resolution of interference (see Chapter 2; Ambrosini & Vallesi, 2017).

It should also be noted that, in the DMC framework, very few studies tried to disentangle the neural oscillations involved in proactive and reactive control. Generally, all these studies reported an involvement of theta frequencies in both proactive and reactive control. For example, Eschmann and colleagues (2018) used two different tasks, one eliciting proactive control (i.e., delayed match to sample task) and the other reactive control (colour-word Stroop task with no PC manipulation), and reported that theta was the main frequency band found in both tasks. However, the authors reported that the distribution of theta in the proactive task was more focally localized over frontal regions, whereas the one from the reactive task had a broader topographical distribution, even though always localized over frontal-midline regions. Other evidence investigating the dissociations between proactive and reactive control came mainly from task-switching studies, where proactive control can be activated in the cue-to-target interval, and reactive control in managing the interference after target onset. These findings showed again that theta band plays an active role in both proactive and reactive control (Cooper et al., 2015; Cooper, Wong, McKewen, Michie, & Karayanidis, 2017). However, also beta band has been reported in some studies investigating proactive and reactive control, but mainly using different paradigms. A recent study using a stop-signal task suggested that the proactive anticipation of conflicts was correlated with theta band, whereas beta band correlated with prediction error (Chang, Ide, Li, Chen, & Li, 2017). Another study using a visual search paradigm suggested that beta band suppression was associated to the use of proactive control, whereas enhancement of delta/theta band was elicited in a condition requiring reactive control (Van Driel, Ort, Fahrenfort, & Olivers, 2019). Moreover, also evidence from interference paradigms, such as the Stroop, needs further investigation.

4.2. Rational and hypothesis

Hence, with this study we aimed at answering multiple questions. First, we wanted to verify if we could find the same neural correlates of the Stroop effect that have been reported in previous literature and that we obtained in Study 1 (see Chapter 2). Second, we wanted to verify if we could find the same behavioural results obtained in our mouse-tracking study (see Study 2 in Chapter 3), analysing the same measures and testing their replicability.

Third, but most importantly, by adding EEG recording, we wanted to extend the findings of the mouse-tracking study, making it possible to investigate the neural mechanisms active during the temporal window before stimulus presentation, where proactive control is mainly supposed to be involved. Indeed, in our Study 2 we found that both LWPC and ISPC manipulations modulated Stroop interference and that the temporal course of their trajectories showed also similar patterns. The findings suggested that the two control modes may work in a similar way. Therefore, by recording EEG signal, it is possible to investigate the neural mechanisms underlying the anticipation of the interference, which can be considered a marker of proactive control employment.

Fourth, if both theta and beta bands play a role in resolving the cognitive interference, it is possible to hypothesize that they may interact in the execution of the temporal cascade of events. In particular, we aimed at testing this hypothesis by means of the analysis of the phase-amplitude coupling (PAC) between these bands. Indeed, it has been demonstrated that the phase of low frequency oscillations can be entrained with external inputs and internal cognitive processes (Canolty & Knight, 2010). Moreover, the connection between the phase of low frequency and the amplitude of high frequency oscillations has been suggested to be a potential mechanism to coordinate the timing of neuronal firing (Szczepanski & Knight, 2014), cortical processing (Axmacher et al., 2010) and possibly long-range information transfer between different networks (Canolty & Knight, 2010). For these reasons, we administered the very same paradigm that we adopted in our mouse-tracking behavioural experiment. However, in this study it was not possible to administer all the PC manipulations that we previously used (at the list and item level), because for the EEG analysis we needed to increase the number of trials in each manipulation, and therefore we adopted only a list-wide manipulation (LWPC).

Behaviourally, we expected to replicate the results of our mouse-tracking experiment, finding a modulation of the Stroop effect as function of the PC, with a consistent pattern for all the mouse measures extracted. For the EEG, we expected the Stroop effect to be characterised by an increase in theta power (Ergen et al., 2014; Hanslmayr et al., 2008), and a main suppression of beta power for incongruent trials. Moreover, we expected to find a modulation of the magnitude of the Stroop effect as function of the PC mirroring the pattern of the behavioural results. We hypothesized blocks with low PC to show the smallest increase in theta and suppression of beta power, because of the additional use of proactive control.

Concerning our predictions for the pre-stimulus period, we expected to find specific spectral correlates of proactive control in this time window. Given the extensive evidence for the involvement of theta band in tasks of interference resolution and of proactive preparation in task-switching paradigms, we assumed to be likely to find this frequencies band also in the time before stimulus appearance. However, we also considered possible to find an involvement of beta band in this temporal window, as it has been previously reported its role in proactive control (Van Driel et al., 2019), and in line with evidence proposing a role of beta in updating and tracking probabilistic quantity (Gould et al., 2012). In respect to the expectation about the PAC between theta and beta frequencies, to our knowledge, there are no previous studies reporting such modulation and involvement in interference paradigms. For this reason, we did not precisely define directional hypotheses and thus investigated this point in an exploratory fashion. Generally, however, we expected the phase of the evoked theta activity to modulate the evoked beta power as a function of cognitive demands and the type of cognitive control exerted (e.g., proactive control in low-PC blocks).

4.3. Methods

4.3.1. Participants

We recruited 44 healthy young participants (females = 36, mean age = 23.61 years, range = [19 39 years]), all Italian native-speaker. We conducted an a priori sensitivity power analysis on G*Power software (Faul et al., 2009) revealing that 36 participants were needed to have a statistical power (1-β) of 0.80 to detect a within-subject significant difference (α = 0.05) corresponding to a medium effect size (Cohen's d) of .34 with a between-measures correlation of .75, as estimated from our previous study. We used the same modified version of the Edinburgh Handedness Inventory (Oldfield, 1971) previously administered (see section 3.3.1), applying the same inclusion criterion for left-handed participants (average handedness score = 74.23, SD = 35.89). All the participants signed an informed consent before taking part to the study and they were reimbursed € 15 for their time. All the experimental methods had ethical approval from the Research Ethics Committee of the School of Psychology of the University of Padua (prot. N. 2714) and was conducted in accordance with the guidelines of the Declaration of Helsinki (World Medical Association, 2013).

4.3.2. Design and stimuli

We administered the same 4-choice spatial Stroop task previously used in Study 2 (see section 3.3.2), with some minor differences. One difference was that we used Psychtoolbox (Version 3, PTB-3; Kleiner, Brainard, & Pelli, 2007) to collect mouse trajectory on the computer screen. Moreover, we also changed the monitor used, as this time we recorded data through a 19-inch monitor, but we maintained the same resolution (1024 x 768 pixels). Stimuli were presented in the very same way as already discussed in the methods of Study 2 (see section 3.3.2) and there were no changes in the instruction of the task. However, another difference concerned the duration of the trial, as we needed to extend the time of the events in order to efficiently compute time-frequency analysis. A trial began when participants clicked on the start square, which caused the four white response squares to appear in the corners of the screen, but no arrow was presented; participants were asked to remain still on the start square until the arrow appeared. After 1500 ms the arrow appeared in one of this white square and participants had up to 750 ms to initiate the movement and had up to 2000 ms to complete their response. After responding an additional blank screen was presented for 1500 ms, constituting the ITI, where participants were instructed to not move the mouse. After this time, the start square appeared again at the center of the screen and participants could move back and click on it to make the following trial appear, at their own pace. Figure 4.1. summarizes the trial events (cf. Figure 3.2 for differences with Study 2).Concerning the PC manipulations adopted in the present study, we could apply only the manipulation at the list-wise level (LWPC), because we needed to raise the number of trials to perform EEG analysis, but we also needed to avoid an excessive task length. Specifically, we presented 8 experimental blocks made by 74 or 98 trials and 3 training phases made by 16 or 24 trials that were presented in a pseudorandom order and were counterbalanced across participants. There were the same three different LWPC conditions previously used: 3 blocks of 98 trials in the low-PC (25%, LW25PC), 2 blocks of 74 trials in the equal-PC (50%, LW50PC), and 3 blocks of 98 trials in high-PC (75%, LW75PC) conditions. Again, blocks with the same manipulation of PC were presented always one after the other and preceded by the same specific training phase. However, participants were not aware of the training phase nor of the change of PC. Between each block there was a break in which participants could rest and decide when to continue with the following one.

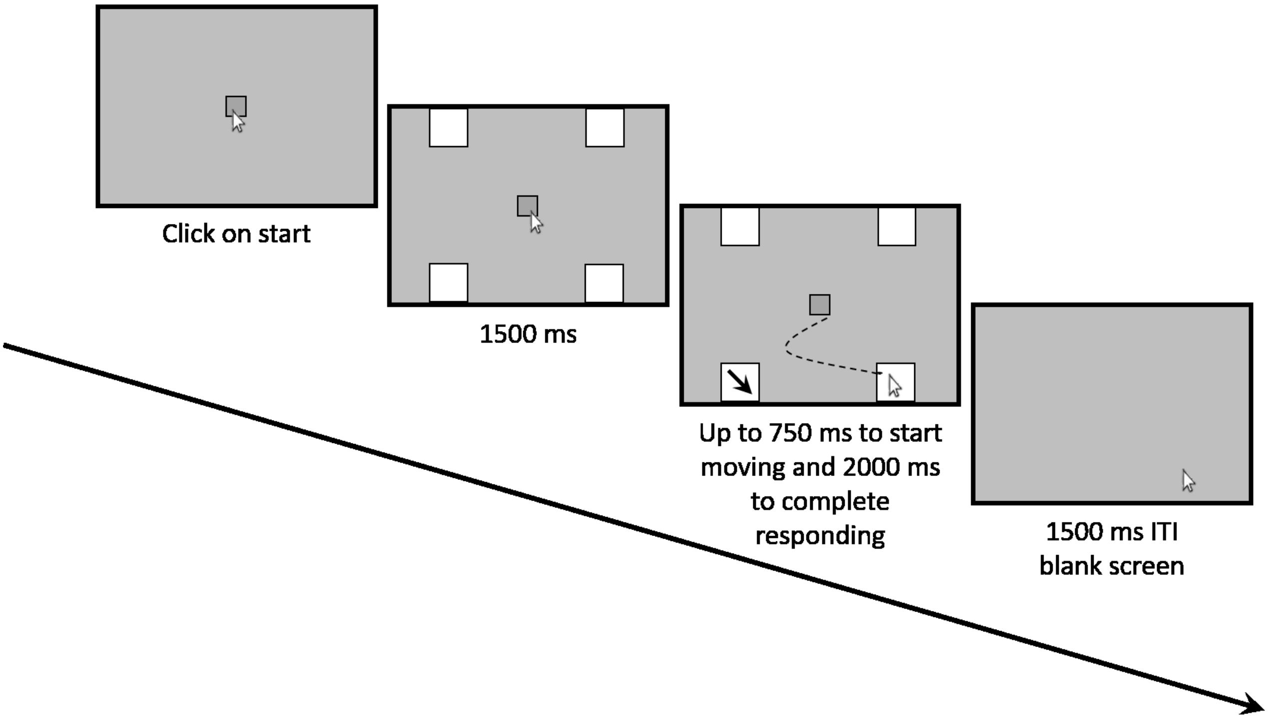

Figure 4. 1. Experimental paradigm
This is an example of incongruent trial, where it is possible to appreciate the differences in events durations (cf. Figure 3.2).

4.3.3. EEG recording

All the data were recorded using BrainAmp amplifiers (Brain Products, Munich, Germany) from 64 Ag/AgCl electrodes mounted on an elastic cap (EASYCAP GmbH, Germany), according to the 10-10 system. We recorded electrooculographic (EOG) activity with an electrode placed under the left eye. All electrodes were adjusted before testing to maintain impedance below 10 KΩ. All electrodes were references to FCz during the recording and an electrode positioned at AFz was used as ground. Raw data were filtered online between 0.1 and 100 Hz and sampled with a rate of 500 Hz.

4.4. Data analysis

4.4.1. Mouse-derived measures

We extracted the very same mouse measures used for Study 2, and we applied the same pre-processing steps in Matlab (version 2017b; The Mathworks, Inc. Natick, MA), as explained in section 3.4.1 more in details.

4.4.2. Behavioural statistical analysis

Statistical analysis on mouse-derived measures were conducted exactly as those for Study 2, for both trial-level and time-level measures. We included the same dependent and independent variables, scaled and centered as previously done. Except for the ISPC regressor, the model fitted the same regressors seen for Study 2, and the final one was similarly re-fitted after excluding observations with absolute standard residuals greater than 3 (never more than 3% and 3.5% of observations were eliminated for the *trial-level* and *time-level* measures respectively). Statistical significance of the coefficients was tested through *lmerTest package* as described in the previous study (see section 3.4.2).

4.4.3. Comparison between mouse-derived measures of Study 2 and Study 3

We compared the mouse-derived measures of this study (Study 3) with those extracted for Study 2. To do so, we applied the same procedure as above (described more in deep in Section 3.4.2.), fitting a new regressor for the study (Study2 vs. Study 3). This procedure was applied for both *trial-level* and *time-level* measures. Therefore, the final model included as fixed effects the total number of trials (cTrialT) and the parameters needed to test for the interaction between LWPC, Congruency and Study. As random effects, we allowed by-subject random slopes for the interaction between LWPC and Congruency. As previously done, the final model was re-fitted after excluding observations with absolute standard residuals greater than 3 (never more than 3% and

3.5% of observations were eliminated, respectively for *trial-level* and *time-level* measures) and then tested for statistical significance.

4.4.4. EEG pre-processing

The analysis of EEG data was performed using MATLAB (Version 2013b; The MathWorks, Inc. Natick, MA) scripts and functions from the EEGLAB toolbox (version 13.4.4b; Delorme & Makeig, 2004). Raw continuous data were filtered offline using zero-phase Hamming windowed sinc FIR high-pass and low-pass filters (cut-off frequencies: 0.1 and 90 Hz, transition bandwidth: 0.2 and 20 Hz) and a notch filter to remove line noise (cut-off frequencies: 49.5 and 50.5 Hz, transition bandwidth: 1 Hz). Then, we applied a stronger pre-processing in order to create a temporary cleaner dataset to be submitted to the independent component analysis (ICA) algorithm, to make the identification and removal of artifacts easier (Winkler, Debener, Müller, & Tangermann, 2015). In particular, the temporary pre-processing steps were as follows: 1) we applied a stronger high-pass filter at 1 Hz, 2) we detected bad channels by means of clean_channels function, using a correlation threshold of 0.5 (this criteria led to the exclusion of 1.73 channels on average, SD = 1.6, range = [0 5]), 3) we segmented data into epochs (from -2500 ms to 3000 ms) with respect to the stimulus onset, 4) we detected and removed bad epochs by means of improbability and kurtosis criteria (SD > 5 for single channel and SD > 3 for global threshold). Subsequently, we performed ICA on this dataset to correct for eye movements, blinks and muscular activity based on scalp topography, evoked time course and the power spectrum of the components. The resulting ICA solution was finally applied to the original dataset after the exclusion of bad channels (so to have the same number of channels in the two datasets) and a segmentation into epochs of the same length of the temporary dataset (from -2500 ms to 3000 ms). In this way, we obtained EEG data cleaned from artifacts detected by ICA. Note that the epochs were created so to fully include the 1500 ms of the screen following the start of the trial and preceding the onset of the experimental stimulus.

At this point, bad channels were interpolated by using a spherical spline method (Perrin et al., 1989), data were re-referenced to a common average reference, and baseline correction was applied from -200 to 0 ms. Afterwards, we used an automatic procedure to detect artifactual epochs based on extreme values thresholding (+/- 125 μV), improbability and kurtosis criteria (SD > 6 for single channel and SD > 4 for global threshold) and abnormal trend in data (maximal slope allowed = 25 μV/s and minimal R2 allowed = 0.3). Moreover, this procedure was joined with the Trial by Trial (TBT) plugin of EEGLAB, which allows to reject and interpolate channels on a trial by trial basis. In particular, if an epoch had more than 6 bad channels, it was removed; on the contrary, if these criteria were not met the channels were interpolated. Finally, we used the Current Source Density (CSD) Toolbox (version 1.1; Kayser, 2009; Perrin et al., 1989) to estimate surface potentials. For this step we re-referenced the EEG data to Oz, and we used the default parameters values (m = 4; lambda (smoothing constant) = .00001). However, we did not recover the data from this channel, so Oz was excluded from further analysis (total number of channels = 63).

4.4.5. Time-frequency analysis

We extracted event-related spectral perturbations (ERSP) in the frequency range between 4 and 80 Hz (linearly spaced, 1 Hz resolution) using wavelets with a temporal window of around 834 ms. This corresponds to a linear increase in the number of wavelet cycles from 3 to 40, from 4 Hz to 80 Hz respectively. Baseline correction was applied trial by trial with the divisive method using the average of power of the entire length of the epoch as baseline in order to avoid any bias due to the choice of the baseline window (note also that we expected to find PC-dependent differences in the pre-stimulus time window -reflecting the engagement of proactive control- so we wanted to avoid using it as a baseline).

Similar to Study 1, statistical differences between the Stroop effect of the different PC manipulations were tested through the Threshold-Free Cluster-Enhancement (TFCE) method, which allows a non-parametric correction for multiple comparison ($p < 0.05$; Smith & Nichols, 2009). This test was applied including all the 63 channels, all the 233 time points covering a time window from -2083 to 2581 ms with a resolution of approximately 22 ms, and all the 77 frequencies ranging from 4 to 80 Hz. Despite the analysis was conducted on each single frequency, in order to facilitate the explanation of the results, we will describe them referring to the following frequency bands: theta (4-7 Hz), alpha (8-12 Hz), beta1 (13-18 Hz), beta2 (19-24 Hz), beta3 (25-30 Hz), gamma1 (31-45 Hz), gamma2 (46-65 Hz) and gamma3 (66-80 Hz).

We first tested for the simple effects of Congruency factor (incongruent vs congruent Stroop condition) in each experimental block (low PC, equal PC, high PC) and then we assessed whether the PC manipulations modulated differently the ERSP Stroop effect (Congruency by PC interaction). For the sake of clarity in the visualization of the results, we reported the simple effects of Congruency separately for the three blocks, but we considered and described only the results emerged from the interaction. As for Study 1, all the results reported in the test were significant at an alpha level of .05 both at the single spatio-temporo-spectral sample level and at the cluster level, thus corresponding to a critical *t* value of ± 2.02 (df = 43).

Lastly, we run a second set of analyses to investigate PC-dependent differences in the power spectrum of the *pre-stimulus* temporal window. For this analysis, it was not our aim to test for the Stroop effect, but only for PC effects. Indeed, it was not possible to predict the congruency of an upcoming trial, so the distinction between congruent and incongruent trials made no sense during the pre-stimulus period. Therefore, we extracted the power spectrum for each PC condition separately, but without distinguishing between congruent and incongruent trials. However, as the relative proportion of congruent and incongruent trials greatly changed across PC conditions, we first balanced their number in each PC condition before extracting time-frequency data by randomly choosing the trials[4]. Finally, we computed the power spectrum in the last 1000 ms of the pre-stimulus epoch (i.e., from -1000 to 0 ms relative to the stimulus onset) with a 20-ms resolution

---

[4] Note that results from the post-stimulus period did not change when balancing the number of congruent and incongruent trials across conditions.

by applying the same wavelet approach described above[5]. However, in this case we did not correct for a baseline, as we aimed to assess the temporal dynamic of the intrinsic, rather than evoked, power spectrum in the pre-stimulus epoch. Moreover, given the characteristics of our paradigm, the use of any time window could have potentially biased the computation of task-related power spectra, especially in the beta band due to the participants' hand movements. Note also that our statistical analysis (see below) contrasted task-related power spectra across conditions but within subjects, so any subject-dependent differences in the overall characteristics of the spectral signals was automatically controlled for.

This was done by means of TFCE method (Smith & Nichols, 2009) to test for existing differences between the PC manipulations we used. Moreover, we included all the 63 channels, 51 timepoints covering the time before stimulus presentation and soon after it (i.e., from -1000 to 0 ms every 20 ms), and the frequencies from 4 to 45 Hz. Frequencies are divided in different bands for descriptive purposes, as reported above. We considered only results that were significant at an alpha level of .05, corresponding to a critical t value of ± 2.02 (df = 43).

4.4.6. Phase-amplitude coupling analysis

We assessed if the phase of theta frequencies modulated the power in beta frequencies. In particular, we chose to test this coupling in the beta2 range (19-24 Hz), also to investigate the functional meaning of the time-frequency findings from the present study and Study 1. To do this, we applied a sinc FIR filter to extract the EEG signals in the bands of interest (cut-off frequencies: 4 and 8 Hz for theta, 18 and 24 Hz for beta; transition bandwidth: 1 Hz). Then, for theta frequencies we extracted the signal from FCz channel (based on the literature reviewed in section 4.1, as well as on the present ERSP results), and we applied the Hilbert transform to extract its instantaneous phase. For beta2 frequencies we considered all the channels in an explorative way, and we applied Hilbert transform to extract the amplitude. We randomly selected a fixed number of trials for each

---

[5] Note that we did not include the first 500 ms of the pre-stimulus window to avoid motor contaminations due to the participants' movements to return with the mouse on the start square and click on it.

condition (congruent/incongruent and PC manipulations), corresponding to the minimum number of trials across all the conditions, so to have unbiased estimates. The amplitudes were then rescaled to z-points, on which a second Hilbert transform was applied to obtain their power envelopes. Then, we selected a temporal window from 200 to 600 ms after stimulus presentation and we computed the strength of the relationship between theta phase and the beta2 power amplitude (PAC). We chose this temporal window based on the present ERSP results, because it showed the earlier involvement of midfrontal theta and the subsequent beta2 involvement. The PAC value was computed by applying the subsequent formula (Canolty et al., 2006):

$$PAC = \left| \frac{\sum_{t=1}^{n} e^{i\Delta_t}}{n} \right|$$

where Δ is the difference between theta phase and the envelope of beta2, n is the length of this vector and t represents the time point. We computed a PAC value for each trial and then we calculated the average for each PC manipulations. Next, to assess the strength of the PAC values, we employed a non-parametric approach. To do so, we created a null-distribution of PAC values by shuffling the temporal information of the theta phase in each trial before computing the PAC as detailed above. We repeated this procedure for 1000 times in order to obtain a null distribution of mean PAC values for each condition. Then, based on this null distribution, we transformed our observed PAC values in z scores (i.e., by subtracting the mean of the permuted PAC values from the observed PAC value and then dividing the result by the SD of the permuted PAC values). Finally, we tested for statistical differences between the Stroop effects in the z-transformed PAC values in the two PC manipulations of interest (LW25PC, LW75PC). This was done by using the TFCE method (Smith & Nichols, 2009), similarly to what we did for the other analyses, but in this case only correcting for multiple comparisons across channels.

4.4.7. Brain-behaviour correlation analysis

We aimed to investigate more thoroughly the functional role of the spectral correlates of proactive control in modulating participants' interference resolution. To this aim, we investigate whether the PC-dependent modulation of participants' Stroop effect in mouse tracking performance could be explained by the PC-dependent differences in power spectrum during the pre-stimulus phase, that is, when participants can use the information about the likelihood of interference occurrence to proactively impose the early attentional bias needed to effectively resolve upcoming interference. To do this, we first computed spectral measures reflecting the degree of proactive control as the difference between high- and low-PC conditions in the power spectra computed during the last 1000 ms of the pre-stimulus temporal window as detailed in section 4.4.5. Then, we computed a composite behavioural score reflecting participants' ability to reduce their Stroop effects in response kinematics based on LWPC information. Specifically, for each of the 15 trial-level mouse tracking measures that we extracted (see section 3.4.1, for a detailed description of these measures), we first computed a cognitive control score as the difference between the Stroop effects (i.e., the difference between incongruent and congruent trials) in the high- and low-PC conditions (i.e., the LW75PC – LW25PC difference in Stroop effect). Then, we submitted these cognitive control scores to a latent variable analysis in order to extract a single latent factor that best explained their common variance (and thus excluding measure-specific effects). Our choice to extract a single latent factor was also validated by an exploratory factor analysis that we performed on mouse tracking measures obtained in Study 2. In this analysis, the optimal number of factors to be extracted was determined by carrying out a permutation-based parallel analysis (Horn, 1965) and the Velicer's minimum average partial correlation test (Velicer, Eaton, & Fava, 2000), and both procedures indicated that only one factor had to be retained, which accounted for 57% of variance in participants' performance.

Finally, we computed Pearson's correlations to assess associations between participants' mouse-tracking scores and pre-stimulus spectral measures. The statistical significance of these associations was assessed again by using the TFCE method (see section 2.3.2) to correct for multiple comparisons across channels, time points, and frequencies.

4.5. Results

4.5.1. Behavioural results

Figure 4.2 gives an idea of the general pattern of movement trajectories, resembling the one already reported for Study 2 (Chapter 3, Figure 3.3). As previously seen, trajectories for congruent trials moved directly toward the target, whereas those for the incongruent ones showed an increase in the magnitude of the interference as a function of the PC.

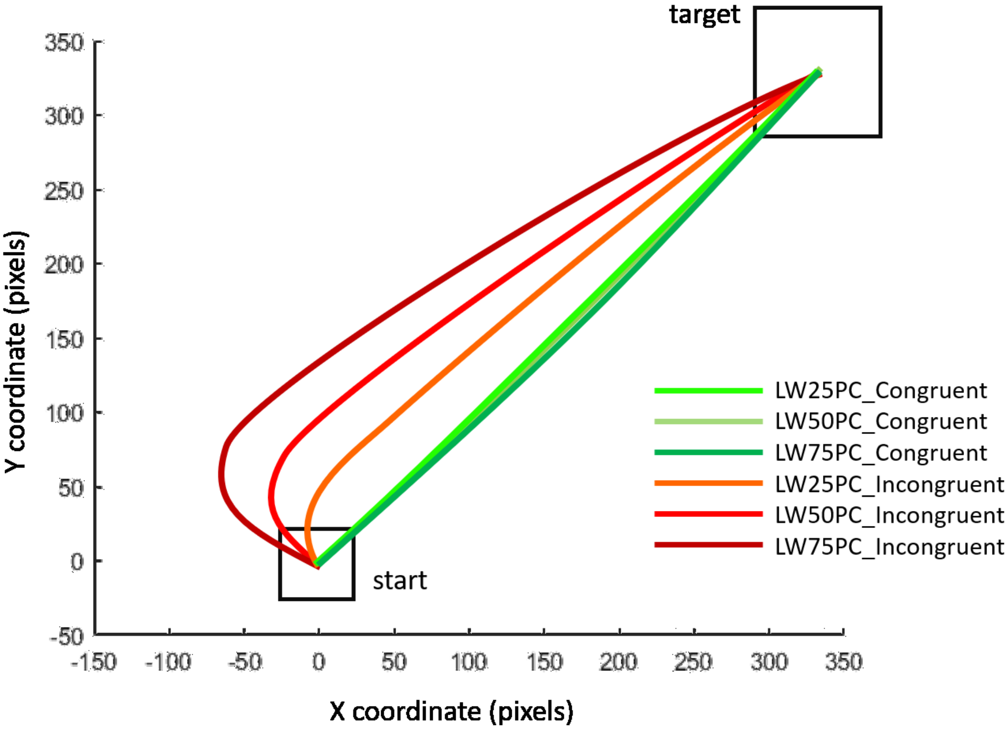

Figure 4.2. Average of trajectories of congruent and incongruent trials for all blocks

The figure represents the upper-right portion of the screen, with the average of the trajectories for congruent (cold, green colours) and incongruent (warm, red colours) trials in all the blocks. On x and y axes there are the x- and y-coordinate in pixels of the mouse-tracking space. All the trajectories are remapped in order to have the target on the upper-right corner and the irrelevant dimension on the upper-left. The start square is at the center of the screen. The plot is similar to the one previously shown in Chapter 3 (cf. Figure 3.3.). Again, we found the same pattern of trajectories, for which congruent trials showed a straight line toward the target and incongruent trials showed a gradual increase in the shift toward the irrelevant and distracting information from the low-PC blocks to the high-PC blocks.

Similar to what we did for Study 2, also in this section we summarized the results for the *trial-level* measures focussing on the effect of main theoretical interest, consisting in the simple effect of Congruency and the interaction between Congruency and LWPC manipulation. For a deeper description of the results of each mouse-derived measure and for a table with the results of the mixed-effects models see Appendix C.

Overall, the analysis showed the same pattern of results for all the measures considered and resembling the one obtained in Study 2. Importantly, all the measures reported the main effect of Congruency, showing a general cost in responding to incongruent trials that was reflected in a greater attraction toward the irrelevant dimension, more spatially complex and less smooth trajectories, more time to complete and initiate the movement. Also, the interaction between Congruency and LWPC manipulation was significant for all the measures, except MDd. We thus found the same consistent pattern (similar to that previously reported) for which the Stroop effect was modulated by PC manipulation, and in particular it was smaller (i.e., less interference) for low-PC condition. Table 4.1 reports the Estimates, Standard Error (SE), degree of freedom (df), t and p values for all the parameters fitted in the final model and for the representative *trial-level* measure used also for Study 2: Xmin. Figure 4.3 shows the effects on this same measure for congruent and incongruent trials.

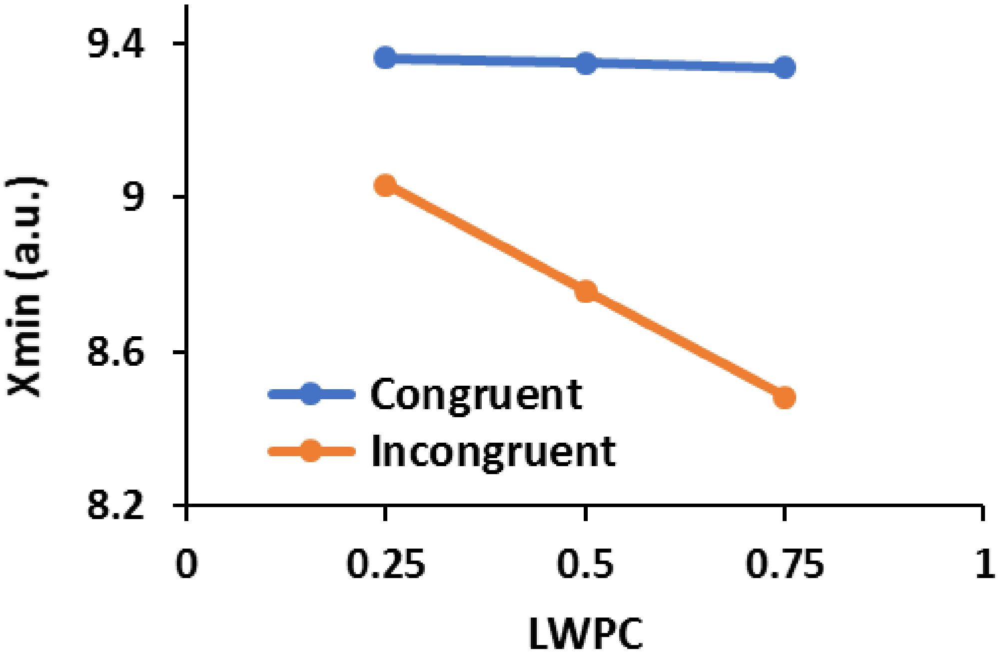

Figure 4.3. Behavioural results, Xmin measure

The figure shows the LWPC by Congruency effect for Xmin measure (y-axis in arbitrary unit, because it was transformed through BoxCox transformation; Box & Cox, 1964). On the x-axis there are the levels of LWPC manipulation, where -.25 corresponds to LW25PC, 0 to LW50PC and .75 to LW75PC. Blue line represents congruent trials, whereas the red line represents incongruent trials.

Table 4.1. Estimates, Standard Error, degree of freedom, t and p-values for the representative measure of Xmin

	Xmin				
EFFECT	Estimate	SE	df	t values	*p* values
Intercept	9.35	0.01	42.72	1820.86	0.000
Trial Tot	-0.01	0.00	4510.46	-6.07	0.000
LWPC	0.01	0.00	103.71	2.62	0.010
Congruency	-0.59	0.05	42.97	-11.11	0.000
LWPC*Congruency	-0.12	0.01	42.97	-11.15	0.000

Concerning the *time-level* analysis, all the measures showed significant effects of the main effect of Congruency, as well as the two-way interaction LWPC by Congruency. In particular, for the x-coordinate we found a significant effect of Congruency in the time bin from 23 to 81, due to the leftward shift of the trajectories for incongruent trials. The LWPC by Congruency interaction was significant in a time window comprising the time bins from 24 to 70. This effect was explained by a linear increase in the magnitude of the Stroop effects from the low-PC to the high-PC condition, with smaller leftward deviations of the trajectories for the incongruent trials in the low-PC condition.

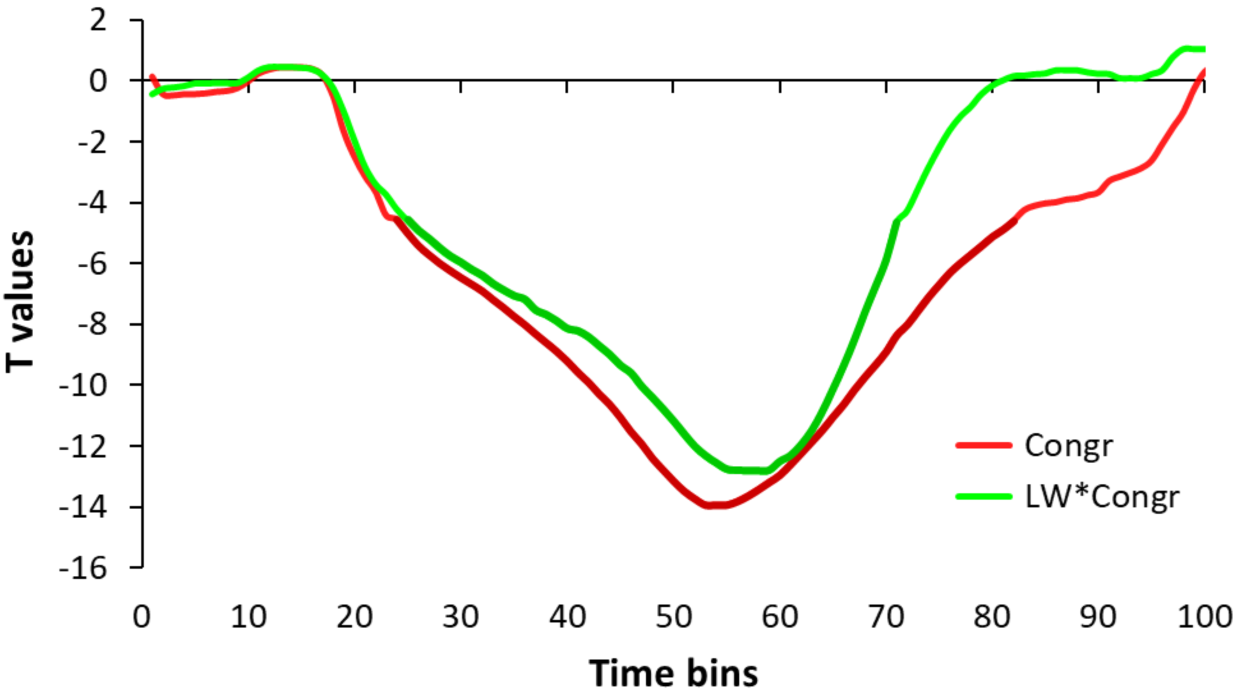

Figure 4.4. Results of time-level analysis on x coordinate

The figure shows the time course of t values (y-axis) for the effects of main theoretical interest: Congruency (Congr in red) and LWPC by Congruency Interaction (LW*Congr, in green). X axis represents the time bins. Darker and thicker portions of the lines indicate time window of statistical significance (corrected for multiple comparisons by means of the Bonferroni method).

Concerning the distance from the target, there was a significant main effect of Congruency for the time bins from 25 to 94, confirming that participants' trajectories reached farther away from the target for the incongruent as compared to congruent trials. The LWPC by Congruency interaction was significant in a time window comprising the time bins from 26 to 94. For this effect we found a similar pattern as the one found for the x-coordinate, with a similar linear increase in magnitude of the Stroop effect as function of the PC. Indeed, the difference in the distance from the target for the incongruent trials was significantly smaller for the low-PC manipulations.

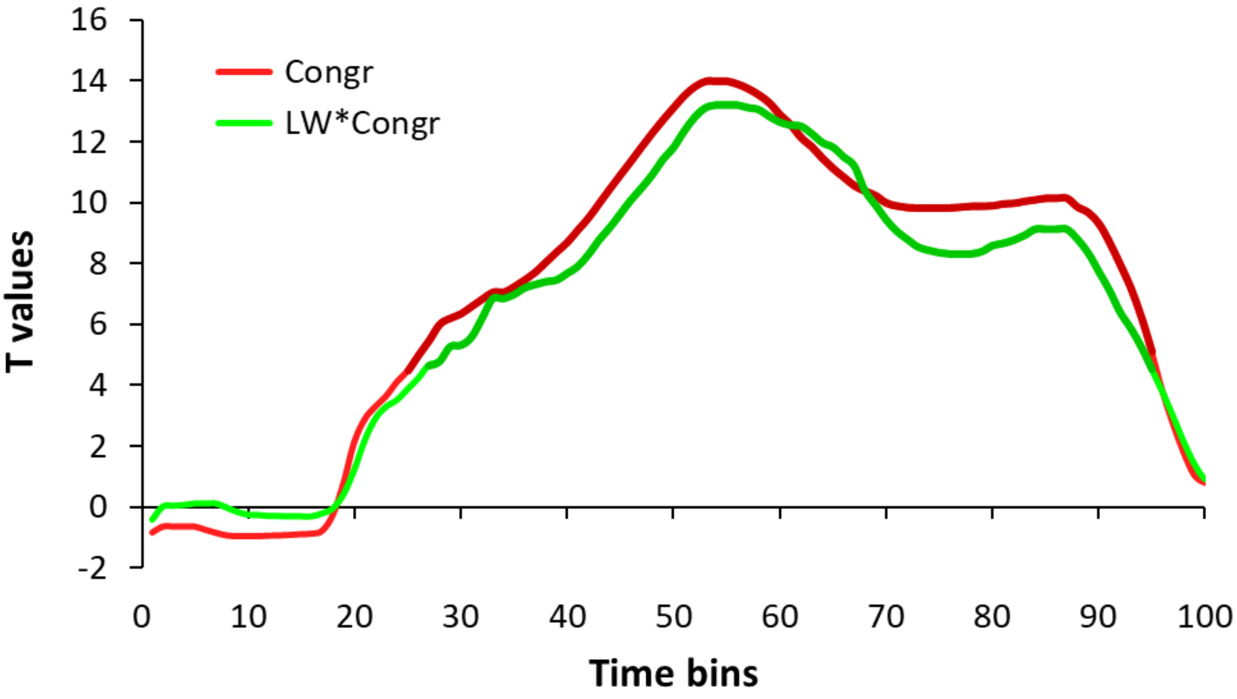

Figure 4.5. Results of time-level analysis on distance from target

The figure shows the time course of t values (y-axis) for the effects of main theoretical interest: Congruency (Congr in red) and LWPC by Congruency Interaction (LW*Congr, in green). X axis represents the time bins. Darker and thicker portions of the lines indicate time window of statistical significance (corrected for multiple comparisons by means of the Bonferroni method).

Finally, the velocity showed a significant main effect of Congruency for three time windows: the first one (time bins from 23 to 35) reflected the greater velocity for incongruent than congruent trials during the initial acceleration phase when the trial began; the second one (time bins from 41 to 49) reflected a decrease in velocity for the incongruent trials due to the need to adjust the trajectories following the erroneous deviation toward the interfering, alternative response option; the third (time bins from 55 to 95) reflected the greater velocity for incongruent than congruent trials during a new increase in velocity needed to give the correct response and counteract the erroneous deviation in the trajectory. The LWPC by Congruency interaction was significant in similar time windows, that is, respectively, in the time bins from 23 to 34, which corresponds to the initial increase in velocity for the incongruent trials; in the time bins from 41 to 49, which corresponds to the decrease in velocity for the incongruent trials; and in the time bins from 56 to 74, which corresponds to the following rebound increase in velocity for the incongruent trials.

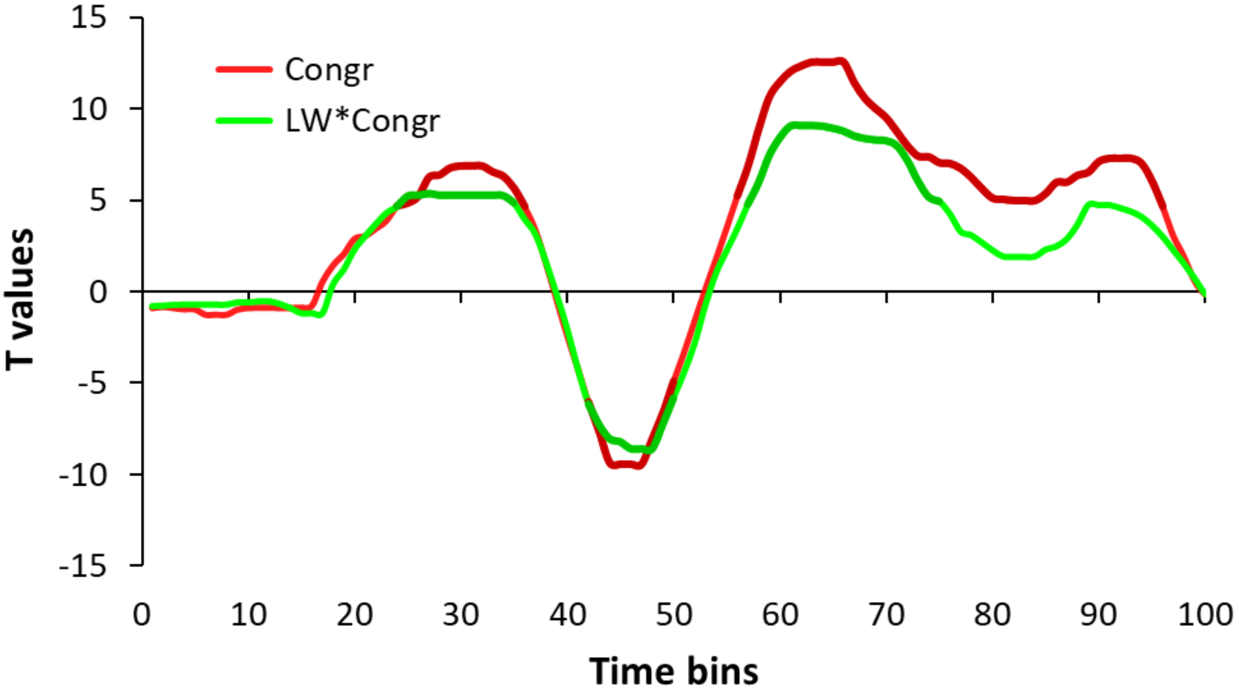

Figure 4.6. Results of time-level analysis on velocity

The figure shows the time course of t values (y-axis) for the effects of main theoretical interest: Congruency (Congr in red) and LWPC by Congruency Interaction (LW*Congr, in green). X axis represents the time bins. Darker and thicker portions of the lines indicate time window of statistical significance (corrected for multiple comparisons by means of the Bonferroni method).

4.5.2. Results of mouse-derived measures comparison for Study 2 and Study 3

Considering *trial-level* measures, from a first glance comparison, we found that almost all the mouse-derived measures in both experiments showed the same pattern of results. Especially focussing on the two primary effects of interest for our hypotheses (i.e., Congruency and the interaction LWPC by Congruency), we found that only IT reported a significant main effect of Congruency in Study 3 (i.e., mouse tracking-EEG), that was not observed in Study 2 (i.e., mouse tracking), whereas concerning the interaction LWPC by Congruency only the Start Angle showed a significant effect in Study 3 that was not present in Study 2. As explained in the data analysis description (see section 4.4.3), we formally tested between-experiment differences through mixed-effects models. We confirmed that all the effects were generally replicated for all the measures. However, focussing on the main effect of interest, which was the interaction LWPC by Congruency by Study, we found that all the measures except IT showed significant results in this three-way interaction. All of them reported weaker effects of the PC-related modulation of interference (i.e., Stroop effect) in Study 3.

Concerning the comparison between *time-level* measures of the two studies, instead, all of them showed the same pattern of results in both experiments. First of all, the main effect of Congruency and the LWPC by Congruency interaction were significant for all the measures in both studies, with only slight differences in the time courses of their effects. However, the mixed-effects models analyses revealed the existence of some between-experiments differences for the x coordinate and the distance from target measures, which were mainly due to weaker effects of the PC-related modulations of interference (i.e., Stroop effect) in Study 3 as compared to Study 2.

In particular, the analysis on the x-coordinate revealed a significant, overall effect of the LWPC by Congruency interaction (i.e., collapsed across studies) that was significant in a time window comprising the time bins from 25 to 68, peaking at the time bin 45. This effect was explained by a linear decrease in the magnitude of the Stroop effects from the high-PC to the low-PC condition. The LWPC by Congruency by Study interaction was significant for the time bins from 41 to 46, thus including the time window of the maximal effect, and was explained by smaller PC-dependent modulations of the Stroop effect for Study 3. Moreover, the analysis on the distance from the target showed a similar pattern of results, with a significant, overall effect of the LWPC by Congruency interaction (i.e., collapsed across studies) that was significant in a time window comprising the time bins from 27 to 86, peaking at the time bin 48. This effect was again explained by a linear decrease in the magnitude of the Stroop effects from the high-PC to the low-PC condition. The LWPC by Congruency by Study interaction was significant for the time bins from 40 to 48, thus including the time window of the maximal effect, and was again explained by smaller PC-dependent modulations of the Stroop effect for Study 3. By contrast, the analysis on the velocity revealed significant, overall effects of the LWPC by Congruency interaction (i.e., collapsed across studies), but no significant effects of the LWPC by Congruency by Study interaction, thus showing that the PC-dependent modulation of the Stroop effect was statistically undistinguishable across studies.

4.5.3. EEG results

Time-frequency-based analysis revealed numerous significant clusters of ERSP Stroop effects. For the purpose of this dissertation, we focussed more in depth on the description of results for beta and theta frequencies, for which we had strong a-priori hypotheses, and on the contrast of main theoretical interest, that is the comparison of the Stroop effects in LW25PC and LW75PC blocks (see Figure 4.3). The contrasts between LW25PC and LW50PC, as well as the one between LW50PC and LW75PC, are mentioned in Appendix C together with the simple effect of LW50PC.

Concerning the Stroop effect in LW75PC condition, there was an general involvement of lower frequencies (i.e., theta and alpha 4-13 Hz) over frontal and occipital channels immediately after stimulus presentation, which was followed by the recruitment of higher frequencies from beta1 up to gamma3 (i.e., 14-80 Hz) mainly over frontal and midfrontal channels and in a temporal window from 200 ms after stimulus presentation to about the end of the epoch.

Specifically, theta band showed two earlier significant clusters in the time window from after stimulus presentation to about 200 ms: one over frontal channels and the other involving posterior channels. Both effects were due to a stronger event-related suppression of power for incongruent trials as compared to the congruent ones. Moreover, there was another significant cluster starting around 200 ms until about 800 ms after stimulus presentation, which was due to a main power increase for incongruent trials compared to the congruent ones and that included also surrounding alpha frequencies. This cluster arose more focally over midfrontal channels and gradually spread on other locations over the scalp, including frontal and occipital channels. Finally, there was a last cluster from around 800 ms to the end of the epoch that interested frontal and occipital channels and was characterized again by a stronger power suppression for incongruent than for congruent trials.

Concerning the beta range, there was a first small cluster interesting just few ms in the temporal window from 0 to around 200 ms. This cluster was due to a stronger power suppression for incongruent trials as compared to the congruent ones, and it was mainly present for lower beta frequencies (14-20 Hz) over left frontal and parietal channels. From about 200 ms another cluster, due to a stronger power increase for incongruent trials, occurred for the entire beta range starting from frontal channels and gradually interesting also occipital regions of the scalp until around 600 ms, even though for the lower range of beta (beta1) it lasted until 800 ms, engaging mainly frontal channels. At the same time, around 400 ms a cluster due to a stronger power suppression for incongruent trials arose over midfrontal channels and interested mainly the upper range of the beta band (beta2, beta3), spreading toward lower frequencies range only after 600 ms. This cluster lasted until the end of the epoch and gradually spread over other channels in the surrounding areas of the scalp.

Concerning the Stroop effect in the LW25PC condition, we found generally a lower number of significant clusters. There was again an involvement of lower frequencies (i.e., theta and alpha) bands mainly over frontal and occipital channels, but not as early as the ones in LW75PC. Also, upper frequencies (mainly from beta2 up to gamma3) showed an involvement around the same time, engaging especially frontal and occipital channels. Instead, from around 600 ms to 1000 ms there was no significant cluster. Specifically, theta band showed a frontal cluster starting from 200 ms that lasted until around 600 ms and gradually involved also occipital channels that remained the only region of the scalp involved until around 800 ms. This cluster interested also surrounding alpha frequencies and was due to a stronger power increase for incongruent trials. Furthermore, around 1000 ms there was another cluster with the same effect, that lasted until the end of the epoch but had a less specific topography, engaging frontal and parietal portions over the scalp.

Beta range reported a less consistent pattern, showing small clusters around 200-600 ms that involved mainly frontal and posterior channels of the upper frequency bands (beta2, beta3).

These clusters were due to a stronger power increase of beta for incongruent trials. Moreover, beta band showed another cluster with the same effect, from around 1000 ms until the end of the epoch. This cluster arose from posterior channels and spread with time also on frontal regions, interesting mainly the lower range of beta frequencies (beta1, beta2). Figure 4.4 shows the ERSP traces for the frequency bands and experimental blocks summarized above.

Thus, the reported results suggest the existence of PC-related modulation of the ERSP Stroop effects, since LW75PC blocks showed earlier and more widespread spectral correlates of interference resolution. Indeed, the interaction analysis contrasting the ERSP Stroop effects in the two experimental conditions showed a number of significant PC-related modulation involving lower frequencies (< 12 Hz) and higher frequency mainly up to beta3 (13-30 Hz). Overall, lower frequencies reported an earlier involvement over midfrontal and frontal channels that lasted until the end of the epoch including also occipital channels, whereas higher frequencies were engaged in a later time window and were more widespread over the scalp.

It is important to note that the pattern of results of the interaction was similar to the simple effect observed for the LW75PC condition. Specifically, we found a midfrontal cluster in theta (and surrounding alpha frequencies) from around 200 ms to 800 ms that gradually interested also frontal and posterior regions. This effect was characterized by a larger Stroop effect in the LW75PC condition as compared to the LW25PC one. In particular, this result was due to the fact that in LW75PC condition there was a stronger power increase for incongruent trials, as compared to the congruent ones, that was almost absent over the midfrontal channels in the LW25PC condition. Regarding the beta range, we observed a significant cluster from around 800 ms involving mainly parietal channels, due to the fact that in LW75PC condition there was a bigger Stroop effect compared to LW25PC. In particular, LW75PC showed a stronger power suppression for incongruent trials, as compared to the congruent ones, that was again almost absent in the same temporal window and range for the LW25PC condition.

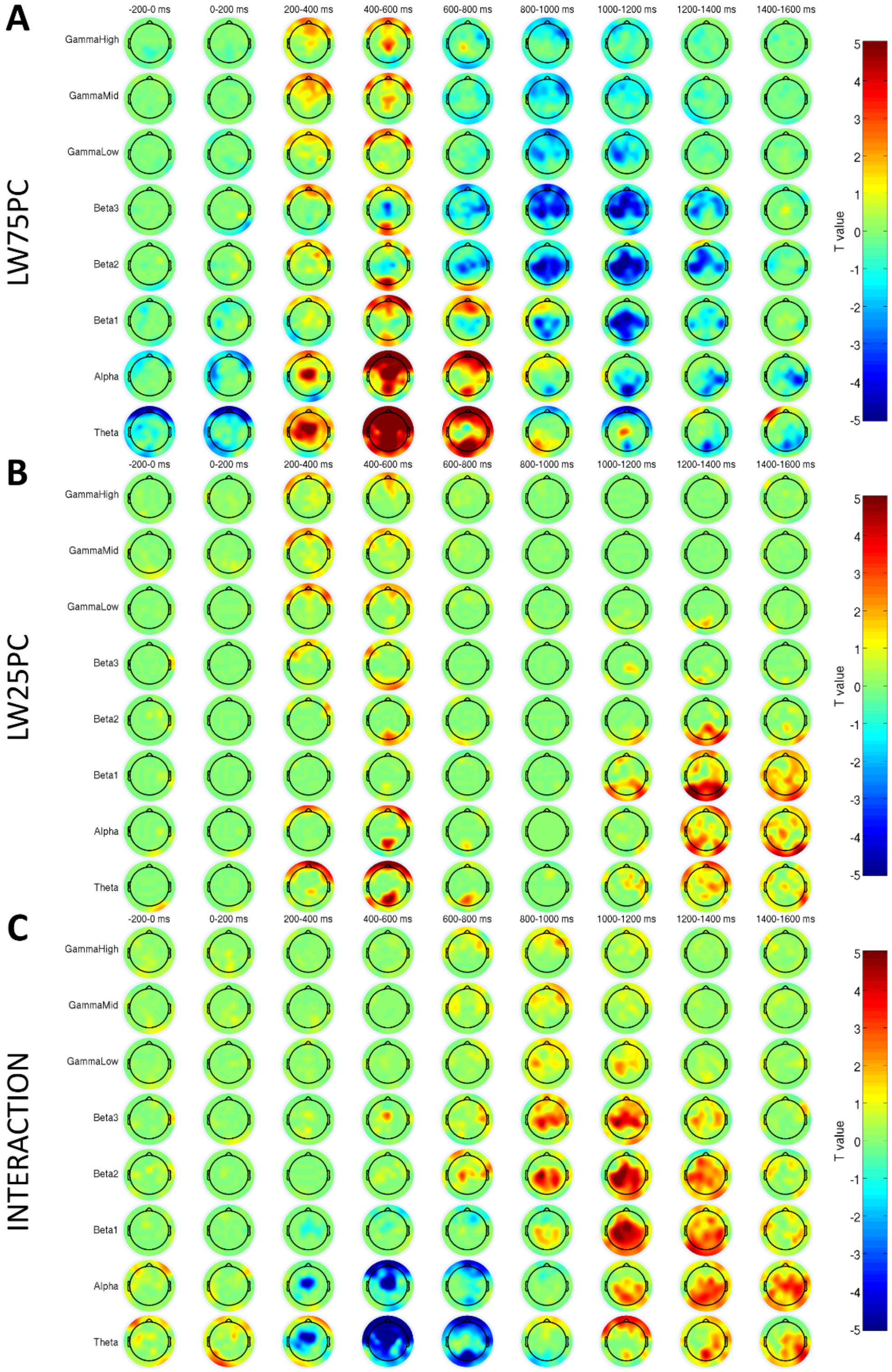

Figure 4.7. Results of the scalp-based ERSP analysis.

The figure shows the topoplots for the results of simple effect analysis in LW75PC (A) and LW25PC (B), as well as the results of the interaction analysis (C). Each row represents the average of each frequency band, whereas the columns represents the average of EEG activity every 200 ms from -200 ms before stimulus presentation. The topoplots show the *t values* of the significant results after TFCE. LW75PC blocks reported that the Stroop effect was characterized by a major involvement of theta frequencies in an earlier temporal window, as well as higher frequencies in a later temporal window. In LW25PC blocks, showed a visible less pronounced Stroop effect. These differences were reflected in the topoplots for the interaction analysis.

Summing up, the results from the interaction between Congruency and PC manipulations revealed a number of significant effects that interested different frequency bands and that were present mainly because of a stronger Stroop effect for the high-PC condition (i.e., LW75PC). Overall, lower frequencies seemed to be especially involved in the earlier processing of interference, with stronger Stroop effects in the high-PC condition. On the contrary, beta range seemed to resemble the results found in the younger group of participants for Study 1 (Chapter 2) and especially involved in the resolution of the interference, which was again stronger for the high-PC condition. Therefore, in line with what we expected, Stroop-related modulations were mainly visible in LW75PC blocks and mainly showed an involvement of lower frequencies soon after stimulus presentation and of higher frequencies (especially up to beta3) in a later temporal window.

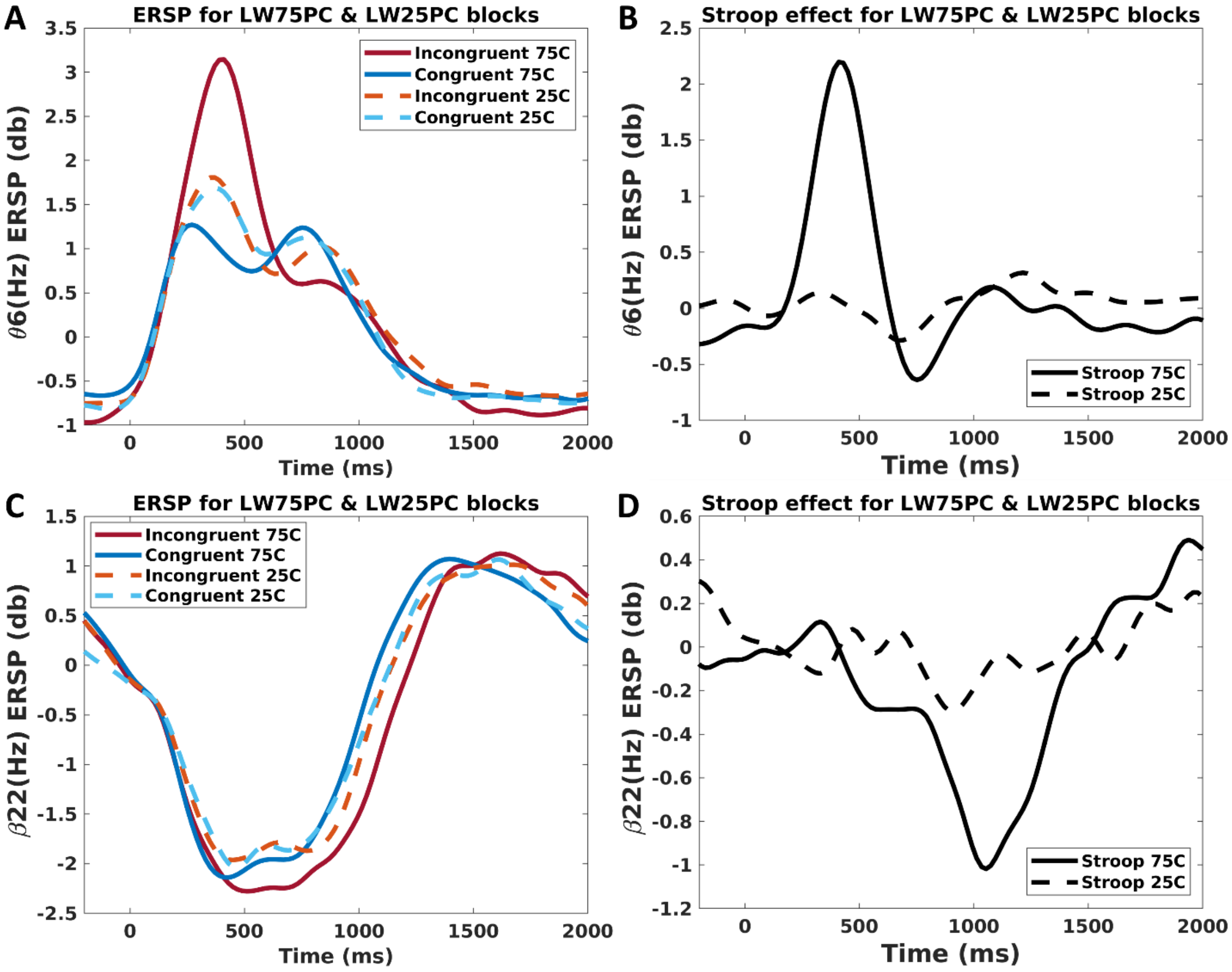

Figure 4.8. Representative results from scalp-based ERSP analysis
The plots show the ERSP traces for the results of simple effect analysis in LW75PC and LW25PC blocks for the theta (A) and beta (C) bands, as well as the results of the interaction analysis for the same frequencies (respectively, B and D). The plots in (A) and (B) depicts representative data for a frequency in the theta band (6 Hz) extracted from FCz channel, while the plots in (C) and (D) depicts representative data for a frequency in the beta range (22 Hz) extracted from FCz channel.

Concerning the results from the *pre-stimulus* window, we observed a number of significant PC-related power modulations. Here we focussed on the main effect of interest: the comparison between LW25PC and LW75PC. In particular, it was possible to recognize two main PC-related power modulations. The first one concerned the lower frequencies, mainly restricted to theta range, for which we found higher power in the low-PC condition (LW25PC), as compared to the high-pc one (LW75PC). This effect mainly involved midfrontal channels, particularly localized around FCz, and medial parieto-occipital channels. The second effect concerned higher frequencies (> 8 Hz), for which we found the opposite pattern of results, where the low-PC condition showed lower power as compared to the high-PC one. Topographically, this effect was less specific and widespread, as it involved most channels over the scalp (i.e., prefrontal, parietal and occipital regions). The topographies and the general power trend for the manipulations of interest are shown in Figure 4.5. A and B for theta, C and D for beta.

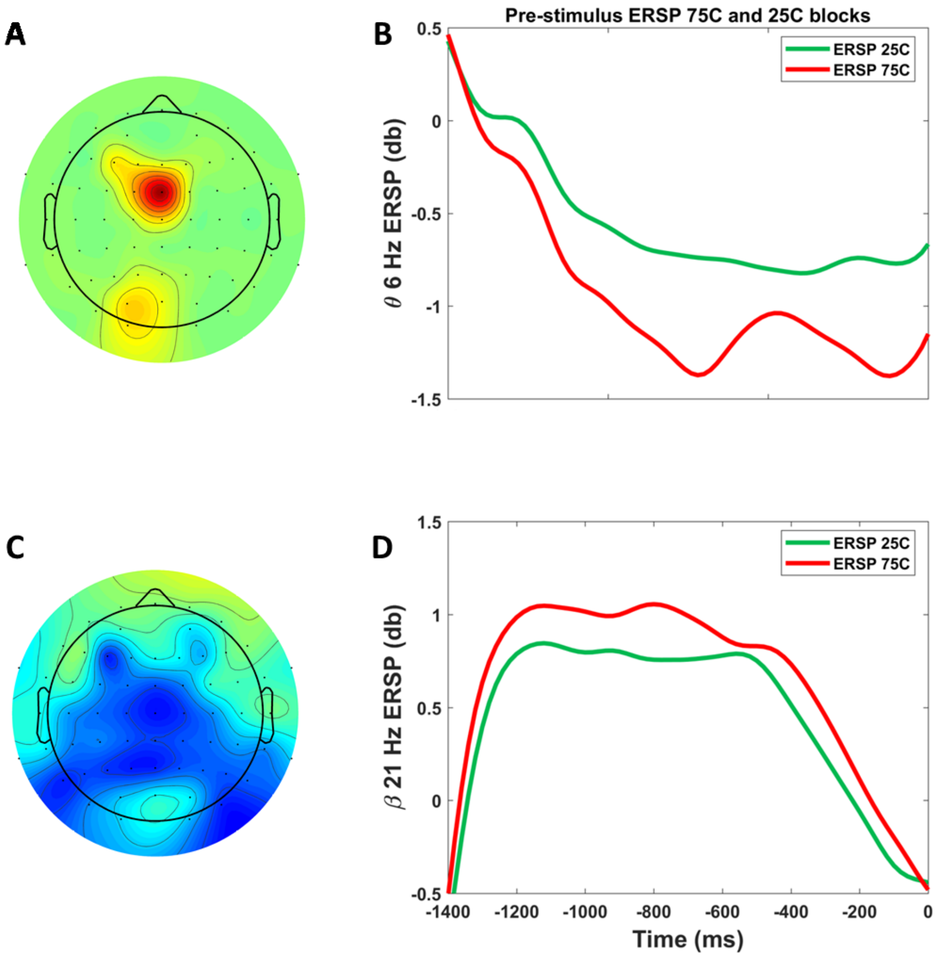

Figure 4.9. Representative results of power spectrum from pre-stimulus temporal window

Plot in A shows the averaged topography for a representative frequency in the theta range (6 Hz) during the time from -1000 ms to the stimulus presentation (time 0). B shows the power modulation, according to the PC manipulations used. It is possible to notice that the higher power was reported for the LW25PC condition (C25 in the legend, corresponding to the green line). C and D represent the same results, but for a representative frequency in beta range (22 Hz).

4.5.4. Phase-amplitude coupling results

We did not find any different significant modulation of theta-beta relationship depending on the PC manipulation used.

4.5.5. Brain-behaviour correlation results

We assessed the significance of the correlations between PC-dependent modulations of participants' mouse-tracking scores and pre-stimulus spectral measures, correcting the results for multiple comparisons through TFCE methods as detailed in section 4.4.7. Here, we focussed on the effects obtained for theta and beta bands. Theta frequencies showed two main clusters. The first one lasted from around -1000 ms to around -500 ms and had a widespread distribution over the scalp, mainly implying frontal, central and parietal electrodes over the left hemisphere and smaller frontal and temporal clusters of channels over the right hemisphere. The second cluster started at around -400 ms and lasted until stimulus presentation and was mainly localized over midfrontal channels, centered around FCz and Cz. Both these clusters showed similar correlations, so that better performance (i.e., greater PC-dependent reduction of Stroop effect in the mouse-tracking measure) was associated to a higher PC-related difference in pre-stimulus theta power.

Concerning beta frequencies, we found one significant cluster starting at around -800 ms and lasting until the presentation of the stimulus and localized mainly over midfrontal and left temporal channels. Similar to the theta clusters, also this one showed that better behavioural performance was associated to a higher PC-related power difference (which in this case was negative, thus explaining the negative correlation).

4.6. Discussion

The principal aim of this study was to shed light on the brain dynamics of proactive control in interference resolution. To this goal, we recorded EEG activity and mouse trajectories while participants were engaged in a spatial Stroop task with blocks at different levels of PC. We also aimed at comparing the EEG results with those previously found in Study 1 (Chapter 2) and the mouse-derived measures with those obtained in Study 2 (Chapter 3).

Our results revealed clear PC-dependent modulations of the Stroop interference, both at the behavioural and the neural level. These modulations confirmed our expectations and showed the same pattern: a smaller Stroop interference for blocks with low PC. Indeed, according to the predictions of the DMC model (Braver, 2012) and in line with previous literature of PC manipulations (e.g., Bugg & Crump, 2012; Bugg, et al., 2011; Gonthier et al., 2016), when PC is low at the block level, participants are able to use this information to impose an early attentional bias that allow them to anticipate the interference, which is considered to be an effect of proactive control. Instead, when PC is modulated at the item level but the probability of occurrence for congruent and incongruent trials is the same at the list-wide level, it is impossible for participants to prepare in advance and reactive control remains the main player to solve the interference. In Study 2 of this dissertation (Chapter 3), we manipulated the PC using both these levels and analysing mouse-derived measures, and we found that the underlying temporal dynamics of proactive and reactive control were more similar than what we expected. Therefore, we turned to study the functional differences between these two modes of control by focussing our investigation on the pre-stimulus temporal window, where only the proactive control can operate in low-PC blocks. This was one of the reasons why we implemented the present study, in which we added the recording of EEG signal to shed light also on this specific time.

The analysis of our mouse-tracking measures revealed a pattern of results very similar to the one found (for the same manipulation) in Study 2. From a first qualitative analysis, the average of the mouse trajectories showed the same pattern of attractions that emerged in Study 2 (cf. Figure 3.3 and Figure 4.2), with an increase in the magnitude of the interference as a function of the PC. Moreover, the mixed-effects analyses on both trial- and time-level mouse tracking measures confirmed this impression, showing significantly smaller Stroop interference in the low-PC block (i.e., LW25PC) as compared to the high-PC one (i.e., LW75PC). This can be taken as evidence that participants can bias more promptly their attention toward the relevant information when they can rely on evidence about the likelihood of interference occurrence. This is in line with the findings of studies proposing that this effect is due to the use of proactive control, which allows participants to anticipate the interference before its occurrence (Bugg, et al., 2011; Gonthier et al., 2016).

One of the aims of the present study was also to test if the results from mouse-derived analysis were the same between Study 2 (mouse tracking) and the present one (mouse tracking and EEG). When we specifically tested for between-experiment differences in mouse tracking results, both at the trial and the time level, we found that the results from Study 2 were confirmed, although there were some subtle differences among the two studies. In particular, for the *trial-level* measures, we found that PC-related effects on the Stroop interference were smaller in the present study as compared to Study 2. Similarly, for the *time-level* measures we found little differences for the x coordinate and the distance from target measures, which were again mostly due to weaker effects of the PC-related modulations of Stroop interference in the present study, as compared to Study 2. There are multiple possibilities for this result, which are evaluated more in details Chapter 5.

Despite this between-experiment difference, it is important to underline that the general pattern of results was replicated across all the measures, showing smaller Stroop interference for low-PC condition and an early time course of this PC-related modulations of the interference during response development. This confirms and extends existing findings from studies investigating the same LWPC effects, even though with other types of responses (e.g., Bugg et al., 2011; Gonthier et al., 2016). However, only few studies used mouse tracking to investigate cognitive control, but they administered only ISPC manipulations (Bundt et al., 2018; Ruitenberg et al., 2019).

To the best of our knowledge, this effect has never been studied through EEG and time-frequency based analysis. Our ERSP results also showed clear PC-related modulations of the Stroop interference, which mirrored the same pattern observed in the mouse-derived measures. Indeed, generally all the frequencies bands showed a decreased magnitude in Stroop interference for the low-PC condition. We identified two leading bands involved in the resolution of Stroop interference: theta and beta. In the high-PC blocks (i.e., LW75PC) we found the engagement of theta activity (but also surrounding alpha) localized over midfrontal channels in an early time window, starting soon after stimulus presentation. The inspection of the time course of this ERSP effect revealed that it was due to a significantly greater increase in the power for incongruent trials, as compared to the congruent ones. Critically, this ERSP Stroop effect was abolished in low-PC blocks (i.e., LW25PC). A similar finding was observed for beta frequencies, for which we also observed a significant reduction in the magnitude of Stroop interference as function of the PC. In particular, we found a main involvement of prefrontal and central channels starting from around 400 ms and lasting until about 1400 ms. This effect was characterized by a significantly greater power suppression for incongruent trials as compared to the congruent ones in high-PC blocks, which was abolished in the low-PC condition. These results thus showed that the same pattern of reduction of Stroop interference for low-PC blocks (i.e., LW25PC) can be observed also at the neurophysiological level.

Taken together, all the results of this study were in line with our expectations, and with previous findings from the literature. Indeed, midfrontal theta has been extensively reported in paradigms involving interference resolution and it has been suggested to be an early interference detection signalling the need to exert cognitive control (e.g., Cavanagh & Frank, 2014; Cohen, 2014). Moreover, evidence from other paradigms eliciting proactive and reactive control (e.g., task-switching) also showed that theta had a role in both modes of cognitive control (e.g., Cooper et al., 2015). Our findings are consistent with this proposed role of theta frequencies. Indeed, the higher increase in early midfrontal theta power we found for incongruent trials especially in the high-PC block (i.e., LW75PC) would correspond to the early detection of the interference signalling the need to exert more control to overcome the interference, which in this PC condition is particularly disrupting. Instead, when participants can rely more on the anticipation of the interference, like in the low-PC block (i.e., LW25PC), this effect disappeared, suggesting that when participants can prepare in advance to respond to the interference, its detection mechanism recruits fewer resources.

The involvement of beta band was also in line with our predictions. Indeed, it has been previously suggested that beta may be involved in interference resolution (Ambrosini & Vallesi, 2017) and may correspond to the mechanism of selection for task-relevant representations, consistent with the results of Study 1. However, our results for the beta band could also reflect an involvement of these frequencies in the online decision processes leading to the build-up and update of the response; this interpretation is consistent with evidence from animal studies proposing that beta band reflects the process of decision-making, and particularly the process of evidence accumulation that leads to the response outcome (Haegens et al., 2011). These findings are particularly relevant for our paradigm, because by means of mouse-tracking, it was possible to capture the kinematic signatures reflecting the process of decision-making and response updating.

Moreover, our results on the beta band are also in line with recent findings proposing that beta band may be involved in maintaining the "status quo" (Engel & Fries, 2010): in our Stroop task the "status quo" may correspond to the preferential elaboration of the stimulus position, which has a processing advantage as compared to the stimulus direction. For this reason, beta suppression may indicate a change in this state to favour the elaboration of the direction of the arrows, and this effect would be stronger for unattended incongruent trials in high-PC blocks (i.e., LW75PC), where there is less cognitive control. On the contrary, in low-PC blocks (i.e., LW25PC) where the degree of cognitive control is high, participants can rely on proactive control mode to impose an early attentional bias toward the relevant dimension (i.e., arrow direction), possibly reducing the need to "change the status quo".

As regards the power spectrum analysis in the pre-stimulus time window, we found again a main contribution of theta and beta frequencies with opposite patterns and specific topographies. Theta frequencies showed an effect focally localized over midfrontal channels, with significantly higher power in the low-PC condition, that is, the condition that entailed more control (i.e., LW25PC), as compared to the high-PC condition. This result confirms and extends previous findings concerning the task-switching paradigm, showing an increase of midfrontal theta power during the cue-to-target interval, when participants knew that they had to switch rule (Cooper et al., 2019). These findings thus provide support for the idea that pre-stimulus midfrontal theta may be a marker of proactive control.

Instead, concerning beta frequencies, we found its PC-related involvement over various portions of the scalp, engaging prefrontal, central and posterior channels, which showed lower pre-stimulus power in the low-PC condition. In the context of proactive and reactive control, previous evidence suggested beta band suppression to be an index of the use of proactive control, because it was associated with switching the target to attend in a visual search paradigm (Van

Driel et al., 2019). Our results showing lower beta power for the condition entailing more control are in line with this result. Moreover, this result is also consistent with the “status quo” account reviewed above (Engel & Fries, 2010). Indeed, the maintenance of the “status quo” may be preferentially implemented in high-PC block (i.e., LW75PC) because it can correspond to the prepotent elaboration of stimulus position, and therefore the lower power observed in the pre-stimulus low-PC condition (i.e., LW25PC) may reflect a change in this state employed as preparatory mechanism to deal with interference.

The present findings thus indicate that our use of PC manipulations can effectively modulate cognitive demands, making it possible to rely on proactive control in low-PC blocks (i.e., LW25PC) as predicted by the DMC model. These interpretations are further corroborated by the results from the correlations between the behavioural Stroop effect and the PC-dependent modulation of the pre-stimulus power in both theta and beta frequencies, which showed that greater power differences between low- and high-PC conditions were associated with a greater PC-dependent reduction of the behavioural Stroop effect. Indeed, participants with greater PC-dependent differences in the pre-stimulus theta and beta power, who thus were more able to exert proactive control, also showed to be more able to reduce the Stroop interference in the low-PC condition as compared to the high-PC one. Our results thus suggest that the recruitment of proactive control reduces the recruitment of additional neural resources after stimulus presentation (i.e., smaller ERSP Stroop interference in LW25PC condition) and explain, at least in part, the forthcoming behavioural performance (i.e., smaller Stroop effects in behavioural measures).

The present findings can also be reconciled with the Cascade of Control model. Concerning our pre-stimulus results, we suggest that they may reflect the early engagement of proactive control especially in low-PC blocks. In particular, the pre-stimulus PC-dependent engagement of midfrontal theta may correspond to the fourth and last step of the Cascade of Control model, which in that model concerns the evaluation of the response carried by the anterior dACC to modulate the degree of control to be employed in next trials. Indeed, it is possible that dACC not only evaluates the responses, but it may also monitor the control demands (based, for instance, on the history of the likelihood of interference occurrence) signalling to DLPFC the need to exert more control in a proactive manner. In turn, the DLPFC engagement corresponds to the first step of the Cascade of Control model, which is the attentional bias toward the relevant processes. We suggest that the more abundant the evidence of the high likelihood of interference occurrence (such as in low-PC blocks) is, the more strongly this bias is imposed. Based on the other pre-stimulus results found, we suggest that this selection process may be carried out by pre-stimulus beta frequencies. Indeed, for this frequency range we observed lower power for the most control demanding condition (low-PC blocks), which we reasoned to be related to a change in the "status quo" in order to bias the elaboration of the arrow direction in place of the (preferential) elaboration of its position.

Our post-stimulus results also revealed a primary involvement of theta and beta frequencies. An extensive body of evidence linked midfrontal theta to a mechanism that detects the interference and signals the need to exert cognitive control, and that is originated in the ACC (Cohen, 2014). In a similar vein, we suggest that the PC- and interference-dependent modulations of midfrontal theta we found may work as an early detection of the interference (and therefore of the need to exert cognitive control) after its occurrence. However, this precise mechanism is not explicitly included in the Cascade of Control model. Nevertheless, it is possible to hypothesize that this theta signal may reactively drive the DLPFC to impose the attentional bias toward the task-relevant process or representations in the earlier steps of the selection processes. This is corroborated by the early involvement of post-stimulus theta starting at around 200 ms, that is, even before participants started moving the mouse to respond and, thus, well in time to allow for the selection bias to take place. Furthermore, we suggest that also our beta results, interpreted in light of the "status quo" account above and as a marker of the selection of task-relevant information, may be in line with the Cascade of Control model, corresponding to one of the early biases imposed by the DLPFC. Indeed, it is possible to hypothesize that the changes in beta power (higher power suppression in responding to incongruent trials) represent the mechanism through which the DLPFC imposes the attentional biases. However, further analysis will be needed to investigate this issue more thoroughly, extending the present results with the estimation of the neural sources. Finally, the reduction of the ERSP Stroop effects we found in low-PC blocks suggests that, when participants can anticipate the interference applying a stronger attentional bias (i.e., proactive control), later mechanisms are less needed and thus recruit fewer resources. This last evidence may be in line with the prediction of the Cascade of Control model, proposing that the more effectively the earlier steps work, the less late steps would need to be recruited.

The last aim of this study was to investigate the functional interplay between theta and beta frequencies, the two bands that we hypothesized to be the key players in interference resolution. In particular, we hypothesized that if theta band is a marker that signals the need to exert control, and if beta band is involved in the selection of task-relevant information, they may be connected and communicate by means of phase-amplitude modulation. Indeed, we aimed at investigating the potential influence of theta phase on the amplitude of beta band. However, our analysis showed no PC-related modulation of this coupling. It may be that theta-beta coupling is not modulated by the control demands elicited by manipulating PC in this task, or it may be that there is a modulation of this coupling but in a different temporal window with respect to the one that we analysed (e.g., pre-stimulus time). It may also be that the coupling between these two bands is not functionally relevant in interference resolution and that other frequencies may have a role in this process (e.g., Jensen, Kaiser, & Lachaux, 2007). Further analysis and future studies can shed light on this aspect.

4.7. Conclusions

To summarize, in the present study, we aimed at investigating more in detail the anticipatory attentional bias that proactive control can impose in interference resolution. With this goal in mind, we analysed mouse-tracking measures together with EEG signal, and we manipulated the PC at the list level in order to elicit proactive control. Our findings showed clear

PC-related modulations of the Stroop effects that were reflected in both the kinematics and neural signatures of cognitive control, showing smaller Stroop interference for the low-PC blocks. Our results showed also clear PC-related differences in the pre-stimulus power in theta and beta frequencies, suggesting that proactive control may be reflected in these neural correlates, in line with the DMC and Cascade of Control models. These results also corroborated and extended the findings that we reported in the two previous studies, replicating the general pattern of the neural oscillations involved in interference resolution (Study 1) and the general modulation of Stroop interference by means of the PC (Study 2), even though with smaller effects.

Chapter 5
General Discussion

5.1. General Discussion

This project aimed at tackling the issue of how cognitive control is exerted to resolve cognitive interference. Specifically, we aimed at shedding light on the brain and temporal dynamics of the mechanisms involved in this process, by capturing their neural and kinematic correlates. Indeed, to address this main question, we took advantage of two different methodologies characterized by high temporal resolution, which were the EEG and the mouse-tracking, and we administered the same version of a spatial Stroop task (originally used in Puccioni & Vallesi, 2012), with small variations depending on the specific aims of each study.

In our Study 1, we aimed at investigating which brain dynamics are involved in interference resolution. As we already mentioned, the study of neural oscillations has been gaining attention only in the last years and evidence about the precise involvement of specific neural oscillations in different cognitive processes is still matter of investigation (Engel & Fries, 2010). Another aim of this first study was to investigate if these neurophysiological correlates and their temporal features change across the lifespan. To this purpose we recorded EEG activity from two samples of participants of different ages, focussing on time-frequency based analysis.

Our results revealed a main role of beta band, a finding that fitted well with the growing body of evidence proposing that beta frequencies play a more “cognitive” role than previously thought (see Ambrosini & Vallesi, 2017; Engel & Fries, 2010; Spitzer & Haegens, 2017). In this vein, we suggested that beta band may be a key player in the process of interference resolution. In particular, given its temporal and spatial features, we suggest that this result can be interpreted in light of the Cascade of Control model (Banich, 2009). Indeed, we hypothesize that beta may reflect the neural marker of the attentional biases toward the relevant information, so one of the earlier steps of the cascade of interference resolution processes.

This interpretation is also consistent with the age-related differences we found in Study 1. Specifically, younger participants showed the engagement of a restricted range of frequencies (i.e., beta2, 19-24 Hz) in an early temporal window and especially localized, through source analysis, over left posterior portions of middle and superior frontal gyri (pMFG, SFG), whereas older participants showed the recruitment of all beta frequencies (13-30 Hz), occurring later in time and with a spread bilateral localization. These age-related differences are in agreement with previous studies reporting that with aging there is an over-recruitment of neural sources, a reduction in hemispheric asymmetry and a dedifferentiation of neural processing that, according to some authors, can be an indicator of compensatory mechanisms adopted to face the functional and structural decline (Cabeza, 2002; Goh, 2011; Reuter-Lorenz & Park, 2014). Together, our beta results suggested that a restricted spectrum of frequencies (i.e., beta2), generated in specific brain areas (left pMFG, pSFG), may be preferentially involved in interference resolution process, but that with aging additional resources are needed to overcome this interference. Indeed, older adults not only recruited the entire spectrum of beta frequencies, but they also did not show any hemispheric specialization, engaging, in a delayed time course, bilateral brain areas and additional neural resources, such as dACC. This result is in line with previous evidence and with the Cascade of Control model (Milham et al., 2002).

Another important result emerged from Study 1 was the involvement of theta band at the source level, which engaged dorsomedial and dorsolateral cortices early in time for the younger participants only. We also found age-dependent differences in the correlation between the behavioural and theta Stroop effects, which was present again in the younger participants only. We suggested that our theta may represent a marker that signals the need to exert cognitive control, especially in contexts of interference, and that this signal may be impaired during aging, in line with previous findings (Cavanagh & Frank, 2014; Cohen, 2014; Ferreira et al., 2019). Importantly, some authors interpreted similar findings in line with the DMC model (Braver, 2012;

Paxton et al., 2007), which proposes that cognitive control may work through the proactive and reactive control mode. Indeed, they suggested that the decline commonly observed in aging may be due to an impairment in the use of proactive control, so in the ability to actively maintain task-relevant information, and that this leads to a stronger reliance on reactive control, that is a mechanism engaged only when needed (Paxton et al., 2007). However, with this first study, we could not examine the specific effects of the two modes of cognitive control. Indeed, for a more precise investigation of proactive and reactive control, it is important to try disentangling their specific contributions. Previous evidence suggested that the manipulation of the percentage of congruent trials (PC) can elicit proactive and reactive control (see Bugg & Crump, 2012, for a review).

Hence, we implemented Study 2, where we aimed at disentangling the underlying temporal dynamics of these two modes of control in interference resolution. For this goal, we used another novel tool with high temporal precision, which consists in the analysis of computer mouse trajectories, and we varied the PC at the list and at the item level (i.e., LWPC and ISPC respectively). Indeed, varying the PC in paradigms of interference can elicit the use of an anticipatory bias toward the relevant dimension (i.e., proactive control), or the use of a late correction mechanism (i.e., reactive control). This study is particularly relevant for different reasons. First of all, despite the extensive investigation of PC manipulations on proactive and reactive control, there is only one study that assessed their independent effects in the same participants (Gonthier et al., 2016). Second, mouse-tracking allows to capture unique aspects of the development and the updating of the decision process when an interference must be resolved, which are fundamental to shed light on the functional differences between the two control modes. Moreover, only two recent studies used this method to investigate interference resolution process, but they only focussed on ISPC manipulations and reactive control (Bundt et al., 2018; Ruitenberg et al., 2019).

Our findings showed that the Stroop effect was replicated also through this tool and showed the same pattern of results in all the mouse-derived measures extracted. These effects were reflected in the greater attraction toward the distracting information, more complex trajectories and longer time to respond to incongruent trials as compared to the congruent ones. Moreover, we found PC-related effects in both kinds of manipulations used. Specifically, we reported a reduction in the magnitude of the Stroop interference as function of the PC, where low-PC blocks showed less interference in line with previous evidence (Bugg & Chanani, 2011; Bugg & Hutchison, 2013; Jacoby et al., 2003), and again constant across all the measures considered. It is important to note that, by means of mixed-effects models, it was possible to disentangle the differential contribution of LWPC and ISPC manipulations (and therefore of proactive and reactive control), despite an ISPC manipulation was necessarily entailed in the LWPC one (e.g., the PC at the block level was manipulated to globally have 25% of congruent trials, leading to a manipulation at the item level for which congruent items were presented in the 25% of cases). This is an important result, because previous evidence argued that LWPC effects were exclusively driven by ISPC, doubting any involvement of proactive control in resolving the interference of this block (Blais & Bunge, 2010). As already mentioned, previous studies tried to prevent this issue by adding additional items with equal PC (i.e., unbiased) embedded in the LWPC block, and explaining the transferred advantage in responding to these items as a proof of the use of proactive control, a global and anticipatory mechanism (Bugg & Chanani, 2011; Gonthier et al., 2016). Therefore, our results suggest the possibility to investigate the same effects without the need of an additional set of unbiased items, which are not possible to create for all the experimental paradigms and settings. Overall, the evidence provided by Study 2 is in line with studies suggesting that, when using LWPC manipulations, participants are able to rely on proactive control and anticipate interference (Bugg & Chanani, 2011; Bugg, et al., 2011; Gonthier et al., 2016).

However, our findings also showed specific effects of ISPC manipulations which, similarly to LWPC blocks, elicited less interference for low-PC conditions. Therefore, even though participants were not able to anticipate the interference because of the equal occurrence of congruent and incongruent trials at the list-wide level, these results suggest that reactive control may work similarly to proactive control. Moreover, the pattern of results of the time-level measures, such as x-coordinate and the distance to target, suggested that also the temporal dynamics of the two control modes may be more similar than what we expected. Interpreting all these results in line with the Cascade of Control model (Banich, 2009), it is possible to hypothesize that proactive control can work as a bias toward the relevant process, therefore corresponding to the first step of the model. The more it is possible to rely on proactive control the stronger this bias will be. However, the finding that the Stroop effect was also reduced for low-PC in the ISPC manipulation suggests that reactive control may also act early in time, imposing a bias toward the relevant information soon after the presentation of the stimulus. Therefore, also reactive control may act by relying on the attentional bias toward the relevant process, even when it is not possible to strengthen the weights for the elaboration of the arrow direction before stimulus appearance. Previous evidence also explained the effects of reactive control as driven by fast stimulus-attention associations, which rapidly impose a bias toward the relevant information to counteract interference (Bugg, 2017; Bugg & Crump, 2012).

Therefore, it is possible that the functional difference between proactive and reactive control can be only highlighted in the time preceding stimulus presentation, where participants can strengthen the bias toward relevant information preparing in advance to cope with the interference. Despite the advantages of this study, it was still not enough to have a clear picture about this important temporal window, where only proactive control can operate, and therefore we implemented Study 3. In the latter study we aimed at investigating further in details the neural correlates of the anticipatory attentional bias that can be imposed through proactive control. For this purpose, we implemented the same task of the previous study, using mouse-tracking method, but we also added the recording of the EEG signal, which allowed us to track the proactive neural processes occurring during the pre-stimulus time window. Moreover, we also aimed at comparing the EEG results with those derived from Study 1, and the mouse-tracking results with those derived from Study 2. However, it is important to notice that, in the present study, it was not possible to apply again both the LWPC and the ISPC manipulations. Indeed, EEG analysis required higher number of trials in each condition, and for this reason we decided to use only the LWPC manipulation.

Our findings showed an influence on the magnitude of the Stroop interference by means of the PC manipulation used, revealing the same pattern of results both at the behavioural and at the neural levels, translated in smaller Stroop interference for the low-PC condition. Generally, all the mouse-derived measures showed this pattern of results, replicating the findings obtained in Study 2. Again, this is in line with previous literature suggesting that for low LWPC block (i.e., LW25PC) it is possible to rely on proactive control, imposing an early attentional bias that helps with the anticipation of interference, and also in accordance to the DMC model (Braver, 2012; Bugg & Chanani, 2011; Bugg & Crump, 2012). ERSP results also revealed the same PC-related effects emerged in the kinematics correlates, with smaller Stroop interference for low-PC blocks. In particular, similarly to the results for Study 1, we observed again a main involvement of theta and beta frequencies in interference resolution.

Theta was mainly involved in high-PC block (i.e., LW75PC) and arose soon after stimulus presentation, over midfrontal electrodes. This result was in line with our expectations and adds to the results of Study 1 in confirming the extensive evidence reporting that theta is involved in paradigms embedding interference (Cavanagh et al., 2012; Cohen, 2014). Therefore, also the findings from Study 3 suggest that these frequencies may be implied in the early detection of the interference, signalling the need to exert cognitive control (Cavanagh & Frank, 2014). Indeed, we found higher theta power for incongruent trials as compared to the congruent ones, especially in high-PC block, but we did not find any power difference in low-PC block, which suggests that, when participants are able to predict interference, this detection mechanism may recruit fewer neural resources. Similarly, beta band showed an involvement starting from around 400 ms after stimulus presentation and engaging mainly prefrontal and central electrodes. Again, these findings are in line with the suggestion that these frequencies may be involved in interference resolution process, already reviewed in Study 1.

More importantly, our analysis on the pre-stimulus window revealed specific PC-dependent modulations of the pre-stimulus power in midfrontal theta as well as in beta, with less spatial specificity in the scalp distribution. In particular, pre-stimulus theta results showed an increase in power for the most control demanding condition (i.e., LW25PC), in line with previous evidence showing an involvement of these frequencies in paradigms engaging proactive control (e.g., task-switching; Cooper et al., 2019). Beta frequencies, instead, reported lower power for the most control demanding condition, result that is again in line with the account of beta as correlate that maintains the "status quo" (Engel & Fries, 2010). We have already mentioned that this state may correspond to the preferential elaboration of stimulus position as compared to the direction, and therefore it is possible that in control demanding blocks (i.e., LW25PC) this state needs to be changed, possibly by means of beta power modulations. Thus, we suggest that these brain dynamics may represent a first evidence of the anticipatory nature of proactive control in the Stroop task.

Moreover, with the latter study we also aimed at comparing these results with those obtained from the previous studies. From the comparison between mouse-tracking measures between this study and Study 2, we found that the general pattern of results was confirmed, and all the measures showed smaller Stroop interference in the low-PC condition. However, the PC-related effects on the Stroop interference were less strong in the present study. This effect can be caused by different factors. First of all, previous authors suggested that when neuro-imaging studies tried replicating behavioural results, the effects are generally less strong (e.g., van Maanen, Forstmann, Keuken, Wagenmakers, & Heathcote, 2016). For instance, neuroimaging studies often require participants to avoid moving, asking to remain still, and this may influence task performance. Another possibility for this effect may rely on the technical differences between these two studies, such as that mouse trajectories have been recorded by means of different tools (i.e., MouseTracker Software, Psychtoolbox), or because of the different duration of trial events (participants had more time to prepare before stimulus presentation in mouse-tracking and EEG study). Alternatively, it may also be possible that monetary reward given to the participants of the latter study influenced their motivation in task execution, increasing their performance (albeit participants were informed that the reimbursement did not depend on the performance). Despite the factors that may have contributed to these differences, it is important to put focus on the general pattern of results that was the same across all the measures and that constantly showed less Stroop interference for low-PC condition, replicating the influence of the use of PC manipulations in modulating the cognitive demands. This is theoretically important because no previous study had administered this manipulation in a mouse tracking experiment, but only the ISPC (Bundt et al., 2018; Ruitenberg et al., 2019).

Concerning the comparison with our electrophysiological results, the results showed some differences. First of all, in Study 1 we did not find any involvement of theta band at the scalp-level, but this result emerged only from neural source estimation, contrary to our expectations. It is important to notice that the present results can be compared only to those obtained from the younger group of participants in Study 1. Indeed, one possibility for the lack of findings for theta band in Study 1 may be that the sample size was not enough to detect this effect. Concerning the results for beta band, they seem to be generally replicated, even though with some subtle differences in the topography of the effect and in the range of frequencies involved. Indeed, in Study 1 beta effect was mainly localized over left prefrontal regions in younger participants (pMFG, pSFG) and mainly included a restricted range of frequencies (19-24 Hz), whereas in Study 3 the localization was not so focal, engaging different channels over central and prefrontal regions of the scalp, and including all the frequencies in the beta range. However, when comparing these results, it is important to notice that in Study 1 we were able to extract a more precise estimation of the neural generators of beta frequencies, whereas in Study 3 the topography is derived by scalp-based results. Moreover, this difference may be also due to the fact that the motor responses required in Study 3 were much more complex of those in Study 1 (i.e., key presses) and may have led to the involvement of more frequencies in the range of beta and more channels over the scalp. The estimation of the neural sources will be computed also for Study 3 in the future and will help to further clarify this point. However, even if it will result that the beta modulation would be related to motor aspects, we still suggest that the neural correlates of motor control are deeply interconnected with the cognitive activity, especially in this paradigm. Indeed, the updating and adjustments of mouse movements are important parts of the decision process that allows dissociating correct and incorrect responses, and that it is particularly relevant in interference resolution (Haegens et al., 2011).

Going back to the Cascade of Control model, we suggest that the evidence collected across the studies of this dissertation can be in line with it. First, we suggest that the midfrontal pre-stimulus theta may reflect an early and anticipatory mechanism carried by the dACC, which not only evaluates the given responses, but also keeps track of the likelihood of potential interference in order to signal the need to increase cognitive control according to contexts. This mechanism may be defined as proactive control and may rely on the process corresponding to the fourth step of the cascade of interference resolution processes. This signal may then arrive to the DLPFC, triggering the imposition of the bias toward the task relevant process (first step). An important prediction is that the more is the evidence that an interference is likely to occur, the stronger will be the DLPFC bias toward regions involved in the elaboration of the relevant information (e.g., arrow direction). This mechanism may be reflected in the beta involvement that follows the predictions of the “status quo” account. Indeed, changes in beta power may represent a change from the “status quo”, which we hypothesize to be the prepotent elaboration of the arrow position. Therefore, we suggest that the early and anticipatory proactive control may be reflected in the main involvement of pre-stimulus theta and beta frequencies that actively regulate control demands, according to the evidence that it is possible to accumulate.

Furthermore, our results showed also a post-stimulus theta involvement, which may represent a signal that detects the interference after its occurrence. This interpretation is in line with a large body of literature suggesting that theta is the main band involved in interference paradigms (Cavanagh & Frank, 2014; Cavanagh et al., 2012; Cohen, 2014; Cooper et al., 2019). However, this specific mechanism is not included in the Cascade of Control model, even though it follows its predictions. Indeed, according to the model, the more is the strength of the attentional bias toward the relevant information, the less the following steps of the cascade will need to be recruited. This is the pattern of results shown for the post-stimulus theta in Study 3, where we found smaller ERSP Stroop effect for the more control demanding condition (low-PC), in which proactive control can be exerted. Therefore, when the weights on the earlier steps are strong before stimulus occurrence (as when it is possible to rely on proactive control), this mechanism may be engaged the less (as evidenced in the Stroop effect of the low-PC condition). However, when it is not possible to prepare in advance, this detection mechanism may play a more important role in order to rapidly recruit control processes to cope with the interference. This signal can thus be communicated again to the DLPFC to start the cascade of processes required to solve the interference. The consequent steps may engage beta frequencies, that we suggest having an important role in this process. Indeed, beta may be involved in the bias toward the relevant information (process and/or representations), but it may also be involved in the selection of the information that should guide response, corresponding to the third step that may be conveyed by the ACC but also by the pre-SMA. This may be also in line with the suggestion that cognitive and motor control are deeply interconnected, especially in this mouse-tracking paradigm, because the updating and adjustments of mouse movements are important parts of the decision process about the correct response to give. Then, the fourth step carried by the anterior dACC may come into play to evaluate the responses and tracking interference occurrence to trigger control adjustments and closing the circle of the processes.

5.2. Future directions

There are still some open issues that we aim at solving with further analysis. First of all, we planned to compute neural source estimation on our mouse-tracking EEG dataset (Study 3) to investigate more in depth the neural generators of the frequencies we found involved in interference resolution. In particular, we aim at studying if there is any PC-related modulation of the brain areas involved in interference resolution process, if there are differences in the neural generators of the pre- and post-stimulus window for theta and beta frequencies, if these areas can overlap with those proposed by the Cascade of Control model, and which is the contribution of motor areas in this paradigm.

Furthermore, we also planned additional PAC analysis to investigate if there is a relation between theta and beta frequencies in the pre-stimulus time, possibly reflecting the mechanism of proactive control adjustments between the dACC and the DLPFC. However, previous literature suggested that a fundamental coupling in cognitive processes is represented by the phase-amplitude relation between theta and gamma frequencies. Indeed, gamma frequencies have been implied in different cognitive functions and have been hypothesized to reflect the activity of synchronously firing neurons in local assemblies (e.g., Jensen et al., 2007), so that theta-gamma coupling may represent a mechanism of coordination of local networks.

Moreover, the present results constitute only a starting point for further investigations. Indeed, different studies can be conducted to further support our interpretations and conclusions. First of all, it would be interesting to administer the same mouse-tracking EEG paradigm of Study 3 but using an ISPC manipulation to investigate the neural and kinematic dynamics of reactive control. The best solution would be to administer both manipulations (i.e., LWPC and ISPC) to the same participants, possibly dividing the experiment in two sessions to avoid fatigue effects due to the length of the task. This experiment would bring to light potential neurophysiological differences in the implementation of proactive and reactive control and would give a more complete picture on the temporal dynamics of these two control modes.

Once these aspects have been clarified, it would be interesting also to administer the same task to older participants, in order to investigate more precisely potential age-related differences in the recruitment of proactive and reactive control. Moreover, even though our results suggest that proactive and reactive control may work through similar mechanisms, it would be interesting to investigate more precisely if one of the two control modes is more efficient than the other (i.e., stronger reduction of the interference).

Moreover, as suggested in previous literature (e.g., Braver, 2012), it would be interesting also to investigate if inter-individual differences (such as personality traits) may influence the use of distinct modes of cognitive control (i.e., proactive and reactive control). Furthermore, decline in this ability have been reported in a variety of clinical conditions (e.g., schizophrenia, anxiety disorders) and also in healthy aging. Therefore, having a clear picture of its functioning, reflected also in the neurophysiological correlates, may help in developing new treatments and preventions. We hope that the present dissertation will encourage future studies in embracing this challenge and in providing new answers to the still open questions.

5.3. Conclusions

Cognitive control is one of the most fascinating and complex aspects of human being, as well as one of the most important functions that flexibly coordinates and adjusts our behaviours. Thus, it is important to shed light on the specific mechanisms that cognitive control implements to achieve goals. This project provides confirmations and new suggestions in the study of interference resolution process, with a particular attention to its neural and temporal dynamics. Our results confirmed the involvement of theta frequencies in interference resolution process, interpreted as an early mechanism of interference detention that signals the need to exert cognitive control. Moreover, our results also showed a main involvement of beta frequencies that we suggest may represent the imposition of early attentional biases toward the relevant information. We interpreted these results in line with the Cascade of Control and the DMC models. Furthermore, to the best of our knowledge, these findings constitute a first evidence of the neural correlates involved in proactive control during Stroop paradigms. This project represents a first attempt to evaluate more in detail the temporal course of proactive and reactive control, taking advantages by two techniques with high temporal resolution.

References

Ambrosini, E., & Vallesi, A. (2017). Domain-general Stroop performance and hemispheric asymmetries: a resting-state EEG study. *Journal of cognitive neuroscience, 29*(5), 769-779.

Antzoulatos, E. G., & Miller, E. K. (2016). Synchronous beta rhythms of frontoparietal networks support only behaviorally relevant representations. *ELife, 5*.

Appelbaum, L. G., Boehler, C. N., Davis, L. A., Won, R. J., & Woldorff, M. G. (2014). The dynamics of proactive and reactive cognitive control processes in the human brain. *Journal of cognitive neuroscience, 26*(5), 1021-1038.

Association, W. M. (2013). World Medical Association Declaration of Helsinki: Ethical Principles for Medical Research Involving Human SubjectsWorld Medical Association Declaration of HelsinkiSpecial Communication. *JAMA, 310*(20), 2191-2194. doi:10.1001/jama.2013.281053

Augustinova, M., Parris, B. A., & Ferrand, L. (2019). The Loci of Stroop Interference and Facilitation Effects With Manual and Vocal Responses. *Frontiers in psychology, 10*.

Augustinova, M., Silvert, L., Spatola, N., & Ferrand, L. (2018). Further investigation of distinct components of Stroop interference and of their reduction by short response-stimulus intervals. *Acta psychologica, 189*, 54-62.

Aulická, Š. R., Jurák, P., Chládek, J., Daniel, P., Halámek, J., Baláž, M., . . . Rektor, I. (2014). Subthalamic nucleus involvement in executive functions with increased cognitive load: a subthalamic nucleus and anterior cingulate cortex depth recording study. *Journal of neural transmission, 121*(10), 1287-1296.

Axmacher, N., Henseler, M. M., Jensen, O., Weinreich, I., Elger, C. E., & Fell, J. (2010). Cross-frequency coupling supports multi-item working memory in the human hippocampus. *Proceedings of the National Academy of Sciences, 107*(7), 3228-3233.

Baayen, R. H., Davidson, D. J., & Bates, D. M. (2008). Mixed-effects modeling with crossed random effects for subjects and items. *Journal of memory and language, 59*(4), 390-412.

Baillet, S., Riera, J., Marin, G., Mangin, J., Aubert, J., & Garnero, L. (2001). Evaluation of inverse methods and head models for EEG source localization using a human skull phantom. *Physics in medicine & biology, 46*(1), 77.

Banich, M. T. (2009). Executive function: The search for an integrated account. *Current directions in psychological science, 18*(2), 89-94.

Banich, M. T., Milham, M. P., Atchley, R., Cohen, N. J., Webb, A., Wszalek, T., . . . Shenker, J. (2000). fMRI studies of Stroop tasks reveal unique roles of anterior and posterior brain systems in attentional selection. *Journal of cognitive neuroscience, 12*(6), 988-1000.

Bates, D., Maechler, M., Bolker, B., & Walker, S. (2014). lme4: Linear mixed-effects models using S4 classes. R package version 1.1-7. *URL http://CRAN. R-project. org/package= lme4*.

Blais, C., & Bunge, S. (2010). Behavioral and neural evidence for item-specific performance monitoring. *Journal of Cognitive Neuroscience, 22*(12), 2758-2767.

Botvinick, M. M., Braver, T. S., Barch, D. M., Carter, C. S., & Cohen, J. D. (2001). Conflict monitoring and cognitive control. *Psychological review, 108*(3), 624.

Botvinick, M. M., Cohen, J. D., & Carter, C. S. (2004). Conflict monitoring and anterior cingulate cortex: an update. *Trends in cognitive sciences, 8*(12), 539-546.

Boulinguez, P., Ferrois, M., & Graumer, G. (2003). Hemispheric asymmetry for trajectory perception. *Cognitive brain research, 16*(2), 219-225.

Box, G. E., & Cox, D. R. (1964). An analysis of transformations. *Journal of the Royal Statistical Society: Series B (Methodological), 26*(2), 211-243.

Braver, T. S. (2012). The variable nature of cognitive control: a dual mechanisms framework. *Trends in cognitive sciences, 16*(2), 106-113.

Braver, T. S., Gray, J. R., & Burgess, G. C. (2007). Explaining the many varieties of working memory variation: Dual mechanisms of cognitive control. *Variation in working memory, 75*, 106.

Braver, T. S., Paxton, J. L., Locke, H. S., & Barch, D. M. (2009). Flexible neural mechanisms of cognitive control within human prefrontal cortex. *Proceedings of the National Academy of Sciences, 106*(18), 7351-7356.

Bugg, J. M. (2014). Evidence for the sparing of reactive cognitive control with age. *Psychology and Aging, 29*(1), 115.

Bugg, J. M. (2017). Context, conflict, and control. *The Wiley handbook of cognitive control*, 79-96.

Bugg, J. M., & Chanani, S. (2011). List-wide control is not entirely elusive: Evidence from picture–word Stroop. *Psychonomic bulletin & review, 18*(5), 930-936.

Bugg, J. M., & Crump, M. J. (2012). In support of a distinction between voluntary and stimulus-driven control: A review of the literature on proportion congruent effects. *Frontiers in psychology, 3*, 367.

Bugg, J. M., DeLosh, E. L., Davalos, D. B., & Davis, H. P. (2007). Age differences in Stroop interference: Contributions of general slowing and task-specific deficits. *Aging, Neuropsychology, and Cognition, 14*(2), 155-167.

Bugg, J. M., & Hutchison, K. A. (2013). Converging evidence for control of color–word Stroop interference at the item level. *Journal of Experimental Psychology: Human Perception and Performance, 39*(2), 433.

Bugg, J. M., Jacoby, L. L., & Chanani, S. (2011). Why it is too early to lose control in accounts of item-specific proportion congruency effects. *Journal of Experimental Psychology: Human Perception and Performance, 37*(3), 844.

Bugg, J. M., Jacoby, L. L., & Toth, J. P. (2008). Multiple levels of control in the Stroop task. *Memory & cognition, 36*(8), 1484-1494.

Bugg, J. M., McDaniel, M. A., Scullin, M. K., & Braver, T. S. (2011). Revealing list-level control in the Stroop task by uncovering its benefits and a cost. *Journal of Experimental Psychology: Human Perception and Performance, 37*(5), 1595.

Bundt, C., Ruitenberg, M. F., Abrahamse, E. L., & Notebaert, W. (2018). Early and late indications of item-specific control in a Stroop mouse tracking study. *PloS one, 13*(5), e0197278.

Cabeza, R. (2002). Hemispheric asymmetry reduction in older adults: the HAROLD model. *Psychology and aging, 17*(1), 85.

Canolty, R. T., Edwards, E., Dalal, S. S., Soltani, M., Nagarajan, S. S., Kirsch, H. E., . . . Knight, R. T. (2006). High gamma power is phase-locked to theta oscillations in human neocortex. *science, 313*(5793), 1626-1628.

Canolty, R. T., & Knight, R. T. (2010). The functional role of cross-frequency coupling. *Trends in cognitive sciences, 14*(11), 506-515.

Cavanagh, J. F., & Frank, M. J. (2014). Frontal theta as a mechanism for cognitive control. *Trends in cognitive sciences, 18*(8), 414-421.

Cavanagh, J. F., Zambrano-Vazquez, L., & Allen, J. J. (2012). Theta lingua franca: A common mid-frontal substrate for action monitoring processes. *Psychophysiology, 49*(2), 220-238.

Cerella, J. (1990). Aging and information-processing rate. In *Handbook of the Psychology of Aging (Third Edition)* (pp. 201-221): Elsevier.

Chang, A., Ide, J. S., Li, H.-H., Chen, C.-C., & Li, C.-S. R. (2017). Proactive control: Neural oscillatory correlates of conflict anticipation and response slowing. *eNeuro, 4*(3).

Cohen, M. X. (2014). A neural microcircuit for cognitive conflict detection and signaling. *Trends in neurosciences, 37*(9), 480-490.

Cohen, M. X. (2017). Where does EEG come from and what does it mean? *Trends in neurosciences, 40*(4), 208-218.

Colás, I., Capilla, A., & Chica, A. B. (2018). Neural modulations of interference control over conscious perception. *Neuropsychologia, 112*, 40-49.

Cooper, P. S., Karayanidis, F., McKewen, M., McLellan-Hall, S., Wong, A. S., Skippen, P., & Cavanagh, J. F. (2019). Frontal theta predicts specific cognitive control-induced behavioural changes beyond general reaction time slowing. *Neuroimage, 189*, 130-140.

Cooper, P. S., Wong, A. S., Fulham, W. R., Thienel, R., Mansfield, E., Michie, P. T., & Karayanidis, F. (2015). Theta frontoparietal connectivity associated with proactive and reactive cognitive control processes. *Neuroimage, 108*, 354-363.

Cooper, P. S., Wong, A. S., McKewen, M., Michie, P. T., & Karayanidis, F. (2017). Frontoparietal theta oscillations during proactive control are associated with goal-updating and reduced behavioral variability. *Biological psychology, 129*, 253-264.

Crump, M. J., Gong, Z., & Milliken, B. (2006). The context-specific proportion congruent Stroop effect: Location as a contextual cue. *Psychonomic bulletin & review, 13*(2), 316-321.

De Houwer, J. (2003). On the role of stimulus-response and stimulus-stimulus compatibility in the Stroop effect. *Memory & Cognition, 31*(3), 353-359.

Delorme, A., & Makeig, S. (2004). EEGLAB: an open source toolbox for analysis of single-trial EEG dynamics including independent component analysis. *Journal of neuroscience methods, 134*(1), 9-21.

Delorme, A., Sejnowski, T., & Makeig, S. (2007). Enhanced detection of artifacts in EEG data using higher-order statistics and independent component analysis. *Neuroimage, 34*(4), 1443-1449.

Derrfuss, J., Brass, M., Neumann, J., & von Cramon, D. Y. (2005). Involvement of the inferior frontal junction in cognitive control: Meta-analyses of switching and Stroop studies. *Human brain mapping, 25*(1), 22-34.

Diamond, A. (2013). Executive functions. *Annual review of psychology, 64*, 135-168.

Egner, T., & Hirsch, J. (2005). Cognitive control mechanisms resolve conflict through cortical amplification of task-relevant information. *Nature neuroscience, 8*(12), 1784.

Engel, A. K., & Fries, P. (2010). Beta-band oscillations—signalling the status quo? *Current opinion in neurobiology, 20*(2), 156-165.

Ergen, M., Saban, S., Kirmizi-Alsan, E., Uslu, A., Keskin-Ergen, Y., & Demiralp, T. (2014). Time–frequency analysis of the event-related potentials associated with the Stroop test. *International Journal of Psychophysiology, 94*(3), 463-472.

Eriksen, B. A., & Eriksen, C. W. (1974). Effects of noise letters upon the identification of a target letter in a nonsearch task. *Perception & psychophysics, 16*(1), 143-149.

Eschmann, K. C., Bader, R., & Mecklinger, A. (2018). Topographical differences of frontal-midline theta activity reflect functional differences in cognitive control abilities. *Brain and cognition, 123*, 57-64.

Faul, F., Erdfelder, E., Buchner, A., & Lang, A.-G. (2009). Statistical power analyses using G*Power 3.1: Tests for correlation and regression analyses. *Behavior Research Methods, 41*(4), 1149-1160. doi:10.3758/brm.41.4.1149

Faust, M. E., Balota, D. A., Spieler, D. H., & Ferraro, F. R. (1999). Individual differences in information-processing rate and amount: implications for group differences in response latency. *Psychological bulletin, 125*(6), 777.

Ferreira, C. S., Maraver, M. J., Hanslmayr, S., & Bajo, T. (2019). Theta oscillations show impaired interference detection in older adults during selective memory retrieval. *Scientific reports, 9*(1), 9977.

Fischl, B., Sereno, M. I., Tootell, R. B., & Dale, A. M. (1999). High-resolution intersubject averaging and a coordinate system for the cortical surface. *Human brain mapping, 8*(4), 272-284.

Fjell, A. M., & Walhovd, K. B. (2010). Structural brain changes in aging: courses, causes and cognitive consequences. *Reviews in the Neurosciences, 21*(3), 187-222.

Floden, D., Vallesi, A., & Stuss, D. T. (2011). Task context and frontal lobe activation in the Stroop task. *Journal of Cognitive Neuroscience, 23*(4), 867-879.

Forstmann, B. U., Tittgemeyer, M., Wagenmakers, E.-J., Derrfuss, J., Imperati, D., & Brown, S. (2011). The speed-accuracy tradeoff in the elderly brain: a structural model-based approach. *Journal of Neuroscience, 31*(47), 17242-17249.

Freeman, J., Dale, R., & Farmer, T. (2011). Hand in motion reveals mind in motion. *Frontiers in Psychology, 2*, 59.

Freeman, J. B., & Ambady, N. (2010). MouseTracker: Software for studying real-time mental processing using a computer mouse-tracking method. *Behavior research methods, 42*(1), 226-241.

Freeman, J. B., & Ambady, N. (2011). A dynamic interactive theory of person construal. *Psychological review, 118*(2), 247.

Friedman, N. P., & Miyake, A. (2004). The relations among inhibition and interference control functions: a latent-variable analysis. *Journal of experimental psychology: General, 133*(1), 101.

Fries, P. (2005). A mechanism for cognitive dynamics: neuronal communication through neuronal coherence. *Trends in cognitive sciences, 9*(10), 474-480.

Gazzaley, A., & D'esposito, M. (2007). Top-down modulation and normal aging. *Annals of the New York Academy of Sciences, 1097*(1), 67-83.

Goh, J. O. (2011). Functional dedifferentiation and altered connectivity in older adults: neural accounts of cognitive aging. *Aging and disease, 2*(1), 30.

Gonthier, C., Braver, T. S., & Bugg, J. M. (2016). Dissociating proactive and reactive control in the Stroop task. *Memory & Cognition, 44*(5), 778-788.

Gould, I. C., Nobre, A. C., Wyart, V., & Rushworth, M. F. (2012). Effects of decision variables and intraparietal stimulation on sensorimotor oscillatory activity in the human brain. *Journal of Neuroscience, 32*(40), 13805-13818.

Gramfort, A., Papadopoulo, T., Olivi, E., & Clerc, M. (2010). OpenMEEG: opensource software for quasistatic bioelectromagnetics. *Biomedical engineering online, 9*(1), 45.

Greenwood, P. M. (2000). The frontal aging hypothesis evaluated. *Journal of the International Neuropsychological Society, 6*(6), 705-726.

Haegens, S., Nácher, V., Hernández, A., Luna, R., Jensen, O., & Romo, R. (2011). Beta oscillations in the monkey sensorimotor network reflect somatosensory decision making. *Proceedings of the National Academy of Sciences, 108*(26), 10708-10713.

Hanslmayr, S., Pastötter, B., Bäuml, K.-H., Gruber, S., Wimber, M., & Klimesch, W. (2008). The electrophysiological dynamics of interference during the Stroop task. *Journal of Cognitive Neuroscience, 20*(2), 215-225.

Hasher, L., & Zacks, R. T. (1988). Working memory, comprehension, and aging: A review and a new view. In *Psychology of learning and motivation* (Vol. 22, pp. 193-225): Elsevier.

He, W., Goodkind, D., & Kowal, P. (2016). US Census Bureau, international population reports. *An Aging World: 2015*, 16-11.

Hehman, E., Stolier, R. M., & Freeman, J. B. (2015). Advanced mouse-tracking analytic techniques for enhancing psychological science. *Group Processes & Intergroup Relations, 18*(3), 384-401.

Horn, J. L. (1965). A rationale and test for the number of factors in factor analysis. *Psychometrika, 30*(2), 179-185.

Incera, S., & McLennan, C. T. (2016). Mouse tracking reveals that bilinguals behave like experts. *Bilingualism: Language and Cognition, 19*(3), 610-620.

Jacoby, L. L., Lindsay, D. S., & Hessels, S. (2003). Item-specific control of automatic processes: Stroop process dissociations. *Psychonomic Bulletin & Review, 10*(3), 638-644.

Jensen, O., Kaiser, J., & Lachaux, J.-P. (2007). Human gamma-frequency oscillations associated with attention and memory. *Trends in neurosciences, 30*(7), 317-324.

Jiang, J., van Gaal, S., Bailey, K., Chen, A., & Zhang, Q. (2013). Electrophysiological correlates of block-wise strategic adaptations to consciously and unconsciously triggered conflict. *Neuropsychologia, 51*(13), 2791-2798.

Jurkiewicz, M. T., Gaetz, W. C., Bostan, A. C., & Cheyne, D. (2006). Post-movement beta rebound is generated in motor cortex: evidence from neuromagnetic recordings. *Neuroimage, 32*(3), 1281-1289.

Kayser, J. (2009). Current source density (CSD) interpolation using spherical splines-CSD Toolbox (Version 1.1). *New York State Psychiatric Institute: Division of Cognitive Neuroscience*.

Kleiner, M., Brainard, D., & Pelli, D. (2007). What's new in Psychtoolbox-3?

Kornblum, S., & Stevens, G. (2002). Sequential effects of dimensional overlap: Findings and issues. *Common mechanisms in perception and action, 19*, 9-54.

Kuznetsova, A., Brockhoff, P. B., & Christensen, R. H. B. (2017). lmerTest package: tests in linear mixed effects models. *Journal of Statistical Software, 82*(13).

Kybic, J., Clerc, M., Abboud, T., Faugeras, O., Keriven, R., & Papadopoulo, T. (2005). A common formalism for the integral formulations of the forward EEG problem. *IEEE transactions on medical imaging, 24*(1), 12-28.

Lindsay, D. S., & Jacoby, L. L. (1994). Stroop process dissociations: The relationship between facilitation and interference. *Journal of Experimental Psychology: Human Perception and Performance, 20*(2), 219.

Logan, G. D. (1998). What is learned during automatization? II. Obligatory encoding of spatial location. *Journal of Experimental Psychology: Human Perception and Performance, 24*(6), 1720.

Logan, G. D., & Zbrodoff, N. J. (1979). When it helps to be misled: Facilitative effects of increasing the frequency of conflicting stimuli in a Stroop-like task. *Memory & cognition, 7*(3), 166-174.

Luo, C. R. (1999). Semantic competition as the basis of Stroop interference: Evidence from color-word matching tasks. *Psychological Science, 10*(1), 35-40.

MacLeod, C. M. (1991). Half a century of research on the Stroop effect: an integrative review. *Psychological bulletin, 109*(2), 163.

MacLeod, C. M., Dodd, M. D., Sheard, E. D., Wilson, D. E., & Bibi, U. (2003). In opposition to inhibition. *Psychology of learning and motivation, 43*, 163-215.

Meindertsma, T., Kloosterman, N. A., Engel, A. K., Wagenmakers, E.-J., & Donner, T. H. (2018). Surprise about sensory event timing drives cortical transients in the beta frequency band. *Journal of Neuroscience, 38*(35), 7600-7610.

Milham, M., Banich, M., Claus, E., & Cohen, N. (2003). Practice-related effects demonstrate complementary roles of anterior cingulate and prefrontal cortices in attentional control. *Neuroimage, 18*(2), 483-493.

Milham, M., Banich, M., Webb, A., Barad, V., Cohen, N., Wszalek, T., & Kramer, A. (2001). The relative involvement of anterior cingulate and prefrontal cortex in attentional control depends on nature of conflict. *Cognitive Brain Research, 12*(3), 467-473.

Milham, M. P., & Banich, M. T. (2005). Anterior cingulate cortex: an fMRI analysis of conflict specificity and functional differentiation. *Human brain mapping, 25*(3), 328-335.

Milham, M. P., Banich, M. T., & Barad, V. (2003). Competition for priority in processing increases prefrontal cortex's involvement in top-down control: an event-related fMRI study of the stroop task. *Cognitive brain research, 17*(2), 212-222.

Milham, M. P., Erickson, K. I., Banich, M. T., Kramer, A. F., Webb, A., Wszalek, T., & Cohen, N. J. (2002). Attentional control in the aging brain: insights from an fMRI study of the stroop task. *Brain and cognition, 49*(3), 277-296.

Miller, E. K., & Cohen, J. D. (2001). An integrative theory of prefrontal cortex function. *Annual review of neuroscience, 24*(1), 167-202.

Miyake, A., Friedman, N. P., Emerson, M. J., Witzki, A. H., Howerter, A., & Wager, T. D. (2000). The unity and diversity of executive functions and their contributions to complex "frontal lobe" tasks: A latent variable analysis. *Cognitive psychology, 41*(1), 49-100.

Mullen, T., Kothe, C., Chi, Y. M., Ojeda, A., Kerth, T., Makeig, S., . . . Jung, T.-P. (2013). *Real-time modeling and 3D visualization of source dynamics and connectivity using wearable EEG.*

Paper presented at the 2013 35th annual international conference of the IEEE engineering in medicine and biology society (EMBC).

Munakata, Y., Herd, S. A., Chatham, C. H., Depue, B. E., Banich, M. T., & O'Reilly, R. C. (2011). A unified framework for inhibitory control. *Trends in cognitive sciences, 15*(10), 453-459.

Nasreddine, Z. S., Phillips, N. A., Bédirian, V., Charbonneau, S., Whitehead, V., Collin, I., . . . Chertkow, H. (2005). The Montreal Cognitive Assessment, MoCA: a brief screening tool for mild cognitive impairment. *Journal of the American Geriatrics Society, 53*(4), 695-699.

Nigbur, R., Ivanova, G., & Stürmer, B. (2011). Theta power as a marker for cognitive interference. *Clinical Neurophysiology, 122*(11), 2185-2194.

Nigg, J. T. (2000). On inhibition/disinhibition in developmental psychopathology: views from cognitive and personality psychology and a working inhibition taxonomy. *Psychological bulletin, 126*(2), 220.

Norman, D. A., & Shallice, T. (1986). Attention to action. In *Consciousness and self-regulation* (pp. 1-18): Springer.

Oldfield, R. C. (1971). The assessment and analysis of handedness: the Edinburgh inventory. *Neuropsychologia, 9*(1), 97-113.

Park, D. C., & Reuter-Lorenz, P. (2009). The adaptive brain: aging and neurocognitive scaffolding. *Annual review of psychology, 60*, 173-196.

Paxton, J. L., Barch, D. M., Racine, C. A., & Braver, T. S. (2007). Cognitive control, goal maintenance, and prefrontal function in healthy aging. *Cerebral cortex, 18*(5), 1010-1028.

Perrin, F., Pernier, J., Bertrand, O., & Echallier, J. (1989). Spherical splines for scalp potential and current density mapping. *Electroencephalography and clinical neurophysiology, 72*(2), 184-187.

Pratte, M. S., Rouder, J. N., Morey, R. D., & Feng, C. (2010). Exploring the differences in distributional properties between Stroop and Simon effects using delta plots. *Attention, Perception, & Psychophysics, 72*(7), 2013-2025.

Puccioni, O., & Vallesi, A. (2012). High cognitive reserve is associated with a reduced age-related deficit in spatial conflict resolution. *Frontiers in human neuroscience, 6*, 327.

Reuter-Lorenz, P. A., & Park, D. C. (2010). Human neuroscience and the aging mind: a new look at old problems. *The Journals of Gerontology: Series B, 65*(4), 405-415.

Reuter-Lorenz, P. A., & Park, D. C. (2014). How does it STAC up? Revisiting the scaffolding theory of aging and cognition. *Neuropsychology review, 24*(3), 355-370.

Roach, B. J., & Mathalon, D. H. (2008). Event-related EEG time-frequency analysis: an overview of measures and an analysis of early gamma band phase locking in schizophrenia. *Schizophrenia bulletin, 34*(5), 907-926.

Roelofs, A. (1997). The WEAVER model of word-form encoding in speech production. *Cognition, 64*(3), 249-284.

Ruitenberg, M. F., Braem, S., Du Cheyne, H., & Notebaert, W. (2019). Learning to be in control involves response-specific mechanisms. *Attention, Perception, & Psychophysics*, 1-12.

Salinas, E., & Sejnowski, T. J. (2001). Correlated neuronal activity and the flow of neural information. *Nature reviews neuroscience, 2*(8), 539.

Salthouse, T. A. (1996). The processing-speed theory of adult age differences in cognition. *Psychological review, 103*(3), 403.

Sauseng, P., Griesmayr, B., Freunberger, R., & Klimesch, W. (2010). Control mechanisms in working memory: a possible function of EEG theta oscillations. *Neuroscience & Biobehavioral Reviews, 34*(7), 1015-1022.

Schmidt, J. R., & Besner, D. (2008). The Stroop effect: why proportion congruent has nothing to do with congruency and everything to do with contingency. *Journal of Experimental Psychology: Learning, Memory, and Cognition, 34*(3), 514.

Siegel, M., Engel, A. K., & Donner, T. H. (2011). Cortical network dynamics of perceptual decision-making in the human brain. *Frontiers in human neuroscience, 5*, 21.

Simon, J. R., & Small Jr, A. (1969). Processing auditory information: interference from an irrelevant cue. *Journal of Applied Psychology, 53*(5), 433.

Smith, S. M., & Nichols, T. E. (2009). Threshold-free cluster enhancement: addressing problems of smoothing, threshold dependence and localisation in cluster inference. *Neuroimage, 44*(1), 83-98.

Spitzer, B., & Haegens, S. (2017). Beyond the status quo: A role for beta oscillations in endogenous content (re) activation. *Eneuro, 4*(4), ENEURO. 0170-0117.2017.

Spivey, M. J., Grosjean, M., & Knoblich, G. (2005). Continuous attraction toward phonological competitors. *Proceedings of the National Academy of Sciences, 102*(29), 10393-10398.

Stroop, J. R. (1935). Studies of interference in serial verbal reactions. *Journal of experimental psychology, 18*(6), 643.

Sturz, B. R., Green, M. L., Locker Jr, L., & Boyer, T. W. (2013). Stroop interference in a delayed match-to-sample task: Evidence for semantic competition. *Frontiers in psychology, 4*, 842.

Stuss, D. T. (2011). Functions of the frontal lobes: relation to executive functions. *Journal of the international neuropsychological Society, 17*(5), 759-765.

Stuss, D. T., & Alexander, M. P. (2007). Is there a dysexecutive syndrome? *Philosophical Transactions of the Royal Society B: Biological Sciences, 362*(1481), 901-915.

Stuss, D. T., & Levine, B. (2002). Adult clinical neuropsychology: lessons from studies of the frontal lobes. *Annual review of psychology, 53*(1), 401-433.

Sullivan, N., Hutcherson, C., Harris, A., & Rangel, A. (2015). Dietary self-control is related to the speed with which attributes of healthfulness and tastiness are processed. *Psychological science, 26*(2), 122-134.

Szczepanski, S. M., & Knight, R. T. (2014). Insights into human behavior from lesions to the prefrontal cortex. *Neuron, 83*(5), 1002-1018.

Tadel, F., Baillet, S., Mosher, J. C., Pantazis, D., & Leahy, R. M. (2011). Brainstorm: a user-friendly application for MEG/EEG analysis. *Computational intelligence and neuroscience, 2011*, 8.

Vallesi, A. (2012). Organisation of executive functions: hemispheric asymmetries. *Journal of Cognitive Psychology, 24*(4), 367-386.

Vallesi, A., Stuss, D. T., McIntosh, A. R., & Picton, T. W. (2009). Age-related differences in processing irrelevant information: evidence from event-related potentials. *Neuropsychologia, 47*(2), 577-586.

Van Driel, J., Ort, E., Fahrenfort, J. J., & Olivers, C. N. (2019). Beta and theta oscillations differentially support free versus forced control over multiple-target search. *Journal of Neuroscience, 39*(9), 1733-1743.

van Maanen, L., Forstmann, B. U., Keuken, M. C., Wagenmakers, E.-J., & Heathcote, A. (2016). The impact of MRI scanner environment on perceptual decision-making. *Behavior research methods, 48*(1), 184-200.

Van Wijk, B., Daffertshofer, A., Roach, N., & Praamstra, P. (2008). A role of beta oscillatory synchrony in biasing response competition? *Cerebral Cortex, 19*(6), 1294-1302.

Velicer, W. F., Eaton, C. A., & Fava, J. L. (2000). Construct explication through factor or component analysis: A review and evaluation of alternative procedures for determining the number of factors or components. In *Problems and solutions in human assessment* (pp. 41-71): Springer.

Verhaeghen, P., & De Meersman, L. (1998). Aging and the Stroop effect: A meta-analysis. *Psychology and aging, 13*(1), 120.

Wang, K., Li, Q., Zheng, Y., Wang, H., & Liu, X. (2014). Temporal and spectral profiles of stimulus–stimulus and stimulus–response conflict processing. *Neuroimage, 89*, 280-288.

Weintraub, S., & Mesulam, M.-M. (1987). Right cerebral dominance in spatial attention: Further evidence based on ipsilateral neglect. *Archives of neurology, 44*(6), 621-625.

West, R. (2004). The effects of aging on controlled attention and conflict processing in the Stroop task. *Journal of cognitive neuroscience, 16*(1), 103-113.

West, R., Bailey, K., Tiernan, B. N., Boonsuk, W., & Gilbert, S. (2012). The temporal dynamics of medial and lateral frontal neural activity related to proactive cognitive control. *Neuropsychologia, 50*(14), 3450-3460.

Winkler, I., Debener, S., Müller, K.-R., & Tangermann, M. (2015). *On the influence of high-pass filtering on ICA-based artifact reduction in EEG-ERP.* Paper presented at the 2015 37th Annual International Conference of the IEEE Engineering in Medicine and Biology Society (EMBC).

Zavala, B., Brittain, J.-S., Jenkinson, N., Ashkan, K., Foltynie, T., Limousin, P., . . . Zaghloul, K. (2013). Subthalamic nucleus local field potential activity during the Eriksen flanker task reveals a novel role for theta phase during conflict monitoring. *Journal of Neuroscience, 33*(37), 14758-14766.

Zhang, H., & Kornblum, S. (1998). The effects of stimulus–response mapping and irrelevant stimulus–response and stimulus–stimulus overlap in four-choice Stroop tasks with single-carrier stimuli. *Journal of Experimental Psychology: Human Perception and Performance, 24*(1), 3.

Zhao, J., Liang, W.-K., Juan, C.-H., Wang, L., Wang, S., & Zhu, Z. (2015). Dissociated stimulus and response conflict effect in the Stroop task: Evidence from evoked brain potentials and brain oscillations. *Biological psychology, 104*, 130-138.

Appendix

A. Supplementary of Study 1

Note on similarity of this Stroop task and Simon task

It is true that our experimental paradigm entails some features in common with the Simon task, in that the spatial position of the response and that of the stimulus (i.e., the task-irrelevant feature) may or may not correspond. However, differently from the Simon task, in our experimental task the task-relevant feature of the stimuli was also spatial in nature (i.e., the arrow direction). Moreover, it is possible to demonstrate that the mechanisms involved in our spatial version of the Stroop task are different from those involved in the Simon paradigm. Indeed, as reported by previous studies, Stroop and Simon tasks can be differentiated assessing the effect of the task-irrelevant information on response time (RT) distributions by means of delta plots (Pratte et al., 2010). In particular, delta plots are derived from percentiles of RT distributions for congruent and incongruent trials and they show opposite patterns of slope for Stroop and Simon tasks. Indeed, in the Stroop task the interference effects are least for the fastest responses and increase with RT, whereas in the Simon task interference effects are maximal for fastest responses and decrease with longer RT. We conducted this analysis and we found that interference effects increase as a function of RT for both groups (blue line corresponds to the percentiles for the younger group and red line is the one for older adults), following the same pattern predicted for Stroop paradigms (figure as follows). We can thus infer that the cognitive interference in our task mainly occurs at the stimulus level (as commonly seen in Stroop tasks). Still, we cannot exclude that interference at the response level is involved in our task.

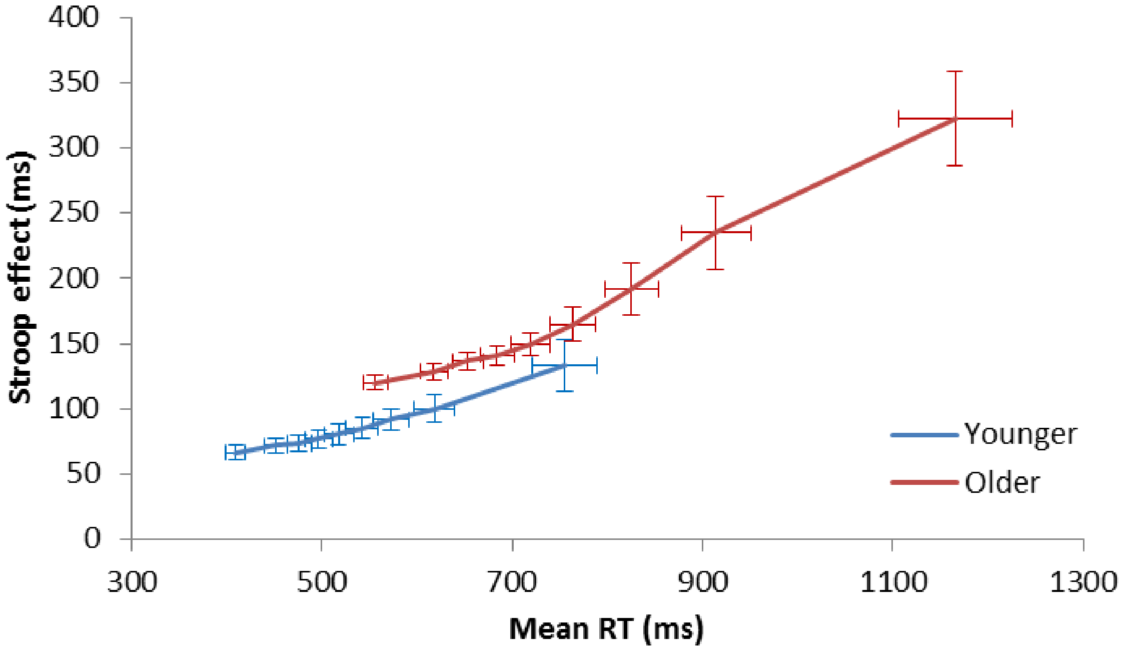

Figure A. 1. Delta Plot

B. Supplementary of Study 2

Results of mixed-effects models for all the *trial-level* MouseTracker measures

Table B.1 reports the Estimates (b), Standard Error (SE), degree of freedom (df), t and p-values for all the parameters and *trial-level* measures in this study. Concerning the results for the IT, the analysis revealed only the main effect of the total number of trials, for which the participants became faster in initiating the movement during the course of the experiment probably due a gradual learning of the task.

The MDd showed again the main effect of the total number of trials with the same pattern of IT measure (i.e., a learning effect), but it also showed a significant main effect of Congruency, with a cost in responding to incongruent trials for which the distance from the optimal trajectory was higher than the congruent ones. Moreover, there was also a significant interaction between ISPC manipulation and Congruency, for which congruent and incongruent trials reported different effects depending on the manipulation used. In particular, incongruent trials in the IS75PC blocks showed the longest distance from the optimal trajectory compared to the incongruent trials of the IS25PC blocks, but this difference was not so pronounced in responding to the congruent trials. This led to a smaller Stroop effect for the highly incongruent ISPC condition (IS25PC).

Concerning the measure of MaxVel we found again the significant main effect of the total number of trials indicating that the performance improved as the experiment went on, and a significant effect of Congruency, where the velocity was higher for the incongruent trials, indicating that participants tried to quickly update and correct their responses. Moreover, this measure showed both a significant interaction between the LWPC manipulation and Congruency, and also between the ISPC manipulation and Congruency, so that the Stroop effect increased as a function of the proportion congruency used.

The Start Angle did not show any significant effect of the total number of trials, but as the measures described above it showed a significant effect of LWPC, ISPC, and Congruency, with the trajectories for incongruent trials that were initially directed toward the alternative response option. There was also a significant interaction between ISPC and Congruency, showing the same pattern reported for MDd.

The measure of MDTime exhibited the same effects of the total number of trials previously reported, as well the main effects of ISPC manipulation and Congruency. It also showed the significant interactions LWCP by Congruency and ISPC by Congruency, mirroring the results found for MaxVel. Similarly, the same pattern of results was found for MD and AUC, with the only difference that for these measures there was also the main effect of LWPC manipulation. The measure of MDx showed significant effects for all the main effects, except the total number of trials, and for all the two-way interactions: LWPC by Congruency, ISPC by Congruency and ISPC by LWPC. The first two interactions reflected the pattern already seen in the other measures, for which the Stroop effect decreased as the PC increased in both types of manipulations. There was also a significant effect of the three-way interaction LWPC by ISPC by Congruency for which incongruent trials showed the biggest interference effect depending on the percentage of congruency adopted (both item and block levels). Finally, RT, MT, TravD, XFlip, VelFlip, MaxVelTime and Xmin showed the same pattern of results, with significant results for all the main effects and all the interactions tested.

Table B.1. Effects for trial-level measures Study 2
The table reports the Estimates, Standard Error, degree of freedom, t and *p-values.*

	IT				
EFFECT	Estimate	SE	df	t values	*p* values
Intercept	3.66	0.13	46.97	28.25	0.000
Trial Tot	0.09	0.01	6454.40	16.25	0.000
LWPC	0.04	0.03	41.30	1.25	0.218
ISPC	0.02	0.01	48.46	1.98	0.054
Congruency	-0.02	0.02	156.34	-1.04	0.299
LWPC*ISPC	0.05	0.04	46.20	1.32	0.192
LWPC*Congruency	0.02	0.02	36.74	1.00	0.322
ISPC*Congruency	-0.01	0.01	49.62	-0.90	0.371
LWPC*ISPC*Congruency	0.00	0.01	69.36	-0.30	0.767

	MT				
EFFECT	Estimate	SE	df	t values	*p* values
Intercept	1.62	0.03	46.97	60.60	0.000
Trial Tot	0.02	0.00	1834.48	15.08	0.000
LWPC	0.01	0.00	47.55	2.71	0.009
ISPC	0.02	0.00	47.27	5.50	0.000
Congruency	-0.24	0.02	47.05	-14.75	0.000
LWPC*ISPC	-0.01	0.00	47.51	-3.81	0.000
LWPC*Congruency	-0.04	0.01	47.23	-6.58	0.000
ISPC*Congruency	-0.03	0.00	50.38	-8.16	0.000
LWPC*ISPC*Congruency	0.00	0.00	84.69	3.31	0.001

	RT				
EFFECT	Estimate	SE	df	t values	*p* values
Intercept	1.08	0.01	47.00	76.71	0.000
Trial Tot	0.01	0.00	2209.83	22.75	0.000
LWPC	0.00	0.00	47.24	2.45	0.018
ISPC	0.01	0.00	47.95	8.70	0.000
Congruency	-0.13	0.01	47.08	-16.12	0.000
LWPC*ISPC	0.00	0.00	47.50	-2.62	0.012
LWPC*Congruency	-0.02	0.00	47.31	-6.13	0.000
ISPC*Congruency	-0.02	0.00	47.97	-9.91	0.000
LWPC*ISPC*Congruency	0.00	0.00	75.22	3.22	0.002

	MD				
EFFECT	Estimate	SE	df	t values	*p* values
Intercept	2.83	0.04	47.07	68.47	0.000
Trial Tot	-0.03	0.01	434.52	-5.08	0.000
LWPC	0.04	0.01	50.13	2.36	0.022
ISPC	-0.07	0.01	47.06	-5.11	0.000
Congruency	1.35	0.07	47.09	20.21	0.000
LWPC*ISPC	0.01	0.00	55.39	1.95	0.056
LWPC*Congruency	0.08	0.02	47.21	3.36	0.002
ISPC*Congruency	0.13	0.02	47.09	7.69	0.000
LWPC*ISPC*Congruency	-0.01	0.01	70.08	-1.34	0.184

	MD Time				
EFFECT	Estimate	SE	df	t values	*p* values
Intercept	6.21	0.01	47.08	425.88	0.000
Trial Tot	-0.01	0.00	1630.53	-8.88	0.000
LWPC	-0.01	0.00	46.31	-1.74	0.088
ISPC	-0.01	0.00	47.63	-3.22	0.002
Congruency	0.02	0.01	55.53	2.24	0.029
LWPC*ISPC	0.00	0.00	44.59	-0.53	0.600
LWPC*Congruency	0.01	0.00	49.52	3.00	0.004
ISPC*Congruency	0.01	0.00	47.44	3.77	0.000
LWPC*ISPC*Congruency	0.00	0.00	56.50	0.41	0.685

	MDx				
EFFECT	Estimate	SE	df	t values	*p* values
Intercept	149.98	3.77	47.31	39.78	0.000
Trial Tot	0.63	0.64	739.50	0.98	0.327
LWPC	3.67	1.41	50.92	2.60	0.012
ISPC	3.04	1.06	52.09	2.86	0.006
Congruency	-167.41	9.14	47.01	-18.32	0.000
LWPC*ISPC	-1.82	0.49	76.45	-3.75	0.000
LWPC*Congruency	-16.29	2.39	47.06	-6.82	0.000
ISPC*Congruency	-14.29	1.64	46.85	-8.72	0.000
LWPC*ISPC*Congruency	2.02	0.83	55.40	2.43	0.018

	MDd				
EFFECT	Estimate	SE	df	t values	*p* values
Intercept	266.86	4.57	46.99	58.46	0.000
Trial Tot	-4.17	0.65	913.53	-6.39	0.000
LWPC	2.31	1.84	47.67	1.25	0.217
ISPC	-0.98	1.35	47.00	-0.73	0.470
Congruency	15.41	5.50	47.30	2.80	0.007
LWPC*ISPC	-0.55	0.55	49.31	-1.00	0.322
LWPC*Congruency	2.16	2.08	51.70	1.04	0.305
ISPC*Congruency	5.48	1.64	51.04	3.34	0.002
LWPC*ISPC*Congruency	0.88	0.72	63.26	1.22	0.226

	AUC				
EFFECT	Estimate	SE	df	t values	*p* values
Intercept	7.30	0.07	46.63	99.09	0.000
Trial Tot	-0.05	0.01	543.47	-4.79	0.000
LWPC	0.06	0.02	1149.13	3.16	0.002
ISPC	-0.11	0.02	57.13	-5.91	0.000
Congruency	2.09	0.12	48.01	17.99	0.000
LWPC*ISPC	0.01	0.01	56.30	1.30	0.197
LWPC*Congruency	0.11	0.03	111.07	3.27	0.001
ISPC*Congruency	0.20	0.02	75.52	8.32	0.000
LWPC*ISPC*Congruency	-0.01	0.01	79.10	-0.88	0.382

	Start Angle				
EFFECT	Estimate	SE	df	t values	*p* values
Intercept	18.67	0.51	38597.86	36.82	0.000.
Trial Tot	-0.29	0.17	462.61	-1.69	0.092
LWPC	-1.76	0.61	49.77	-2.89	0.006
ISPC	2.29	0.55	50.55	4.17	0.000
Congruency	-17.42	0.93	103.91	-18.80	0.000
LWPC*ISPC	-0.08	0.23	57.51	-0.34	0.737
LWPC*Congruency	1.15	0.78	50.94	1.48	0.146
ISPC*Congruency	-3.33	0.75	49.03	-4.46	0.000
LWPC*ISPC*Congruency	0.17	0.29	57.10	0.58	0.564

	TravD				
EFFECT	Estimate	SE	df	t values	*p* values
Intercept	6.34	0.01	46.95	496.31	0.000
Trial Tot	-0.01	0.00	1632.58	-8.15	0.000
LWPC	-0.01	0.00	45.69	-3.02	0.004
ISPC	-0.01	0.00	46.51	-7.65	0.000
Congruency	0.33	0.02	46.97	16.52	0.000
LWPC*ISPC	0.00	0.00	45.58	4.18	0.000
LWPC*Congruency	0.05	0.01	47.02	8.54	0.000
ISPC*Congruency	0.03	0.00	46.52	11.56	0.000
LWPC*ISPC*Congruency	0.00	0.00	46.91	-2.41	0.020

	MaxVel				
EFFECT	Estimate	SE	df	t values	*p* values
Intercept	4.68	0.02	47.00	190.09	0.000
Trial Tot	-0.02	0.00	4498.63	-13.37	0.000
LWPC	-0.01	0.00	46.61	-1.76	0.085
ISPC	0.00	0.00	47.02	0.06	0.954
Congruency	0.18	0.01	47.01	12.86	0.000
LWPC*ISPC	0.00	0.00	46.99	-0.02	0.981
LWPC*Congruency	0.03	0.01	46.80	5.50	0.000
ISPC*Congruency	0.01	0.00	46.94	3.25	0.002
LWPC*ISPC*Congruency	0.00	0.00	47.01	-0.64	0.524

	MaxVelTime				
EFFECT	Estimate	SE	df	t values	*p* values
Intercept	6.02	0.01	47.00	431.11	0.000
Trial Tot	-0.01	0.00	2412.14	-12.77	0.000
LWPC	-0.01	0.00	46.93	-3.64	0.001
ISPC	-0.02	0.00	46.90	-8.84	0.000
Congruency	0.20	0.01	46.94	17.63	0.000
LWPC*ISPC	0.00	0.00	46.84	2.98	0.005
LWPC*Congruency	0.03	0.00	46.85	7.20	0.000
ISPC*Congruency	0.03	0.00	46.82	10.40	0.000
LWPC*ISPC*Congruency	0.00	0.00	46.56	-2.24	0.030

	XFlip				
EFFECT	Estimate	SE	df	t values	*p* values
Intercept	0.91	0.05	47.00	18.57	0.000
Trial Tot	-0.03	0.00	1362.38	-6.73	0.000
LWPC	-0.03	0.01	47.08	-3.10	0.003
ISPC	-0.04	0.01	47.77	-6.55	0.000
Congruency	0.66	0.03	47.69	22.09	0.000
LWPC*ISPC	0.01	0.00	47.02	2.84	0.007
LWPC*Congruency	0.09	0.01	47.52	6.77	0.000
ISPC*Congruency	0.05	0.01	50.80	5.73	0.000
LWPC*ISPC*Congruency	-0.02	0.00	79.31	-3.99	0.000

	VelFlip				
EFFECT	Estimate	SE	df	t values	*p* values
Intercept	3.58	0.07	47.01	51.49	0.000
Trial Tot	-0.08	0.01	1376.16	-11.42	0.000
LWPC	-0.06	0.02	50.69	-3.34	0.002
ISPC	-0.07	0.01	84.05	-6.52	0.000
Congruency	1.17	0.06	47.91	19.15	0.000
LWPC*ISPC	0.03	0.01	48.47	3.65	0.001
LWPC*Congruency	0.20	0.03	48.09	6.50	0.000
ISPC*Congruency	0.14	0.02	53.09	7.95	0.000
LWPC*ISPC*Congruency	-0.03	0.01	123.50	-4.05	0.000

	Xmin				
EFFECT	Estimate	SE	df	t values	*p* values
Intercept	8.69	0.05	47.06	169.46	0.000
Trial Tot	0.02	0.01	1364.06	2.55	0.011
LWPC	0.04	0.01	59.94	2.96	0.004
ISPC	0.05	0.01	230.33	5.88	0.000
Congruency	-2.37	0.09	46.97	-25.58	0.000
LWPC*ISPC	-0.02	0.01	53.91	-4.52	0.000
LWPC*Congruency	-0.21	0.03	46.48	-7.27	0.000
ISPC*Congruency	-0.18	0.02	53.78	-11.85	0.000
LWPC*ISPC*Congruency	0.03	0.01	50.76	3.34	0.002

C. Supplementary on Study 3

C.1. Results of mixed effects models for mouse-derived trial-level measures

Table C.1 reports the Estimates (b), Standard Error (SE), degree of freedom (df), t and p-values for all the parameters and trial-level measures in this study. As mentioned above, we calculated the very same measures of Study 2. Concerning the results of MDd, the analysis revealed only the main effects of Congruency, for which the distance from the optimal trajectory was higher for incongruent than congruent trials, and of LWPC manipulation, for which the distance was higher for high-PC blocks.

MT reported also the main effects of Congruency and LWPC manipulation, so that MT was generally longer in responding to incongruent trials and in responding to high-PC blocks when compared to the others. Moreover, there was also a significant effect of the interaction Congruency by LWPC manipulation, for which the Stroop effect increased as function of the PC.

The measures of MD, AUC, Start Angle and MaxVel showed the same pattern of results, for which there were the main effects of the total number trials and Congruency and a significant interaction between Congruency and LWPC manipulation. However, the pattern of the total number of trials seemed to be less consistent compared to the one previously found in Study 2, because some measures showed an improvement in performance as the experiment went on, whereas other seemed to be probably affected by fatigue. Concerning Congruency, all the measures showed a general cost in responding to the incongruent trials, and we also found an interaction with the manipulation, for which the Stroop effect was generally smaller for low-PC manipulations. All the other measures (i.e., IT, RT, MDTime, MDx, TravD, MaxVelTime, Xflip, VelFlip, Xmin) showed significant effects for all the regressors, reporting the main effects of the total number of trials, Congruency, LWPC manipulation and also the interaction Congruency by LWPC. These measures exhibited the same effects and patterns already described for the others above. In addition, they also showed the main effects of LWPC for which they were better in low-PC conditions.

Table C.1 Effects for trial-level measures Study 3
The table reports the Estimates, Standard Error, degree of freedom, t and *p-values.*

	MDd				
EFFECT	Estimate	SE	df	t values	*p* values
Intercept	342.83	5.17	43.32	66.32	0.000
Trial Tot	1.10	1.09	354.41	1.00	0.316
LWPC	3.44	0.99	114.64	3.45	0.001
Congruency	18.68	5.37	43.34	3.48	0.001
LWPC*Congruency	1.37	1.74	52.80	0.79	0.434

	MT				
EFFECT	Estimate	SE	df	t values	*p* values
Intercept	1.87	0.04	42.96	49.82	0.000
Trial Tot	0.00	0.00	3327.49	-1.57	0.117
LWPC	0.01	0.00	43.00	2.12	0.040
Congruency	-0.18	0.02	42.98	-9.65	0.000
LWPC*Congruency	-0.04	0.00	43.02	-8.29	0.000

	MD				
EFFECT	Estimate	SE	df	t values	*p* values
Intercept	2.47	0.04	43.06	61.35	0.000
Trial Tot	0.03	0.01	565.62	3.30	0.001
LWPC	0.00	0.01	43.00	0.44	0.661
Congruency	0.92	0.08	43.05	11.17	0.000
LWPC*Congruency	0.14	0.02	42.79	8.21	0.000

	AUC				
EFFECT	Estimate	SE	df	t values	*p* values
Intercept	6.18	0.07	43.10	89.57	0.000
Trial Tot	0.04	0.02	506.25	2.14	0.033
LWPC	0.02	0.02	42.96	0.94	0.353
Congruency	1.43	0.14	43.07	10.54	0.000
LWPC*Congruency	0.20	0.03	42.64	7.00	0.000

	Start Angle				
EFFECT	Estimate	SE	df	t values	*p* values
Intercept	39.12	0.78	42.86	50.01	0.000
Trial Tot	-0.61	0.16	1094.22	-3.88	0.000
LWPC	0.21	0.14	194.28	1.55	0.123
Congruency	-20.47	1.92	43.52	-10.64	0.000
LWPC*Congruency	-3.44	0.39	46.82	-8.86	0.000

	Max Vel				
EFFECT	Estimate	SE	df	t values	*p* values
Intercept	5.10	0.04	43.00	130.11	0.000
Trial Tot	0.01	0.00	8542.03	4.84	0.000
LWPC	0.00	0.00	42.95	-0.03	0.976
Congruency	0.04	0.01	43.02	3.23	0.002
LWPC*Congruency	0.01	0.00	43.04	4.59	0.000

	IT				
EFFECT	Estimate	SE	df	t values	*p* values
Intercept	2.90	0.04	42.99	68.22	0.000
Trial Tot	0.06	0.00	10227.24	19.71	0.000
LWPC	0.05	0.01	42.95	8.66	0.000
Congruency	-0.15	0.02	43.05	-7.67	0.000
LWPC*Congruency	-0.04	0.01	43.01	-7.12	0.000

	RT				
EFFECT	Estimate	SE	df	t values	*p* values
Intercept	1.12	0.02	42.95	64.78	0.000
Trial Tot	0.01	0.00	4187.83	9.51	0.000
LWPC	0.01	0.00	42.98	6.42	0.000
Congruency	-0.10	0.01	42.93	-13.61	0.000
LWPC*Congruency	-0.03	0.00	42.95	-13.44	0.000

	MD Time				
EFFECT	Estimate	SE	df	t values	*p* values
Intercept	6.23	0.02	43.00	403.18	0.000
Trial Tot	-0.02	0.00	1023.47	-11.28	0.000
LWPC	-0.01	0.00	42.31	-6.22	0.000
Congruency	0.07	0.01	42.86	7.24	0.000
LWPC*Congruency	0.02	0.00	42.80	8.51	0.000

	MDx				
EFFECT	Estimate	SE	df	t values	*p* values
Intercept	217.20	3.18	43.87	68.29	0.000
Trial Tot	-3.11	0.90	639.75	-3.45	0.001
LWPC	2.98	0.78	420.80	3.80	0.000
Congruency	-112.69	12.34	43.31	-9.13	0.000
LWPC*Congruency	-26.67	2.69	45.92	-9.93	0.000

	TravD				
EFFECT	Estimate	SE	df	t values	*p* values
Intercept	6.57	0.01	43.18	884.54	0.000
Trial Tot	0.01	0.00	754.13	9.01	0.000
LWPC	0.00	0.00	41.89	-2.82	0.007
Congruency	0.15	0.02	43.53	7.97	0.000
LWPC*Congruency	0.04	0.00	43.34	8.49	0.000

	Max Vel Time				
EFFECT	Estimate	SE	df	t values	*p* values
Intercept	6.08	0.01	42.67	435.05	0.000
Trial Tot	-0.02	0.00	2798.69	-18.19	0.000
LWPC	-0.02	0.00	43.05	-9.43	0.000
Congruency	0.15	0.01	43.20	14.71	0.000
LWPC*Congruency	0.04	0.00	42.97	19.38	0.000

	XFlip				
EFFECT	Estimate	SE	df	t values	*p* values
Intercept	0.56	0.04	43.08	15.14	0.000
Trial Tot	0.01	0.00	1733.63	2.54	0.011
LWPC	-0.02	0.01	42.89	-3.68	0.001
Congruency	0.35	0.03	43.02	10.30	0.000
LWPC*Congruency	0.08	0.01	42.89	10.28	0.000

	VelFlip				
EFFECT	Estimate	SE	df	t values	*p* values
Intercept	3.26	0.06	43.06	56.07	0.000
Trial Tot	-0.01	0.01	815.73	-1.29	0.196
LWPC	-0.02	0.01	42.98	-2.50	0.016
Congruency	0.67	0.07	42.95	10.32	0.000
LWPC*Congruency	0.16	0.02	42.82	9.76	0.000

	Xmin				
EFFECT	Estimate	SE	df	t values	*p* values
Intercept	9.35	0.01	42.72	1820.86	0.000
Trial Tot	-0.01	0.00	4510.46	-6.07	0.000
LWPC	0.01	0.00	103.71	2.62	0.010
Congruency	-0.59	0.05	42.97	-11.11	0.000
LWPC*Congruency	-0.12	0.01	42.97	-11.15	0.000

C.2. EEG results for LW50PC and its interaction with LW75PC and LW25PC

Concerning the Stroop effect in LW50PC condition, there was a main involvement of lower frequencies (i.e., theta and alpha ranges) that started around 200 ms until around 800 ms. Higher frequencies were mainly involved starting around 400 ms, showing a more specific involvement of beta range with the time passing. Focussing on theta and beta results, we found a main cluster for theta frequencies, that started soon after stimulus presentation with a more focal localization over midfrontal channels and became more spread over the scalp with time, engaging also frontal and posterior channels. This cluster diminished until almost disappearing around 1200 ms and was due to an increase in power for incongruent trials as compared to the congruent ones. Beta range showed a frontal cluster starting mainly from 400 to 600 ms, with the range of beta1 lasting also until 800 ms. This effect was due to a higher increase in power for the incongruent as compared to the congruent trials. From around 800 to 1400 ms, there was a second cluster mainly engaging left lateralized parietal and prefrontal channels, that was characterized by a stronger power suppression for incongruent than for congruent trials.

As regard to the interaction between the Stroop effects of LW50PC and LW75PC, there was a small midfrontal cluster in theta frequencies starting from around 200 ms and lasting around 600 ms. This exclusively involved the upper range of theta (6-7 Hz) and was due to the fact that the Stroop effect was smaller in the LW50PC condition. After 600 ms there was another cluster localized initially over frontal channels and that, as the time passed, involved also posterior channels. This effect was due to the fact that, in this temporal window, there was still a stronger power increase for incongruent trials, as compared to the congruent ones, but mainly present in the LW75PC. Concerning beta frequencies, there was one cluster due to the same effect, that started around 400 ms mainly involving the upper range of the band (beta3) over midfrontal channels, and gradually engaging more portions over the scalp and the lower range of beta (beta1 and beta2), until around 1400 ms.

Finally, about the interaction between LW25PC and LW50PC and the frequencies bands of interest, we found one main cluster involving theta frequencies (and surrounding alpha), starting from around 200 ms to 800 ms from midfrontal channels and spreading also on occipital portion of the scalp. This cluster was due to the fact that there was a main power increase for incongruent trials in LW50PC blocks, as compared to the congruent ones, whereas this difference was not pronounced in the LW25PC. A cluster due to this same effect was present also in the beta range, but was mild from around 200 ms, engaging only beta1 and localized over midfrontal and frontal channels. Mainly from 800 ms there was another cluster spreading over central and posterior channels and lasting until around the end of the epoch, that was due to the fact that the power suppression for incongruent trials, as compared to the congruent, was less pronounced in the LW25PC condition as compared to the LW50PC. Stated differently, also these results showed that the Stroop effect was stronger as function of the PC and in line to what already reported for LW25PC and LW75PC interaction.

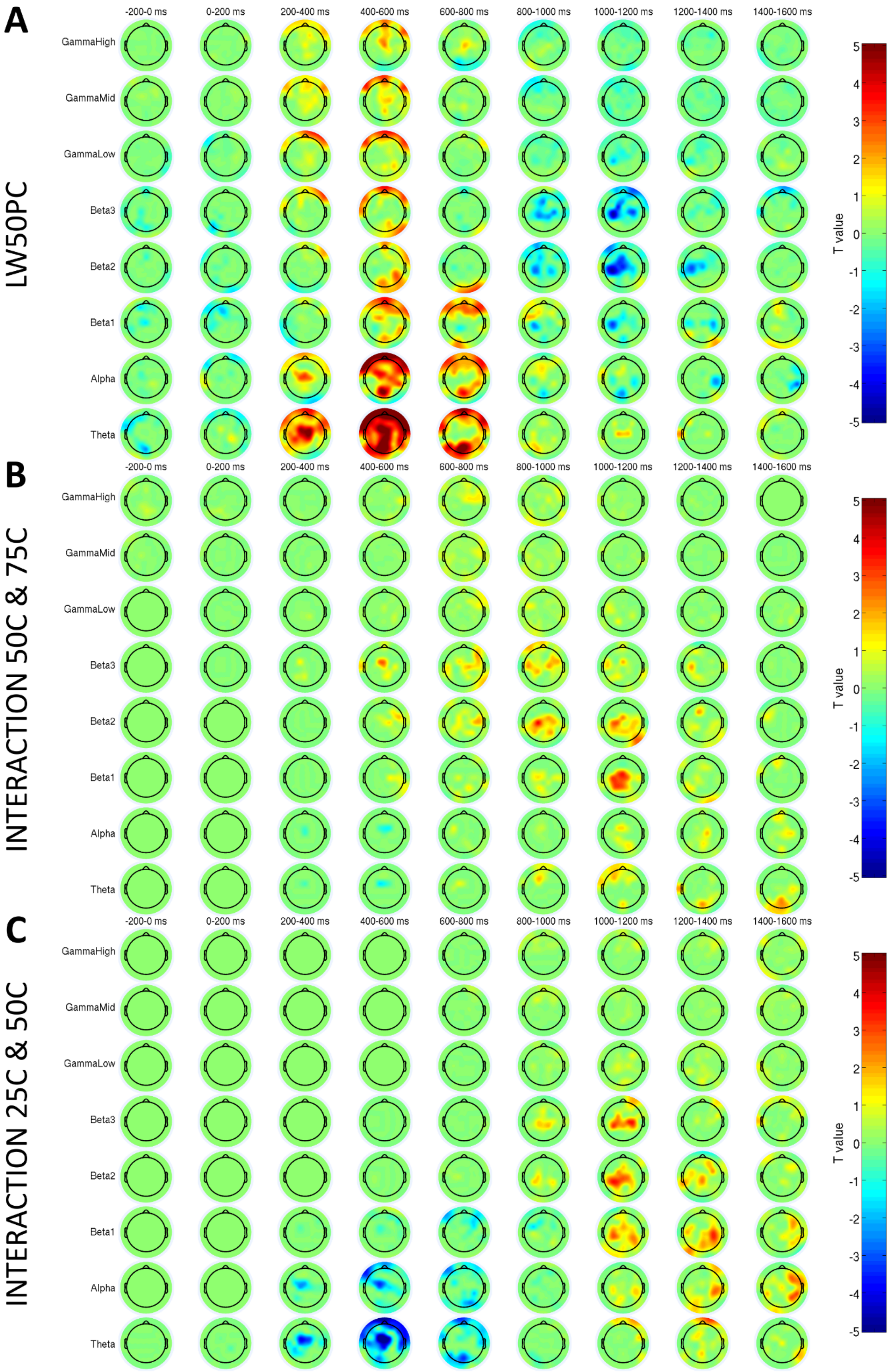
A
LW50PC
B
INTERACTION 50C & 75C
C
INTERACTION 25C & 50C
-200-0 ms
0-200 ms
200-400 ms
400-600 ms
600-800 ms
800-1000 ms
1000-1200 ms
1200-1400 ms
1400-1600 ms
GammaHigh
GammaMid
GammaLow
Beta3
Beta2
Beta1
Alpha
Theta
T value
5
4
3
2
1
0
-1
-2
-3
-4
-5

Figure C.1. Results of the scalp-based event-related spectral perturbation (ERSP) analysis.

The figure shows the topoplots for the results of simple effect analysis in LW50PC (A) and its interaction with LW75PC blocks (B), and its interaction with LW25PC blocks (C). Each row represents the average of each frequency band, whereas the columns represents the average of EEG activity every 200 ms from 200 ms before stimulus presentation (time 0). The topoplots show the *t values* of the significant results after TFCE.